COOLING EFFICIENCY IMPROVEMENT OF A DATA CENTER USING OPTIMIZED CABINET DESIGN AND HYBRID COOLING WITH HIGH INLET CONDITIONS OF SINGLE-PHASE COOLANT AND AIR

by

USCHAS CHOWDHURY

Presented to the Faculty of the Graduate School of

The University of Texas at Arlington in Partial Fulfillment

of the Requirements for the Degree of

DOCTOR OF PHILOSOPHY

THE UNIVERSITY OF TEXAS AT ARLINGTON

May 2021

Copyright © by Uschas Chowdhury 2021

All Rights Reserved

Acknowledgements

I am grateful to Dr. Dereje Agonafer for his excellent guidance and academic support over the course of my doctoral degree. He has engaged and exposed me to work on industry-funded projects and help me to attend conferences which increased networking by presenting papers and posters.

I would also like to thank Dr. Haji-Sheikh, Dr. Miguel A Amaya, Dr. Zeynep Celik and Dr Saket Karajgikar for serving on my dissertation committee. I owe a great deal of gratitude to Dr Ali Heydari for serving my mentor regarding industry-related topics during my internship at NVIDIA. My special thanks to Mr. Walter Hendrix, Mr. Thomas Craft and Mr. Willis James of CommScope to teach and guide me in my industry related projects.

I would like to thank Ms. Ayesha Fatima and Ms. Wendy Ryan for their timely assistance with administrative matters during my time with the EMNSPC. Special thanks to Md Malekkul Islam, Dr Manasa Sahini and Ashwin Siddharth for not only being co-authors but also helping to learn from our funded projects and for their valuable input on my research.

Most importantly, I would like to thank my father (Ashish Kumar Chowdhury) and mother (Supriya Chowdhury) and wife (Chanda Das Gupta) who have always provided me emotional support and hope for pursuing my PhD degree.

May 04, 2021

Abstract

COOLING EFFICIENCY IMPROVEMENT OF A DATA CENTER USING OPTIMIZED CABINET DESIGN AND HYBRID COOLING WITH HIGH INLET CONDITIONS OF SINGLE-PHASE COOLANT AND AIR

Uschas Chowdhury, PhD

The University of Texas at Arlington, 2021

Supervising Professor: Dereje Agonafer

The objective of this study is to improve and optimize the cooling efficiency of liquid and air cooling from server to room level while applying best practices in the industry. The effect of increased air and coolant temperature has been explored through a literature survey and studies are conducted from device level to room level for air and liquid cooling. Three major aspects are considered. A closed-form air cooling solution is proposed for high-powered racks in a modular data center equipped with in-row coolers. Direct-to-chip liquid cooling technology is extensively studied at the server level for raised air and coolant inlet temperature for determining thermal performance and reliability of IT equipment. A cost analysis for liquid cooling has been conducted with a TCO model for the

performance improvement and holistic evaluation of a data center with air and liquid cooling.

The first part consists of a room-level numerical study conducted with high-powered racks in a modular data center with regular low-powered racks. Typical modular data centers are cooled by perimeter or outdoor cooling units. A comparative analysis is performed for a typical small-sized non-raised facility to investigate the efficacy and limitations of in-row coolers in thermal management of IT equipment with variation in rack heat load and containment. Several other aspects like a parametric study of variable opening areas of duct between racks and in-row coolers, the variation of operating flow rate, and failure scenarios are also studied to find proper flow distribution, uniformity of outlet temperature, and predict better performance, energy savings and reliability. The results are presented for general guidance for flexible and quick installation and safe operation of in-row coolers to improve thermal efficiency.

The Second Part consists of a server-level numerical and experimental study with raised inlet air and coolant temperature for a hybrid cooled server. A detailed numerical study of an enterprise 1U hybrid cooled server is performed to predict the effect of raised inlet air temperature on the component temperatures following the limits of ASHARE air cooling classes. Then, an experimental study is performed in an environmental chamber with high inlet air temperatures. Results

for both studies are compared. Previously warm water cooling or increased coolant inlet temperature has been experimentally tested on the respective server. Thus, the effect of both air and liquid coolant temperature has been presented and scaled up to a data center level with help of industry-standard tools for 1D flow network analysis to address the cooling efficiency improvement.

The third part consists of a cost analysis of a data center with air and liquid cooling using an established TCO model. The ASHRAE cooling classes for air and liquid cooling are used based on the experimental findings. Also, the effect of cooling efficiency improvements at component and server level and increased inlet conditions are used to compare with a baseline model with air cooling.

TABLE OF CONTENTS

Acknowledgements iii

Abstract iv

List of Illustrations x

List of Tables xvi

Nomenclature 17

Chapter 1 Introduction 20

1.1 ASHRAE Air Cooling Guidelines 22

1.2 ASHRAE Liquid Cooling Guidelines [9] 23

1.3 Power Consumption and Data center Efficiency 23

Chapter 2 Literature Review 30

2.1 Optimal Design and Modeling of Server Cabinets with In-Row Coolers and Air conditioning Units in a Modular Data Center 30

2.2 Failure Scenarios of Fan and Pumps and Optimization for Liquid Cooling 32

2.3 Effect of Raised Inlet Air Temperature on Cooling Efficiency of Hybrid Cooled Server 35

2.4 Effect of Raised Inlet Coolant Temperature on Cooling Efficiency of Hybrid Cooled Server 36

2.5 Total Cost of Ownership (TCO) Analysis for Air and Liquid Cooled Data Center for Increasing Cooling Efficiency of Data Center 38

Chapter 3 Air Cooling: Room Level and Rack Level 43

3.1 Optimal Design and Modeling of Server Cabinets with In-Row Coolers and Air Conditioning Units in a Modular Data Center 43

3.1.1 Data Center Description 44

3.1.2 Description of MEC Cabinet 46

3.1.3 Boundary Conditions 47

3.1.4 Case Studies 49

3.1.5 Without Containment and In-row Coolers for MEC Cabinet 51

3.1.6 With Containment and In-row Coolers for MEC Cabinet 53

3.1.7 Reduced Cooling Capacity of External ACUs 55

3.1.8 Air Flow Optimization 57

3.1.9 Variable Air Flow Rate from In-Row Coolers 62

3.1.10 Failure Scenarios for In-row Coolers 63

3.1.11 Failure Scenario-1 63

3.1.12 Failure Scenario-2 65

Chapter 4 Hybrid Cooling: Server Level 67

4.1 Server Under Study 67

4.2 Effect of Raised Inlet Coolant Temperature 69

4.3 Effect of Raised Inlet Air Temperature on Air Cooler Server 70

4.4 Effect of Raised Inlet Air Temperature on Hybrid Cooler Server 71

4.5 Numerical Analysis 72

4.5.1 Modeling and Validation 72

4.5.2 CFD Results 74

4.5.3 Discussion 78

4.6 Experimental Analysis of Raised Inlet Temperature for Hybrid Cooled Server 79

4.6.1 Experimental Setup 80

4.6.2 Single Server in Environmental Chamber 83

4.6.3 Server on Top in Environmental Chamber 86

4.6.4 Power Consumption 89

Chapter 5 Flow Network Analysis: Rack and Room Level 91

5.1 Governing Equations 91

5.2 FNM and Results 92

Chapter 6 Total Cost of Ownership (TCO) Analysis for a Hybrid Cooled Data Center 98

6.1 TCO model 99

6.2 Assumptions 102

6.3 Case Studies and Results 103

Conclusion 109

6.4 Optimal Design and Modeling of Server Cabinets with In-Row Coolers and Air Conditioning Units in a Modular Data Center 109

6.5 Raised Inlet Temperature of Air and Coolant for Hybrid Cooled Server........110

6.6 One Dimensional Flow Network Analysis 111

6.7 Total Cost of Ownership (TCO) Analysis for Hybrid Cooled Data Center 112

References 113

Biographical Information..136

List of Illustrations

Figure 1 Multilevel energy efficiency enhancement and thermal management of Datacenter [7]... 21

Figure 2 The progress on power, clock frequency, number of cores and transistors in microprocessors over the last 42 years. 25

Figure 3 Air Cooled 2U Two-Socket Server Power Trends [16] 26

Figure 4 Schematic of Air-Cooled Data Center.. 27

Figure 5 Typical Liquid Cooled Data Center with Chiller and Cooling Tower ... 27

Figure 6 Heat Transfer Coefficient Limitations for Different Cooling Technologies [22].. 28

Figure 7 Schematic (Isometric View) of the Data Center Containing It Equipment Racks, ACUs, and In-Row Coolers. 45

Figure 8 Top View of Shelter Showing Modular Equipment Controller (MEC) Cabinet Showing Racks, Servers, and Ducts with Inlet Vent Openings. . 46

Figure 9 Isometric View of MEC Cabinet with 3 Racks and Vents for Guiding the Air flow.. 47

Figure 10 Configuration-1: 11 Servers per Rack in MEC Cabinet (4.125KW/Rack) 50

Figure 11 Configuration-2: 21 Servers per Rack in MEC Cabinet (7.875 KW/Rack) 50

Figure 12 Mesh Sensitivity Analysis 51
Figure 13 Temperature Contour for Without Containment for MEC Cabinet for Configuration -1. 52
Figure 14 Temperature Contour Plot for Without Containment for MEC Cabinet for Configuration-2. 53
Figure 15 Temperature Contour Plot Containment for With for MEC Cabinet for Configuration -1. 54
Figure 16 Temperature Contour Plot for With Containment for MEC Cabinet for Configuration -2. 55
Figure 17 Temperature Contour Plot at the Height of Maximum Temperature for with Containment for MEC Cabinet for Configuration-2 56
Figure 18 Streamlines Showing Flow Pattern and Temperature of Supply and Return Air for External ACU and Outlet Air from the Existing Legacy Racks. 57
Figure 19 The Location and Vent Opening Areas for Ducts on Both Sides of In-Row Cooler 58
Figure 20 Dimensions and Numbering of the vents at the front and rear for rack at the middle in MEC Cabinet. 59
Figure 21 Mean Inlet and Outlet Temperature of IT Equipment With full opening for all vents (1, 2, 3, and 4) 60

Figure 22 Mean Inlet and Outlet Temperatures for 100% (front) and 50% (rear) Vent Opening Areas of the Two Ducts for Middle Rack. 61
Figure 23 Mean Inlet and Outlet Temperatures for 64%(front) and 32%(rear) Vent Opening Areas of the Two Ducts for Middle Rack 61
Figure 24 Mean Outlet Temperatures and Flow Rate for Racks (I9, I15, I21) inside MEC for Different Air Flow Rate. 62
Figure 25 Fan Failure of single in-row cooler (24.62KW): Doors of MEC are closed 64
Figure 26 Mean Inlet and outlet temperature of IT equipment for Failure Scenario-1.. 64
Figure 27 Fan Failure of single in-row cooler (12.34 KW) while doors for MEC are closed 65
Figure 28 Mean Inlet and outlet temperature of IT equipment for Failure Scenario-2.. 66
Figure 29 Hybrid and Air Cooled 1U Server. [107] 68
Figure 30 (a) Isometric View of Server (b) Validation of Resistance Curve of CFD and Experiment. 74
Figure 31 Component temperatures at different inlet air temperatures (5 fans at 3450 rpm).. 75

Figure 32 Component temperatures at different inlet air temperatures (5 fans at 7000 rpm). 76

Figure 33 Contour Plot for surface temperature at 3450 RPM for 25˚C 77

Figure 34 Contour Plot for surface temperature at 3450 RPM for 45˚C 77

Figure 35 Schematic of Experimental Setup for Testing Hybrid Cooled Server in Environmental Chamber 82

Figure 36 Two Scenarios for Experimentation Inside the Environmental Chamber 83

Figure 37 CPU Temperatures for Single Hybrid Cooled Server in Environment Chamber for max. utilization of CPUs and Memory and Variation of Fan PWM: (a) 40% (b) 70% (c) 100% 84

Figure 38 DIMMs Temperatures for Single Hybrid Cooled Server in Environment Chamber for max. utilization of CPUs and Memory and Variation of Fan PWM: (a) 40% (b) 70% (c) 100% 85

Figure 39 PCH temperature for Max. CPU and Memory Utilization at different inlet air temperature and fan PWMs (40%, 70%, 100%) 86

Figure 40 CPU Temperatures for Server on top in Environment Chamber for max. utilization of CPUs and Memory and Variation of Fan PWM: (a) 48% (b) 75% (c) 100% 87

Figure 41 DIMMs Temperatures for Single Hybrid Cooled Server in Environment Chamber for max. utilization of CPUs and Memory and Variation of Fan PWM: (a) 48% (b) 75% (c) 100% 88

Figure 42 PCH temperature for Max. CPU and Memory Utilization at different inlet air temperature and fan PWMs (48%, 75%, 100%)................................. 89

Figure 43 Server (IT) Power Consumption for (a) Single server (b) Server on top inside the Environmental Chamber.. 90

Figure 44 Rack Setup for FNM and Server Loop with cold plates, QDs connected to Rack Manifolds.. 93

Figure 45 Pressure-drop and thermal resistance curve generated for the rack 94

Figure 46 Caloric Thermal resistance curve generated for the rack 94

Figure 47 Liquid Cooling loop of a data center with 4 racks (34 servers/rack) ... 95

Figure 48 Flow resistance Curve for Data Center Cooling Loop with 4 Racks ... 96

Figure 49 Overview of Cost Model 99

Figure 50 Relative TCO of Different Kind of Cooling Technology with Respect to CRAC.. 104

Figure 51 Percentage of costs for infrastructure, maintenance, power, network equipment and server acquisition with (a) CRAC and (b) IDEC 104

Figure 52 Relative contribution of costs for infrastructure, maintenance, power, network equipment and server acquisition with CRAC, IRC, OCU, BCU and IDEC 105
Figure 53 Relative TCO of Different Kind of Cooling Technology with Respect to CRAC.. 106
Figure 54 Percentage of costs for infrastructure, maintenance, power, network equipment and server acquisition with (a) CRAC and (b) LC................ 106
Figure 55 Relative contribution of costs for infrastructure, maintenance, power, network equipment and server acquisition with CRAC, RDHX, OCU, LC and IDEC 107
Figure 56 Relative TCO of Different Kind of Cooling Technology with Respect to CRAC when PUE for LC is increased. 108

List of Tables

Table 1 ASHRAE Air Cooling Guidelines [8] 22

Table 2 ASHRAE Liquid Cooling Guidelines... 23

Table 3 Boundary Conditions Applied for Numerical Analysis........................... 48

Table 4 Brief Summary of Components and Cooling in Server [108] 68

Table 5 Cooling Power Consumption vs IT Power Consumption[109] 71

Table 6 Cooling power for the liquid cooling loop for 4 racks and pPUE values 97

Nomenclature

ρ	Density of Fluid (kg/m^3)
Q	Volumetric Flow rate (m^3/s)
S_{CR}	Quantity added to denote the departure from curve to linear variation
R	Slope from the PQ curve
P	Pressure (N/m^2)
Nu	Nusselt Number
Re	Reynold's Number
Pr	Prandtl Number
K	Loss co-efficient
A	Flow Area (m^2)
C	Constant
C_{sqm}	Cost of land and building per square meter ($/month)
A_{rack}	Area of Rack (m2)
N_{rack}	Number of Racks
$K_{occupancy}$	Factor ratio of total area to IT area
$SPUE$	Server PUE (ratio of IT Energy to useful server energy)
P_{server}	Power of Server

P_{net}	Power of Network Equipment
$C_{cp,w}$	Cooling infrastructure acquisition cost per watt
$T_{building}$	Building depreciation in years
$T_{cooling}$	Cooling depreciation in years
N_{server}	Number of Server
C_{server}	Cost of Server Acquisition
T_{server}	Server depreciation in years
OR	Online-rate
$C_{server-v}$	Lumped Server cost from vendor
$N_{server-IT}$	Number of on-line servers
N_{comp}	Number of Component
C_{comp}	Cost of Component
$C_{core-node}$	Cost per Core Node
$C_{netperrack}$	Cost of Network Equipment per Rack
T_{core}	Core/cable depreciation in years
$T_{net-rack}$	Depreciation for Network equipment inside the rack in years
C_{e-KWh}	Electricity cost ($/KWh)
ARR_{server}	Annual Replacement Rate for server

$C_{rep-cost}$	Cost of replacement for components
AFR_{comp}	Annual Failure rate for components
$T_{warranty}$	Period of warranty in years
C_{labor}	Cost of labor ($/hr.)

Chapter 1

Introduction

Data centers are infrastructures or spaces containing continuously operating servers, racks, and IT equipment for computing, storage, and network. The heat generated through the usage of IT hardware requires cooling for ensuring uninterrupted service, high performance, and long-term reliability. According to the ASHRAE TC 9.9 2011, average power consumptions for IT equipment and cooling (power and related infrastructures) are around 50% and 45% [1]. In 2018 [2], it was estimated that global data center energy use rose to 205 TWh or around 1% of global electricity consumption. Some of the world's largest data centers can each contain many tens of thousands of IT devices and require more than 100 megawatts (MW) of power capacity—enough to power around 80,000 U.S. households (U.S. DOE 2020) [3]. Power Usage Effectiveness (PUE), one of the metrics to measure to determine the efficiency of a data center [4], is the ratio of energy consumption of IT equipment compared to total energy consumption in a data center. In a recent report, the PUE is reported as 1.2 for hyperscale data centers with improved cooling [5]. Traditionally IT equipment in data centers is cooled by air with or without containment. There have been many research works conducted on improving total cooling power consumption and improving cooling efficiency through various methods. To meet the limitations of air-cooling for high power

density IT equipment and avoid critical issues, hybrid cooling can be employed with liquid cooling to the high heat-generating components. Dividing the heat load thus helps to improve the cooling efficiency by reducing the amount of heat load on air-cooling. This paper discusses the options to improve cooling efficiency by providing increased inlet air temperature. Providing proper inlet air temperature can also reduce the total cost for cooling. The conventional method of calculating the benefit of higher operational temperature is just to find the balance between the IT power consumption and IDC cooling energy savings [6].

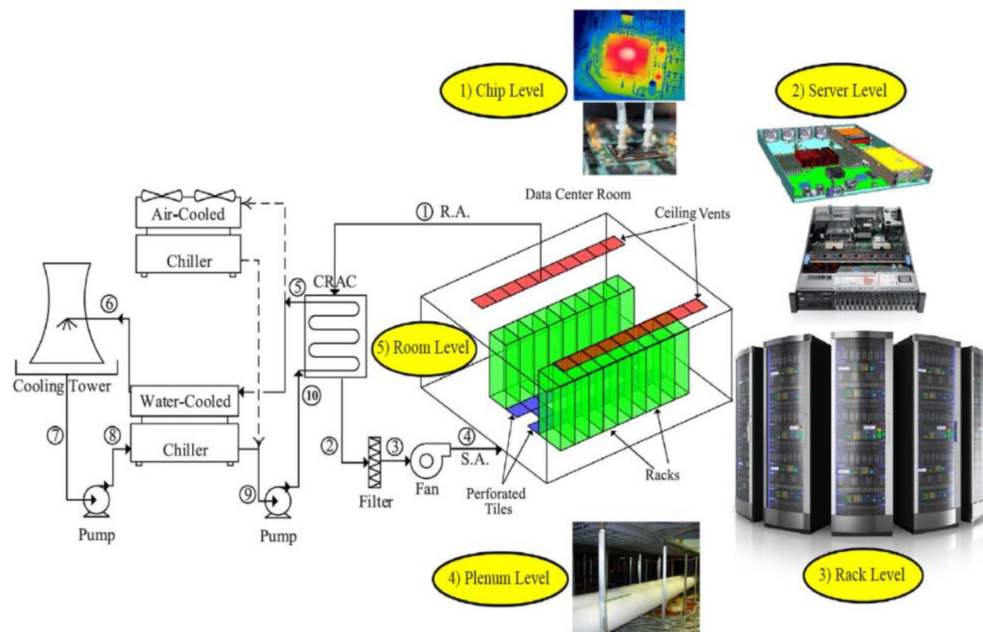

Figure 1 Multilevel energy efficiency enhancement and thermal management of Datacenter [7]

1.1 ASHRAE Air Cooling Guidelines

American Society of Heating, Refrigeration and Air-Conditioning Engineers (ASHRAE) TC 9.9 chapter has published codes, guidelines, and standards for air cooling as well as liquid cooling.

Table 1 ASHRAE Air Cooling Guidelines [8]

Class[a]	Equipment Environmental Specifications for Air Cooling						
	Product Operations[b,c]					Product Power Off[c,d]	
	Dry-Bulb Temperature[e,g] ˚C	Humidity Range, Non-Condensing[h,i,k,l]	Maximum Dew Point[k] ˚C	Maximum Elevation[e,j,m] m	Maximum Temperature Change[f] in an Hour (˚C)	Dry-Bulb Temperature ˚C	Relative Humidity[k] %
Recommended (Suitable for all 4 classes)							
A1 to A4	18 to 27	-9˚C DP to 15˚C DP and 60% RH					
Allowable							
A1	15 to 32	-12˚C DP & 8% RH to 17˚C DP and 80% RH[k]	17	3050	5/20	5 to 45	8 to 80
A2	10 to 35	-12˚C DP & 8% RH to 21˚C DP and 80% RH[k]	21	3050	5/20	5 to 45	8 to 80
A3	5 to 40	-12˚C DP & 8% RH to 24˚C DP and 85% RH[k]	24	3050	5/20	5 to 45	8 to 80
A4	5 to 45	-12˚C DP & 8% RH to 24˚C DP and 90% RH[k]	24	3050	5/20	5 to 45	8 to 80
B	5 to 35	8% to 28˚C DP and 80% RH[k]	28	3050	NA	5 to 45	8 to 80
C	5 to 40	8% to 28˚C DP and 80% RH[k]	28	3050	NA	5 to 45	8 to 80

Based on the extensive study over the years, the established classification provides a set of classes for IT equipment and their respective operational envelope. The table below shows the classes and the temperature and humidity range for recommended and allowable zones.

1.2 ASHRAE Liquid Cooling Guidelines [9]

For liquid cooling, the classification is based on primary loop configuration and inlet temperature to the facility. The classes are described as W1-W5. The table below shows the details of classification.

Table 2 ASHRAE Liquid Cooling Guidelines

Classes	Typical Infrastructure Design		Facility Supply Water Temp (C)	IT Equipment Availability
	Main Cooling Equipment	Supplemental Cooling Equipment		
W1	Chiller/Cooling Tower	Water-side Economizer Chiller	2 – 17	Now available
W2			2 – 27	
W3	Cooling Tower	Chiller	2 – 32	Not generally available, dependent on future demand
W4	Water-side Economizer (with drycooler or cooling tower)	Nothing	2 – 45	
W5	Building Heating System	Cooling Tower	> 45	Specialized systems

The cooling classes are chosen for the high inlet temperature of coolant entering the building and choice cooling units (chillers, cooling tower, economizer etc.).

1.3 Power Consumption and Data center Efficiency

The power of the microprocessors has been increasing with the invention new technology nodes for transistors. Looking back from the start of 1970, the

power growth has been proportional to the rise of clock frequency. Denard Scaling [10] suggests the power density to be similar for increase in number of transistors per generation and increasing the clock frequency which allowed the manufacturer to decrease or keep the same footprint of processor but have gain in performance without causing extra power consumption. During the time around 2003, the scaling broke down as the excessive increase of clock frequency became difficult and single core processors has transformed into multi-core processors. Also in small area, the leakage current can pose thermal issues leading to thermal runaway and increase energy cost [11]. After the end of Dennard's scaling, the next period is term as Amdahl's law [12] which is used by multiple processors for parallel computing to predict the theoretical speedup. Even with multi-core processors (CPUs and GPUs), a certain portion of the chip is powered off and the percentage increases with decrease of transistor gap size. This is known as dark silicon[13] which makes the multi-core scaling power limited. But the progress of putting more transistors is on the increase and number of cores are also increasing, while the frequency and power are flattening out. As a result, there is need for new language and architecture (such as Domain Specific Language and Architecture) [14]. A brief overview of the progress over the last 42 years is shown in Figure 2.

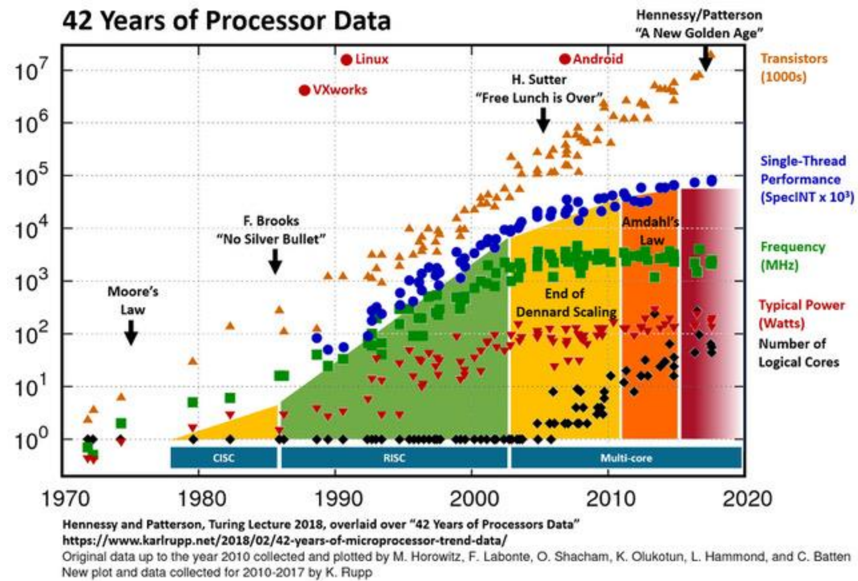

Figure 2 The progress on power, clock frequency, number of cores and transistors in microprocessors over the last 42 years.

Traditionally, air cooling has been used in the data center cooling for a long time. But due to limitations for air cooling and operating conditions inside a data center, other cooling technologies are adopted. Liquid cooling is not a new technology, and it has been extensively used and developed for high heat generating components. From early days of Bi-polar circuit technology (early 1980s) liquid cooling has been used. Later arrival of Complementary Metal Oxide Semiconductor (CMOS) by 1990s has made the heat flux lower and air cooling has become the cheap and feasible way of cooling semiconductor devices [15]. But over the years the number of transistors is increasing in the same footprint of processors with increase in performance for each generation. Heat dissipation is still an issue for the high package density and liquid cooling as an alternative to air

cooling is appreciated for cooling high powered processors especially in hyperscale data centers. The typical and expected power consumption per rack can be seen from the Figure 3.

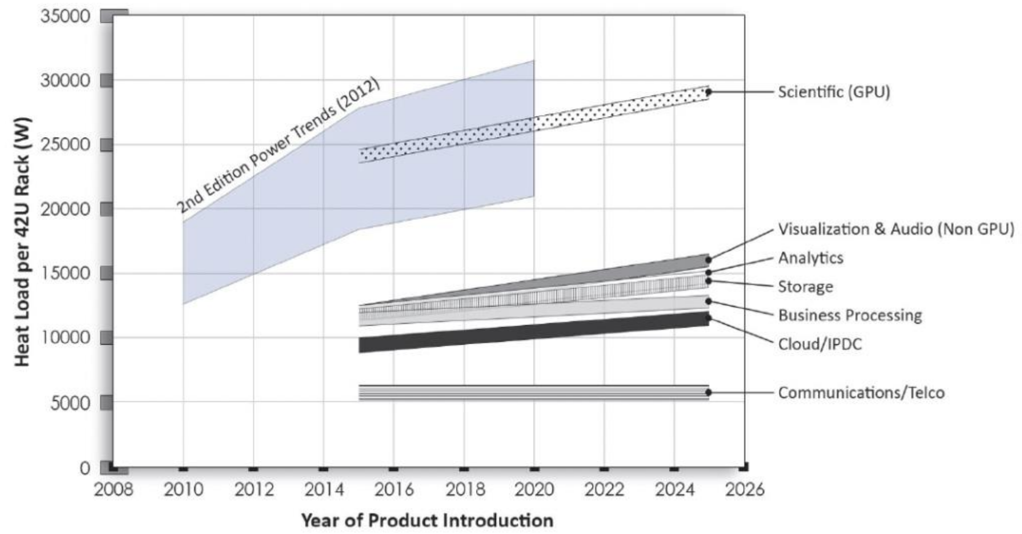

Figure 3 Air Cooled 2U Two-Socket Server Power Trends [16]

Typically, with air cooling the data center is equipped with Computer Room Air Conditioning (CRAC) or Computer Room Air Handler (CRAH) units [17]. There is raised or non-raised plenum and hot and cold aisle containment to contain the hot and cold air and guide the supply air from the CRAC/CRAH to rack and the return air from the racks again to CRAC/CRAH units. The difference between the CRAC and CRAH is that CRAC cools the air by refrigerant-based system with outdoor condenser units whereas the CRAH uses the facility water supply in liquid to air heat exchanger to cool the return air from the racks. There are other methods

of indirect air cooling which uses liquid to air heat exchanger closer to the racks such as Rear Door Heat Exchanger (RDHX)[18], Sidecar Heat Exchanger (SCHX)[19], top and bottom located cooling units (TCU, BCU) [20] [21] inside a rack in a data center to manage the high heat loads.

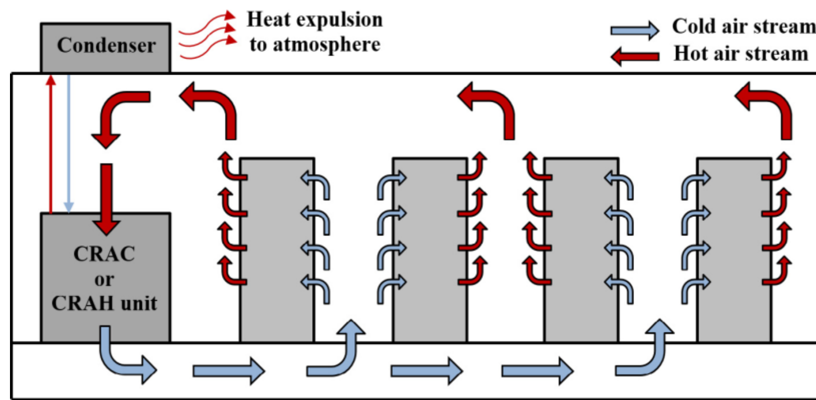

Figure 4 Schematic of Air-Cooled Data Center

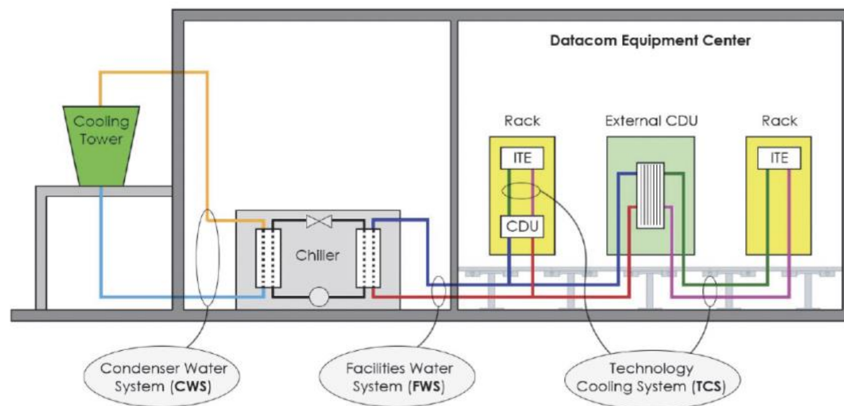

Figure 5 Typical Liquid Cooled Data Center with Chiller and Cooling Tower

The use of liquid cooling in a data center can categorized into two broad classes depending on the interaction of coolant with the surface of electronics:

direct and indirect liquid cooling [22]. Direct cooling refers to the cooling technologies where coolant comes in direct contact with the electronics and indirect liquid cooling uses an intermediary heat exchanger such as cold plate to remove the heat from the processor to the coolant. As such, indirect liquid cooling includes single-phase[23] and two-phase cold plates [24] [25], heat pipes[26], vapor chamber[27]. On the other hand, direct liquid cooling includes immersion cooling [28], pool boiling[29], submersed jet impingement[30], spray cooling [31] etc. There are heat transfer limitations with each kind of cooling technologies such as in the heat transfer co-efficient shown in Figure 6.

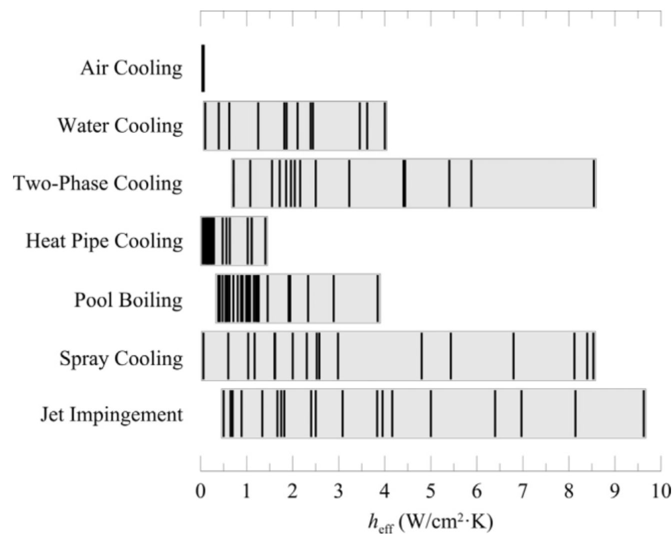

Figure 6 Heat Transfer Coefficient Limitations for Different Cooling Technologies [22]

There has been continuous drive to increase the cooling power consumption and optimizing each technology for increasing cooling efficiency. For example, for air cooling plenum height[32], depth of hot/cold aisle [33], ducting under the

plenum, modular heat exchanger in pod level deployment[20], predicting the air flow pattern[34] [35], controlling, and quantifying particulate contaminates[36], corrosion [37] etc. In liquid cooling, there has been tremendous amount of research on the improvement of cold plate design[38], [39], comparison of cold plate[40], system level design[41], use of nanoparticles [42], rack level, flow network modeling[43], warm water cooling [44], wetted material and coolant degradation[9] and corrosion detection and control[45], increasing the cooling efficiency by proper choice of configuration on primary side[46]. For immersion cooling, the pumping power is very low[47] and cooling power is reported to be very low but there is a concern for material reliability[48]. There has been research going on the material compatibility and proper handling guidelines.

The green grid has defined a metric called Power Usage Effectiveness (PUE) [49]which is extensively used to measure power consumption and energy efficiency. A closed form of PUE, also known as partial PUE (pPUE) is used when the domain becomes smaller inside the data center. There are energy metrics such as Data Center Energy Productivity (DCeP) [50] invented by green grid to calculate the net useful work based on the consumed energy. The definitions are given below.

$$PUE = \frac{Total\ Facility\ Energy}{IT\ Equipment\ Energy} \tag{1}$$

$$DCeP = \frac{Useful\ Work\ Produced}{Data\ Center\ Energy\ Consumed\ to\ Produce\ the\ Work} \tag{2}$$

Chapter 2

Literature Review

This section includes the literature review for the optimal design of server cabinets with liquid to air heat exchangers for a modular data center and methods to increase the cooling efficiency of a hybrid cooled data center using dynamic control and raised inlet conditions for both liquid and air.

2.1 Optimal Design and Modeling of Server Cabinets with In-Row Coolers and Air conditioning Units in a Modular Data Center

The operating temperature and humidity for cooling IT equipment in a data center are standardized by ASHRAE and Network Equipment Building Standards (NEBS) in collaboration with manufacturers and researchers. The recommended zone for air temperature and humidity inside a data center according to ASHRAE TC 9.9 is 18-27 °C and 60% maximum relative humidity (-9 °C to 15 °C Dew Point) [8]. There are other zones (A1, A2) and allowable zones with limited operating hours. The most widely used method for controlling hot-air recirculation and cold-air bypasses are hot aisle containment (HAC) and cold aisle containment (CAC). In recent years, many novel cooling solutions were successfully launched to further improve the Power Usage Effectiveness (PUE) in data centers, such as the liquid cooling systems, the rack-level cooling with heat exchanger, and hybrid cooling with heat pipes. The traditional room cooling system can be replaced with

rack cooling to improve cooling efficiency. Rack and room level simulations and experiments were also conducted based on the location of the Air Conditioning Unit (ACU) such as Computer Room Air Handling (CRAH) or Computer Room Air Conditioner (CRAC), positioning of racks. The heat exchanger is the key equipment in the enclosed rack-level cooling system, and the thermo-hydraulic performance of the crossflow water-and-air heat exchangers was investigated in many application areas. In a minimum footprint to cool the high heat generating IT equipment, the rear door heat exchanger can be a solution. Parametric and experimental studies had been done to improve the cooling capacity and utilize the facility water in the secondary loop. Room-level cooling for unmanaged high-density racks can cause destabilizing effects such as lower cooling efficiency, loss of cooling redundancy, hot spots, thermal shutdown, and circuit overload [51]. It has also been shown that how row-based data center cooling works with a Rack Cooling Index (RCI) and Return Temperature Index (RTI) [52]. The advantages of the row and rack-oriented cooling architectures for data centers were also described comparing the balance of high predictability, high power density, and adaptability, at the best overall Total Cost of Ownership (TCO). Rack level modification, use of snorkels, blanking panels, and cabinet chimneys have been studied previously to improve airflow management and prevent mixing of hot and cold air.

2.2 Failure Scenarios of Fan and Pumps and Optimization for Liquid Cooling

Hybrid cooling uses liquid cooling for high heat-generating components while the rest of the components are cooled by air. Hybrid cooling coupled with warm water cooling provides provisioning for reducing cooling power and costs, which is shown in a separate study [53]. Using coolant above ambient conditions can be a viable option for cooling IT equipment taking advantage high specific heat and thermal conductivity of coolant. Characterization of hybrid liquid-air cooled servers was done in a study showing key performance indicators including both heat recovery effectiveness and thermal loss parameters [54]. But operating at high temperatures also poses the risks of affecting the operation, serviceability, or reliability of the IT equipment. Safety precautions and decisions for immediate response are necessary for the smooth operation of the servers. Analysis of failure scenarios can provide a better perspective of the situations and prevent damage to any IT equipment. A study on failure scenarios of the dry cooler in a chiller-less liquid-cooled data center showed parametric analysis with a dynamic model [55]. It is also found that, by decreasing the external fluid flow rate, the safety time can be extended. Another paper by Alkharabsheh et al [56] suggested the failure scenarios of liquid cooling in a data center. The time delay for CPU throttling of three types of liquid-cooled servers is experimentally investigated. The leakage

current effect during full and partial scenarios is discussed with the change server power, chip power, coolant, and chip temperature. The remedies are suggested as using an uninterrupted power supply (UPS), long lifetime of a pump, load migration, precise sensor placement, rapid live migration of load and data. A similar set of failure scenarios are investigated by Puvvadi et al [57] for the failure of the pump in the heat exchanger as well as for the single and dual pump failure. The paper suggested and demonstrated the use of task migration to other servers as fans ramp up detecting high CPU temperature in a server. This technique utilizes the time lag caused for frequency throttling of CPUs at elevated temperatures. But the optimization for latency has been studied in a different paper by the same author [58]. Similar work with load balancing for liquid cooling was also suggested by Li Li [59] to minimize power consumption. The smart cool algorithm showed a 38% efficiency improvement for a traditional data center configuration for air and hybrid cooled servers with CRAH, chiller, cooling tower, and air-side economizer on the primary side. The chip leakage power is an issue for high heat generating CPUs. Providing the required flow rate to servers with high CPU temperatures is essential which is addressed in a paper by Wei et al [60]. This paper highlighted the efficiency gain for air to the liquid heat exchanger by intelligent data-driven cooling power allocation. Full pump failure is a rare phenomenon, and it can certainly happen if there is a power outage in an emergency. Such a condition is investigated by Zavřel et al [61] and numerical modeling was performed after calibration with

real-time data for a full failure scenario of pumps for finding possible solutions such as the use of a short-term energy backup plan for pumps and the use of additional storage tank in the loop. A whitepaper from Intel [62] also suggested the use of a low-cost thermal storage tank in the event of chiller cooling failure for an electric power outage. The paper successfully showed case studies on the efficient use of storage tanks on the primary side to run the servers inside the data center on UPS without causing overheating. Another paper by Sahini et al [44] showed that reduced flow rate at different temperatures of coolant can help to keep the junction temperature within limitations. A mini-rack with 4 servers was tested with variable CPU utilization for elevated coolant temperature at two different pump speeds for centralized cooling. Approximately 55% reduction of total cooling power was achieved from the experimental findings. A similar study on the server level for fan and pump failure was experimented by Chowdhury et al [63]. Possible scenarios for the partial and full failure of fans and pumps are experimentally investigated and redundancy for cooling power was quantified with a scope of saving 46% of cooling per server. A novel dynamic flow control method on rack-level was suggested by Kasukurthy et al [64]. Approximately 64% of pumping power can be saved by modulating flow rate based on the temperature of coolant with a pPUE range of 1.007-1.01. Scaling up to the data center level, Parida et al [65] showed a servo control algorithm to control the inlet coolant temperature to the racks by controlling the recirculation valves. The algorithm provided an energy saving of

25% and over 90% as compared to the refrigerant-based cooling system of the data center. The use of different PID controllers for pumps is discussed in [66], [67]. The lumped parameter method is used with different control algorithms for both papers.

2.3 Effect of Raised Inlet Air Temperature on Cooling Efficiency of Hybrid Cooled Server

The recommended and allowable envelopes are provided by ASHRAE TC 9.9 for the server inlet temperature and humidity in a data center. Chiller less data center results in higher inlet temperature to rack and IT equipment. The reliability and thermal management for inlet temperature has been studied in a paper. An experimental for a 1 MW data center suggested that only one-degree rise in the temperature set point can save 2-5% of the overall energy consumption in data centers [68]. There has been a continuous effort from the manufacturers and operators of CRAH/CRAC to control the supply air temperature for various unprecedented events. Thus, control system for on-demand cooling has been presented in a research paper with the application of high operational temperatures in data centers. It is crucial to have resilient server design and performance metric for thermal safety in the case of the high inlet conditions as with benefit in cooling efficiency server reliability should not be impacted [67]. A separate numerical analysis has shown that increasing the ambient conditions up to 35°C along with

best practices such as hot aisle/cold aisle containment, removing cable obstructions, configuring by-pass and re-circulation reduction for a CRAH based cooling system has improved data center level power savings with the use of economizers [69]. With temperature the corrosion becomes an issue. So, before choosing the high ambient with free air-cooling technology, corrosion-resistant hardware design should be checked. The ASHRAE class A3, A4 classes require the balance between the IT and cooling infrastructures [70]. Increasing inlet temperature leads to the power consumption increase per server for leakage current effect and may cause thermal runaway and degradation or damage of microprocessors. In a study, the chip leakage power has been modeled with respect to increase in inlet air temperature and reported that the COP of the data center cooling infrastructure has been affected by the leakage current. So, chip operating temperature is also factor before choosing the high inlet air temperature in a data center. This study suggests for optimum operating point between cooling efficiency and leakage current affect while increasing the inlet air temperature [71].

2.4 Effect of Raised Inlet Coolant Temperature on Cooling Efficiency of Hybrid Cooled Server

As mentioned above, there are some adverse effects from the increase of inlet air temperature of servers. Similar effect is also examined for higher inlet coolant temperature for liquid cooled components in servers. The study found that

the total data center power consumption is a function of coolant temperature, the computational state of the chip, weather factors that employ free cooling has not shown improved energy efficiency even during maximized free cooling due to additional leakage power incurred by the associated higher coolant temperatures [72]. The cooling classes for liquid cooling provided by ASHRAE liquid cooling guidelines have higher inlet conditions for liquid entering the data center operating without chillers. So, significant energy saving is expected for the elimination of chiller but the study shows that cooling energy usage was as low as 3.5% of the typical air-cooled chiller-based data center [73]. The use of increased coolant temperature for liquid cooling is also known as warm water cooling. In a separate study, warm water cooling has been applied where the return water is as high as 95°F and the hot return water is used as a primary heating source for building for energy reuse [74]. Aquasar project shows the experimental and analytical studies conducted to show that the PUE and ERE can be improved with reduced use or elimination of chiller and use of warm water cooling of data centers [75]. A comprehensive study on liquid cooling design guidelines has been presented for building-supplied warm water-cooled IT at 15 national laboratory sites and the total cost of ownership calculations that showed reduced capital as well as ongoing energy consumption costs [76] . Based on the mentioned research, the high ambient inlet coolant conditions have better prospects on the performance and cooling

efficiency of liquid cooling in a data center, but precautions must be made before choosing the appropriate cooling envelope for liquid cooling.

2.5 Total Cost of Ownership (TCO) Analysis for Air and Liquid Cooled Data Center for Increasing Cooling Efficiency of Data Center

There has been tremendous work on the efficiency improvement of data center cooling and newer methods for TCO calculation were introduced by the researchers, facility owners, industry leaders. Chandrkanth D Patel [77] proposed a TCO model which takes into account the latest improvement in cooling technologies. The model gives the results based on some assumptions and best practices for increasing cooling efficiency and changing the layout of data center. W. Pitt Turner [78] emphasized on misuse of a parameter (cost per area metric) and proposed a model based on engine cost plus the cost per area. The author also advised to take initiative at an early stage based on the variations of result with the practical deployment experiences. M.K. Patterson [79] used a TCO model by considering a work cell with a bounding box around the rack to understand the rack power density properly. Layout efficiency is evaluated based on cooling cost and suggested some best practices to implement in the data center for lower TCO. Jonathan Koomey [80] suggested a simple spreadsheet method to determine the

cost and provided the model as opensource from uptime institute with precautions of application and best practices to avoid a large error. This TCO model has been extensively used by researchers and industry as a benchmarking tool considering the ease of use and availability of the model. There are also some open sources for TCO tools APC (Scheider Electric) [81] for traditional and modular data centers. Christopher G Malone [82] pointed out the performance gains by server inlet temperatures, flow rates, control mechanisms, and coupling concepts to determine the infrastructure cost structure. Cloud computing was included in the TCO model by Xinhui Li [83] and a method for calculating the TCO was explained. A web tool was developed, and the cost distribution and utilization imbalance factor were added to the model. Jose E Moreira [84] studied the effect of the size of servers (big to mid-size) based on the number of processors per server and finalized that mid-sized servers with 4 to 12 processors per server are cost-optimal. So, it was recommended to turn off the server that is not used based on workload distribution. Srini Chari [85] compared the IBM blue Gene/Q server with traditional x86 based cluster systems with Graphics Processing Units (GPUs) by the cost model developed by the uptime institute. A new parameter was introduced named RAS (reliability, availability, and serviceability) related to downtime cost considering some assumptions. To reduce the power consumption in a data center, Stijn Polfliet [86] suggested the heterogeneity of workload to run a job most efficiently in a data center. This parameter showed a driving force to increase the cost efficiency of a

data center as compared to homogenous high-end and low-end server data centers. Damien Hardy [87] provides a detailed TCO model which takes into account the environmental conditions. The model shows the trade-offs offered by different server configurations, performance variability, and ambient temperature. An interesting study on the processor core size of a 1U server was carried by Boris Grot [88] to point the consequences on the TCO model developed by D.Hardy[87]. A point of optimization was investigated and reported for scale-out processors. In another study, government and corporate data center costs are analyzed and a new TCO model is proposed by Ajay Ahuja [89]. An analytical framework was suggested by Damien Hardy [87] while taking into consideration about the design space of data center. In this study, assess tradeoffs, among other, between server configurations, performance variability, datacenter ambient temperature, and 3D processor integration are discussed. Shaoming Chen [90] investigated the maintenance costs in a hybrid cooled data center and suggested optimization of electricity and server maintenance cost by server consolidation, high inlet temperature, and sleeping time threshold. Brandon Rubenstein [91] suggested using an optimized setpoint for cold aisle by optimization of the TCO model. A metric has been suggested to identify the operational overhead and reduce server maintenance costs. Another study by Georges da Costa [92] suggested a new tool for power and capacity management with power capping and proper cooling configuration. The chiller sizing was also suggested for energy savings based on

the model. Dustin W. Demetriou [93] compared traditional air cooling, rack-level cooling by a rear door heat exchanger, and direct water cooling by cold plates by a TCO model. Based on the study it was suggested that no significant increase in cost was noticed for the adoption of liquid cooling. Sorell Vali [94] developed a TCO model for liquid-cooled IT equipment in data centers. Best-in-class air-cooled data center design has been compared to two different data center design with separate air and liquid cooling loops to identify the cost benefits for the liquid-cooled data center. Dustin Demetriou [95] again evaluated the TCO of liquid cooling by comparing a purpose-built vs retrofit liquid-cooled data center. The author showed when the electricity cost is lower energy savings are not impactful but additional cost from additional equipment increases the cost of hardware required for liquid cooling. Several authors also suggested TCO models for flash storage [96], cooling strategies [97], installation of adsorption chillers [98], using hardware acceleration [99] etc. The cooling technology is evolving in the data center owing to the limitations of previous cooling technology and the emergence of power-hungry processors. A TCO model by Yan Cui [100] showed the major components in a TCO explicitly and evaluated rear door cooling, cost plate cooling, high-efficiency power solutions, and parametric study to identify the differences and find a point of comparison. A survey [101] was conducted and presented by analyzing previous publications and available spreadsheets. The paper pointed out the TCO based on Tier Levels with some assumptions taken in the models and parameters discussed

in the paper. Other aspects such as cost related to virtual content and cost of licenses are included in a separate TCO model by Doaa Bleidy [102]. The cost of all components for power distribution are added in that model. Bob van den Berg [103] conducted a comprehensive study on the cost savings for changing network technologies (ethernet, glass fiber, plastic optical fiber). In a recent paper, Wenrui Ya [104] showed a TCO model to understand the cost of long-term data preservations, constructions and operation of a data center considering the capital and operational expenditures.

Chapter 3

Air Cooling: Room Level and Rack Level

3.1 Optimal Design and Modeling of Server Cabinets with In-Row Coolers and Air Conditioning Units in a Modular Data Center

(Reprinted with permission © 2019 ASME) [105]

The purpose this study is to determine the optimum configuration for cooling capacity of in-row coolers and wall mount air conditioning units used for modular data center. In addition to the existing low power density rack, the deployment of high-powered racks creates hot spot and recirculation inside the data center. The use of in-row cooler uses an air to liquid heat exchanger where the secondary loop carries the heat away from the data center to environment by Direct Expansion (DX) cooling or refrigeration cooling. Proper selection of cooling capacity, floor space requirement, compactness in design and customized cabinet design were performed for modular deployment of racks. The numerical analysis on the effect of raised inlet temperature per ASHARE A1 class for the IT equipment was performed in a Computational Fluid Dynamics (CFD) model developed in 6SigmaRoom[106] with the help of built-in library items for a typical small-sized non-raised facility. The efficiency and limitations of in-row coolers in thermal management of IT equipment with variation in rack heat load and containment were studied in detail. Several other aspects like a parametric study of variable opening

areas of duct, variable flow rate, and failure scenarios are studied for flexible and quick installation.

3.1.1 Data Center Description

A non-raised telecom data center is constructed in 6SigmaRoom which consists of IT equipment stacked in racks of different dimension and power density. The room dimension is 20x13x9 (ft^3). The room is cooled with two external walls mounted ACUs where condenser part is situated in the outside environment to reject the heat with DX cooling. The cabinets inside can be subdivided into two broad categories (Figure 7). One type of cabinet (existing legacy equipment racks) that uses traditional room cooling by pulling the air from the room to cool the equipment without enclosures such as HAC or CAC and the other type of cabinet named as Modular Equipment Controller (MEC) cabinet in Figure 8, which is closed or open cabinet with three 42U racks. This custom designed MEC cabinet is situated at the periphery of the room and cooled by in-row coolers and external ACUs. The cabinet is constructed with built-in items from library such as cabinet, IT equipment, solid obstructions. The required power and capacity of each rack, in-row cooler and ACU are modified for the cases studied. By bringing in new servers, the heat load increases, but footprint is limited in terms of floor space required. As a result, high temperature and hotspots are expected. To avoid hotspots, the racks

in MEC cabinet can be cooled by in-row coolers separated by ducts with inlet and outlet openings for supply and return air same as in hot and cold aisle containment.

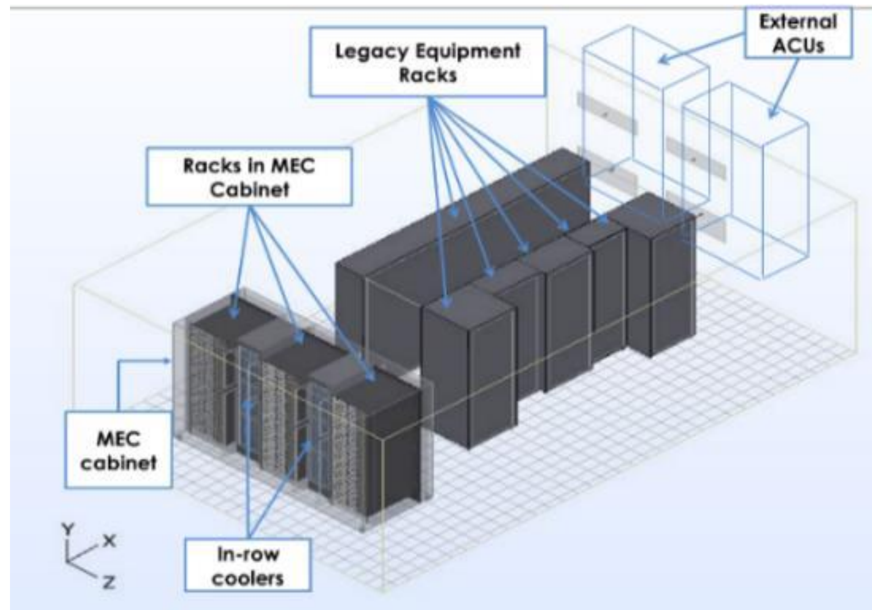

Figure 7 Schematic (Isometric View) of the Data Center Containing It Equipment Racks, ACUs, and In-Row Coolers.

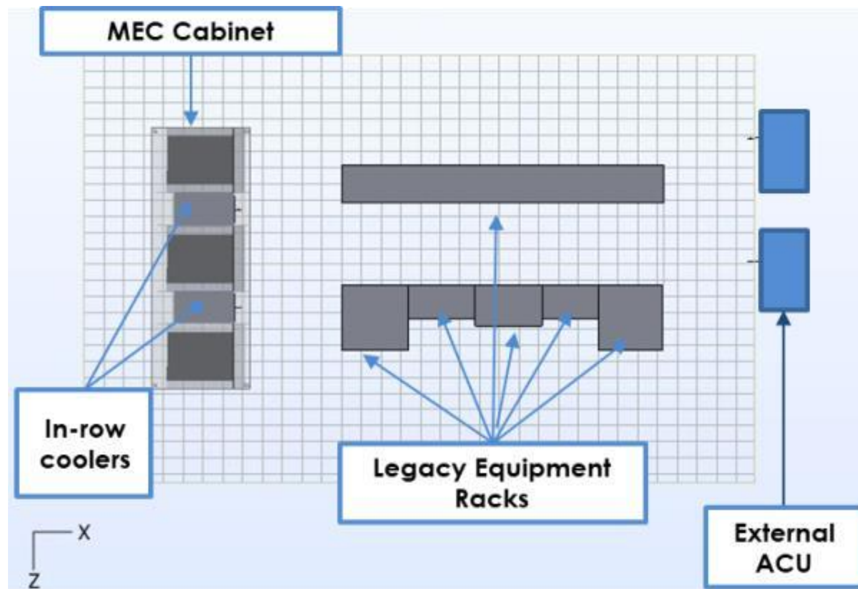

Figure 8 Top View of Shelter Showing Modular Equipment Controller (MEC) Cabinet Showing Racks, Servers, and Ducts with Inlet Vent Openings.

3.1.2 Description of MEC Cabinet

The cabinet is a custom-made enclosure for housing 3 racks with 2U servers. There are two in-row coolers situated inside the cabinet, in between the racks. The rack dimension is same as standard 42U unit rack. The doors for racks and in-row coolers can be opened and closed if needed for installing servers, maintenance, and other reasons. The cooling capacity and type of in-row coolers are selected based on required cooling capacity and flow rate requirement of the IT equipment.

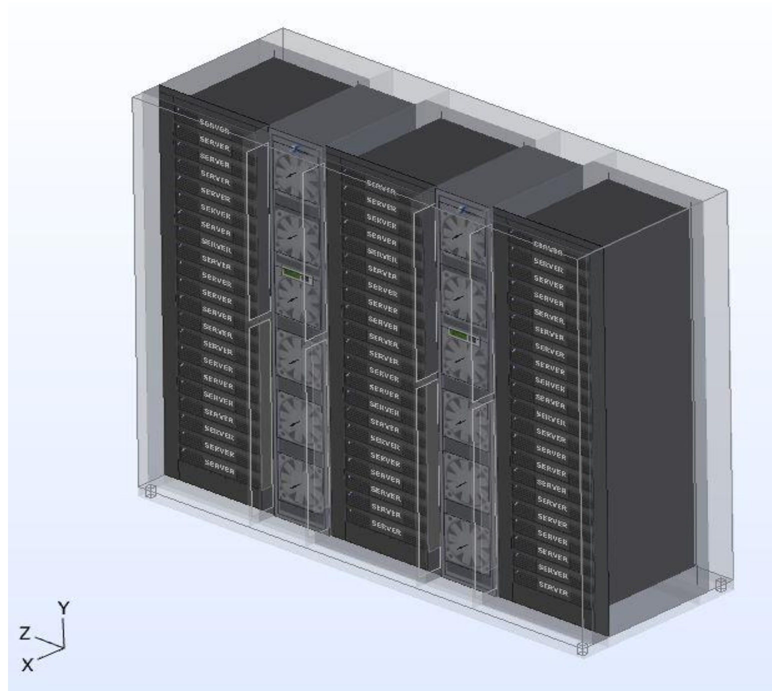

Figure 9 Isometric View of MEC Cabinet with 3 Racks and Vents for Guiding the Air flow

3.1.3 Boundary Conditions

Proper and realistic boundary conditions are needed to improve the cooling efficiency by reducing the amount of work needed to cool the air inside the data center to opt for higher Coefficient of Performance (COP) [18]. The servers and the racks were dragged and dropped from library and used as a compact model. The server when used as a black box model determines the required air flow from the energy balance equation $Q=\dot{m} C_p \Delta T$ if power and temperature rise given for forced flow condition. The air flow rate is fixed but excess flow coefficient is to default as 0.05. Racks in MEC cabinet are populated with 2U servers while legacy

equipment racks are considered as a black box model with given power and temperature rise to fix the flow. Higher inlet temperatures are applied for IT equipment considering the A1 and A2 zones recommended by ASHRAE. Maximum possible supply air temperature is chosen as 28 °C from the ACUs and 30 °C from in-row coolers as inlet to the IT equipment and the temperature rise across the servers is set for 20 °C. So, each cabinet and IT equipment were given 375 W power and constant temperature difference (ΔT=20°C) as boundary condition. When the cold aisle in the data center is contained, there is potential it will become pressurized. In this situation more air will be forced through the server than if the server was placed in open space.[19] The doors in the MEC cabinet can be opened or closed and cooling capacities of in-row coolers and external ACUs are applied as described in the table below.

Table 3 Boundary Conditions Applied for Numerical Analysis

Components	**Dimensions (ft^3)**	**Specifications**	
MEC Cabinet	6.6794x7.98x2.9 614	doors can be opened or closed	
Servers in MEC Cabinet	Depth 1.9684 ft. (600mm) Width 1.4764 ft. (450 mm) Height 2U (88.9 mm)	375 W, ΔT=20°C Forced convection Excess flow co-efficient 0.05	
Racks (3) in MEC Cabinet	6.67x1.973x2.3	21 or 11 servers per rack, 7.88KW or 4.13 each, air cooled	
Legacy Equipment racks (as black box model)	6.9975x9.6123x1.164 (1) 6.9974x2x2 (2) 6.9974x2x1.03 (2) 6.9974x2x1.25 (1)	1st Row	4KW, air cooled, front to back, ΔT=20°C
		2nd Row	0.8kW per rack, Air Cooled, front to back, ΔT=20°C

External ACU (2)	6.0833x4.33x2.9	DX cooled, 15.97 KW, 1850 CFM
In-Row Cooler (2)	6.6794x1.01x1.8	DX cooled, 12.31 KW, 1500 CFM or 24.62 KW, 2900 CFM

Solar loading is not applied as the building material is considered as an insulating material. Mesh sensitivity is also performed, and grid sizes were varied to find optimum grid setting based on overserving variations in maximum temperatures.

3.1.4 Case Studies

Two configurations of a MEC cabinet are studied with two in-row coolers and two external ACUs for the shelter. As we are using in-row coolers for the MEC cabinet the general idea is to reduce the cooling capacity needed for legacy racks. Results are compared for full and half heat load for the racks in MEC cabinet with and without containment.

The racks are given customized names as I21 (left), I15(middle), I9 (right). The configurations are given below:

1. Configuration-1: The open compute racks are filled with 11 servers (2U) with the blank panel in between each server (Figure 10). Each server has 375 W and each rack in MEC cabinet has 4.13 KW.

2. Configuration-2: The open compute racks are filled with 21 servers (2U) with the blank panel in between each server (Figure 11). Each server has 375 W and each rack in MEC cabinet has 7.88 KW

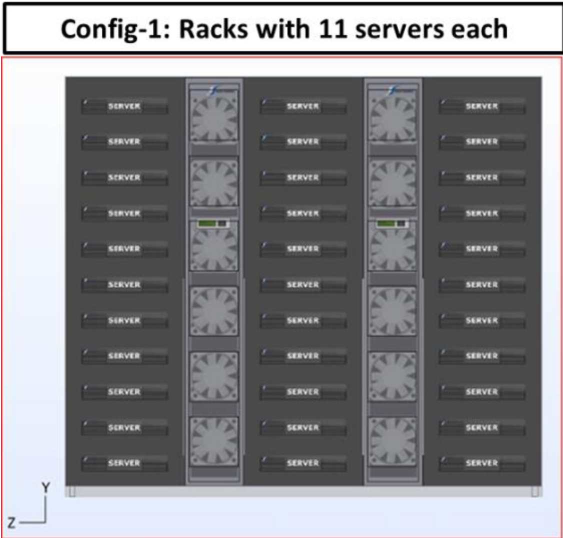

Figure 10 Configuration-1: 11 Servers per Rack in MEC Cabinet (4.125KW/Rack)

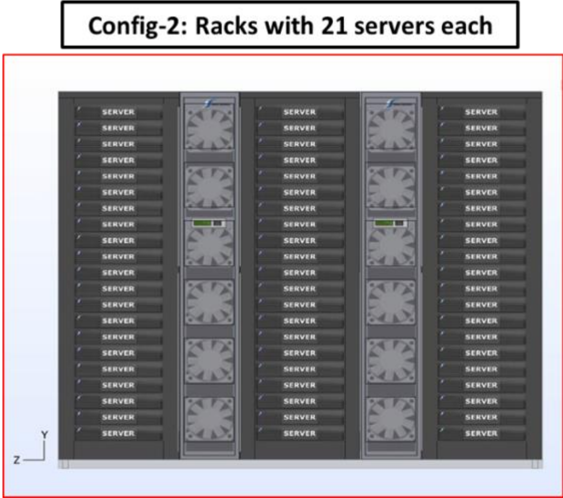

Figure 11 Configuration-2: 21 Servers per Rack in MEC Cabinet (7.875 KW/Rack)

The optimum mesh was found to be approximately 215000 cells for maximum heat load with 21 servers per rack in MEC cabinet (doors closed), two in-row coolers at (12.31 KW each) and two external ACUs (15.97KW each). Other boundary conditions are applied as described in table. The results are shown for maximum temperature in the model. Gridding is varied by changing minimum gap size and size of maximum cell. The cell count is less due to the use of the compact models from library for servers, racks, in-row coolers and ACUs (Figure 12).

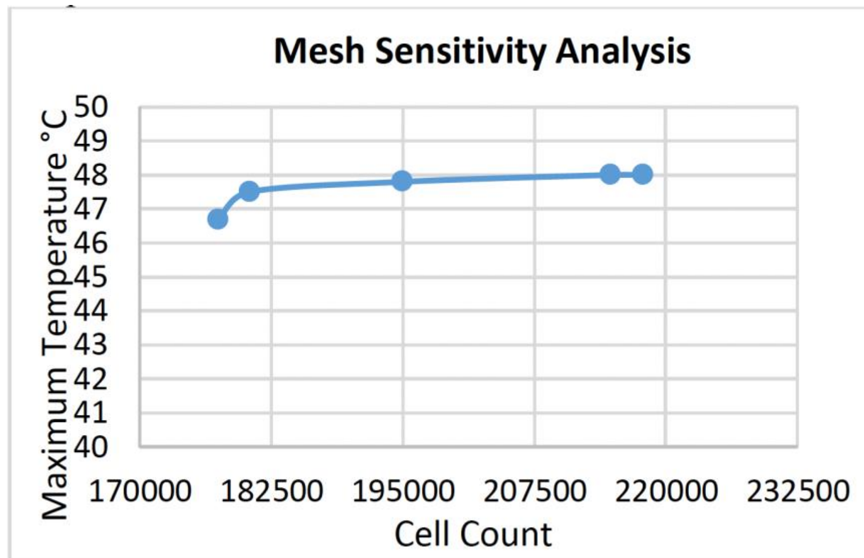

Figure 12 Mesh Sensitivity Analysis

3.1.5 Without Containment and In-row Coolers for MEC Cabinet

The doors for MEC cabinet are kept open and the rack power density is varied by populating more servers into the racks. The in-row coolers are turned off and the supply air from ACUs provides cooling to all IT equipment. Due to mixing of inlet air and the return air, the average inlet temperature for IT equipment is

increased and hotspots are generated at the outlet of IT equipment. As the rack power density is increased from 4.13 KW to 7.88 KW as external ACUs cannot manage the high heat load of the shelter. With 11 servers per rack maximum temperature rises to 60.7 °C and with 21 servers per rack the temperature rises even further to 92.4 °C which is unacceptable. The contour plots are given in Figure 13 and Figure 14 showing the rise of temperature for racks in MEC cabinet (without containment) at higher heat load.

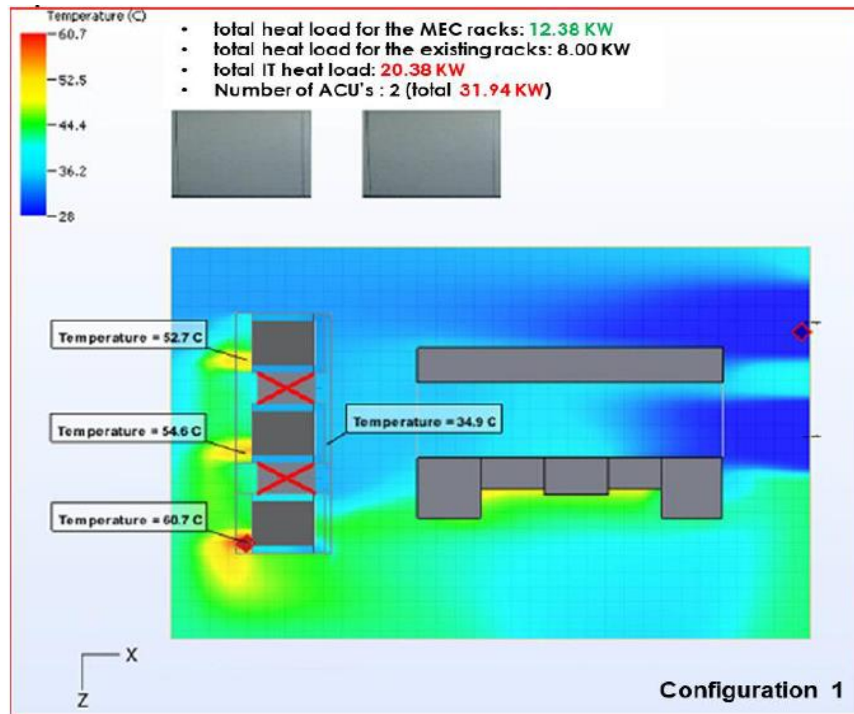

Figure 13 Temperature Contour for Without Containment for MEC Cabinet for Configuration -1.

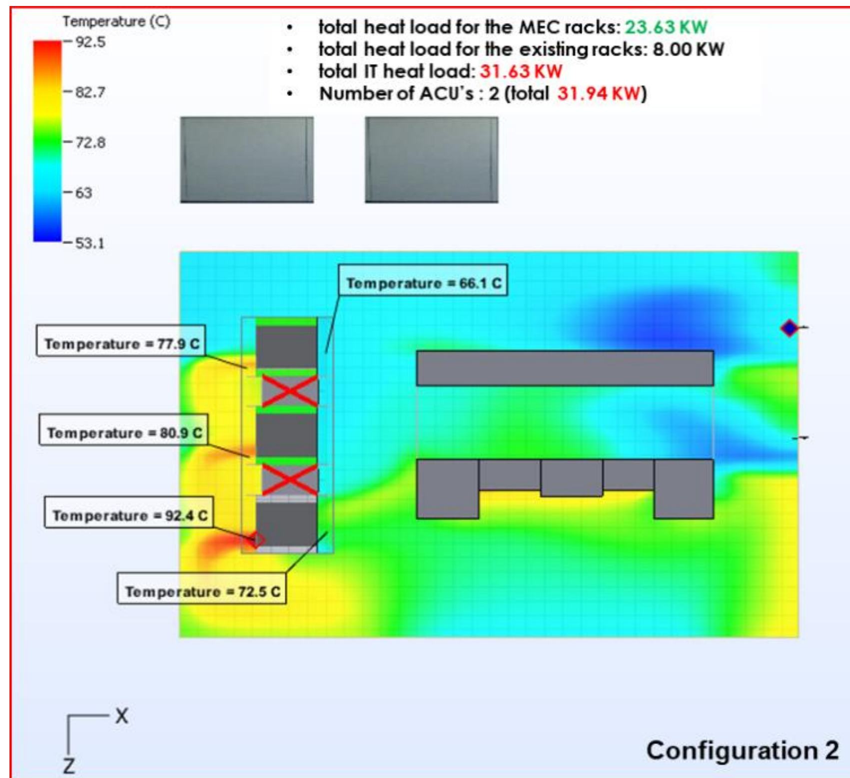

Figure 14 Temperature Contour Plot for Without Containment for MEC Cabinet for Configuration-2.

3.1.6 With Containment and In-row Coolers for MEC Cabinet

The MEC cabinet doors are closed, and the in-row coolers are turned on. The inlet and outlet air for IT equipment are separated by ducts with vent openings as an open hole. The air recirculates within the MEC cabinet and remain contained. External ACUs provides cooling to existing legacy racks. Both in-row coolers are supplying air at 30 °C. Total heating load for the data center and cooling capacities are mentioned in Figure 15 and Figure 16. The results in the contour plot for both configuration 1 and 2, show the benefit of containing the cabinet while managing

temperature rise for half and full of heat load of racks in MEC cabinet. In both configurations, it is observed that the mean outlet temperature from the IT equipment does not exceed 50 °C.

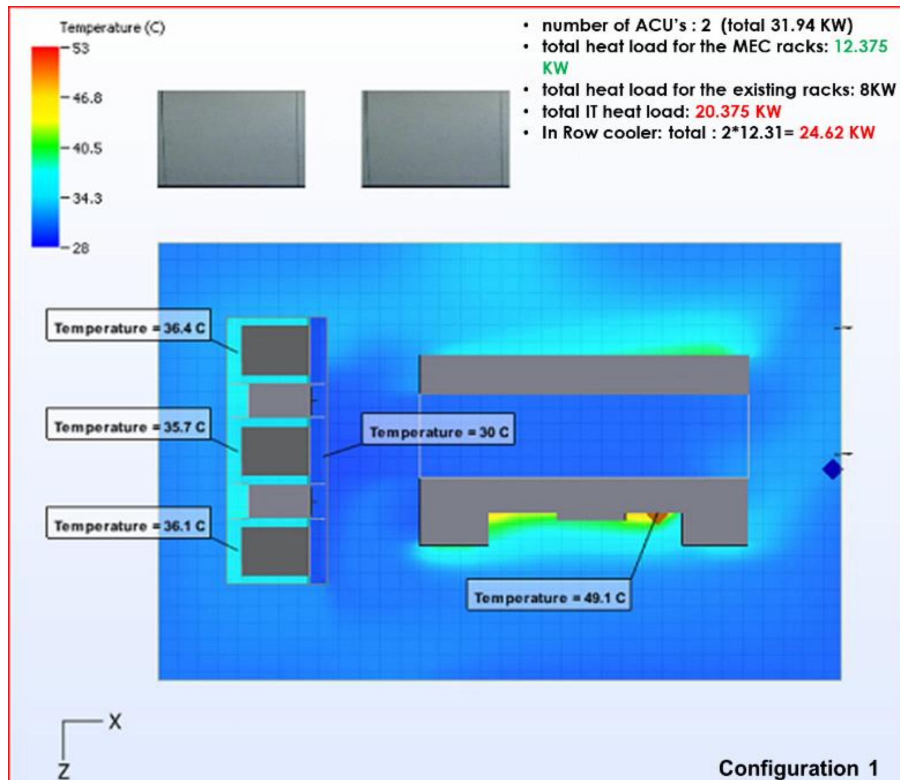

Figure 15 Temperature Contour Plot Containment for With for MEC Cabinet for Configuration -1.

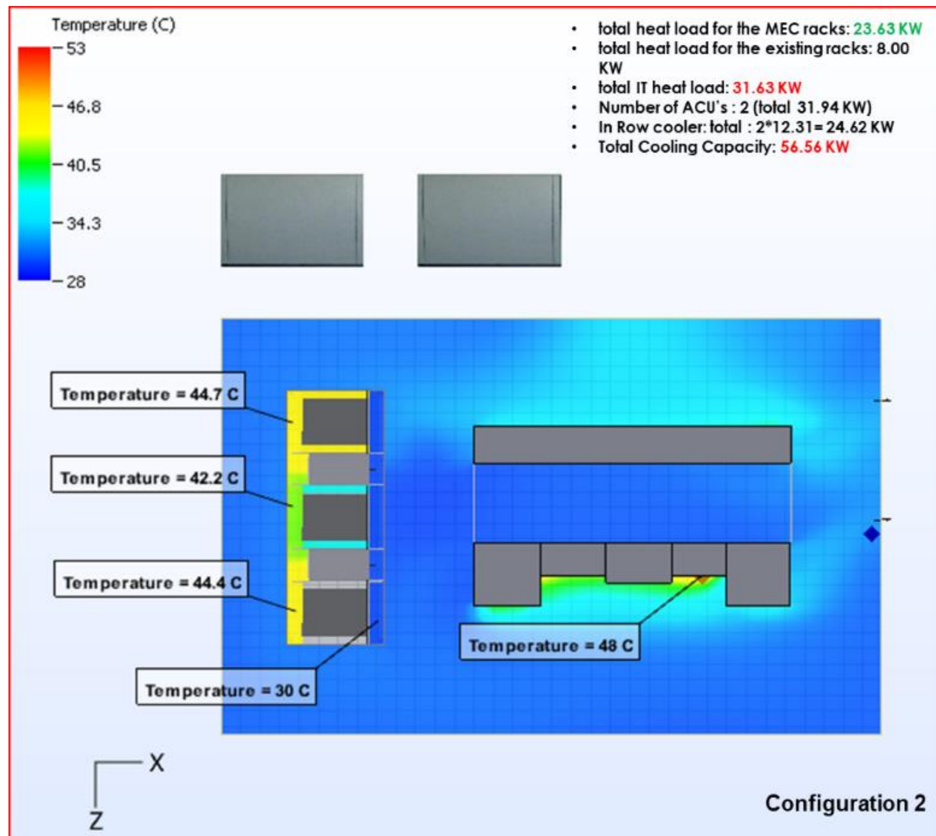

Figure 16 Temperature Contour Plot for With Containment for MEC Cabinet for Configuration -2.

3.1.7 Reduced Cooling Capacity of External ACUs

As the in-row coolers are used to cool the IT equipment inside the MEC cabinet, rest of the cabinets situated outside of the MEC cabinet can be cooled with reduced number of external ACUs with lower cooling capacity. So, one external ACU of 15.97 KW is used to cool 8 KW existing legacy racks while the two in-row coolers (12.31 KW, 1500 CFM each) provide cooling to the MEC cabinet to manage heat load of 23.63 KW. As a result, local hotspots are avoided as well as

number of external ACUs are reduced to one with a decrease of 15.97 KW in total cooling capacity. From Figure 17, it is shown that the inlet temperature for racks in MEC cabinet is 30 °C, but the outlet temperature from each rack is different as middle rack is getting more airflow from each of the in-row coolers compared to other racks.

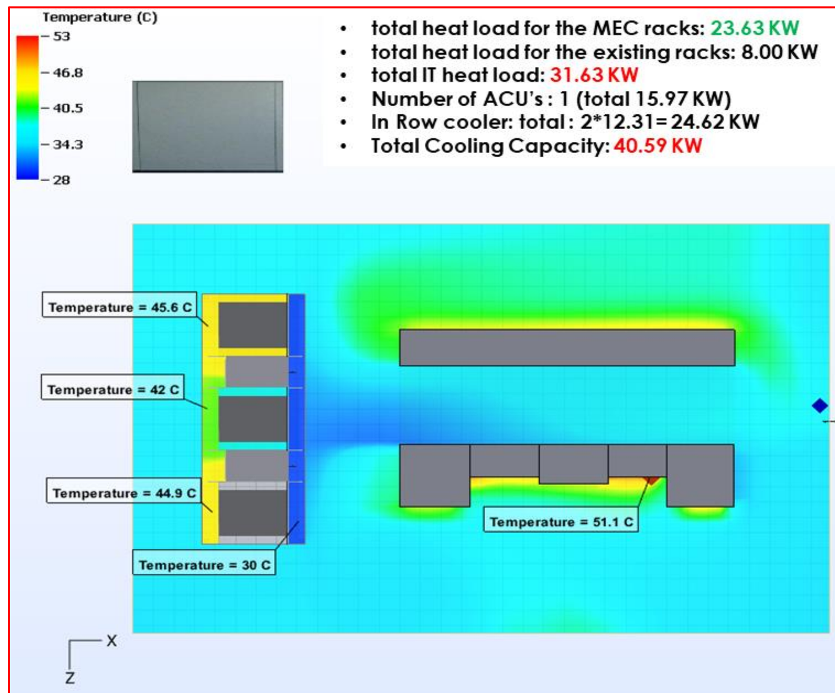

Figure 17 Temperature Contour Plot at the Height of Maximum Temperature for with Containment for MEC Cabinet for Configuration-2.

The blue region between the MEC cabinet and legacy equipment racks shows lower temperature than rest of the room. The reason is for high velocity of supply air from the external ACUs through the small supply vent. The inlet and outlet vents are designed for wall mount air conditioning units. Figure 18 is given

to show the streamlines from and to the vents, superimposed with temperature gradients. The outlet air from the existing legacy racks gets mixed with supply air from external ACU, but in front of the MEC cabinet the temperature remains approximately at 30°C as the air moves with high velocity.

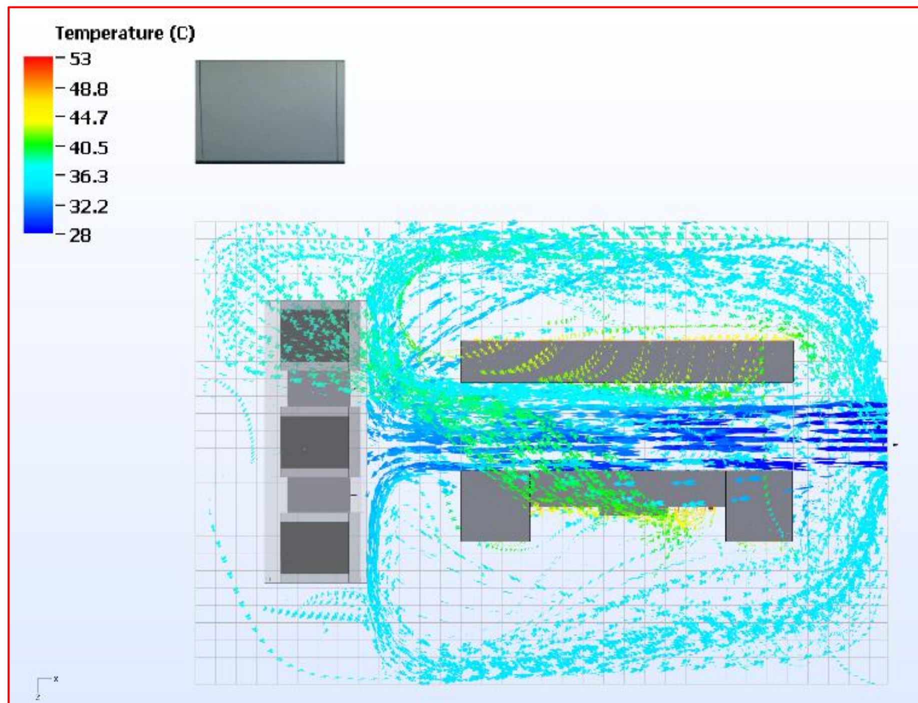

Figure 18 Streamlines Showing Flow Pattern and Temperature of Supply and Return Air for External ACU and Outlet Air from the Existing Legacy Racks.

3.1.8 Air Flow Optimization

The inlet air temperature for the IT equipment for three racks is observed to be different as there was overflow mostly in the middle rack relative to the side racks. So, the scope of optimizing air flow was studied for different vent openings for the duct on both sides of in-row cooler.

Two Cases studied:

1. Case-1: Inlet Flow vents for middle racks to 50% and rear vents are 100

2. Case-2: Inlet Flow vents for middle racks are 32% and rear vents are 64%

The in-row coolers are separated from the racks with a duct as part of custom designing for the MEC cabinet. Ducts increases the resistance and causes reduction in flow rate, but as a part of the design, duct vents were modified to create less temperature and flow rate variation.

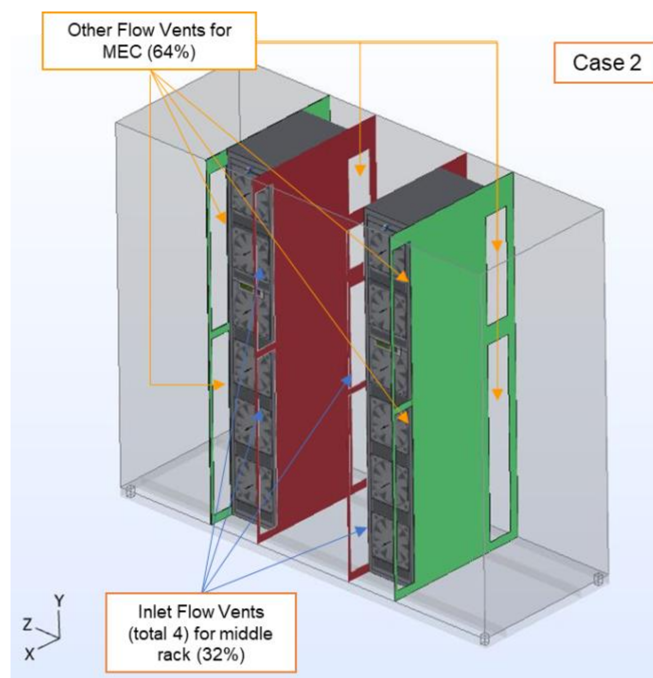

Figure 19 The Location and Vent Opening Areas for Ducts on Both Sides of In-Row Cooler

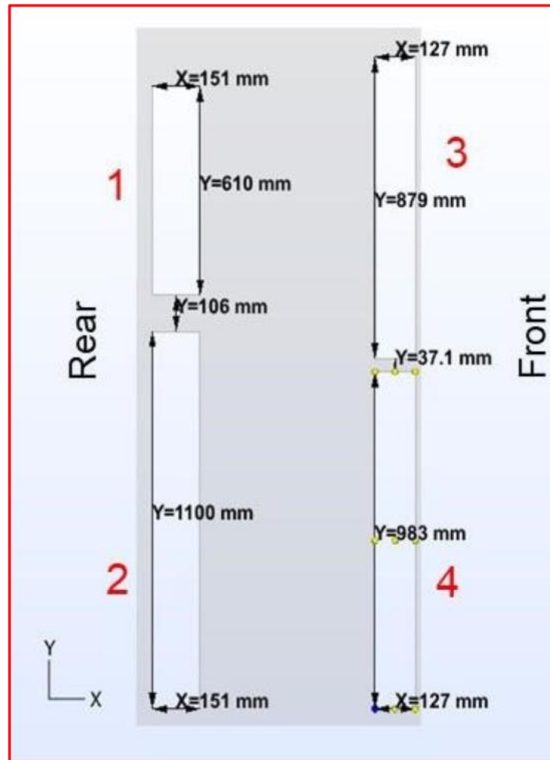

Figure 20 Dimensions and Numbering of the vents at the front and rear for rack at the middle in MEC Cabinet.

Opening areas at the inlet of the middle duct between in-row cooler and middle rack are varied to detect the change in the flow rate and temperature. With the decrease in the opening area, the variation in mean outlet temperatures from the servers in all racks have become less. The impedance for the vents increases as the percentage of opening area is reduced. The flow is reduced for middle rack through the vents and mean outlet temperature increases but approaches to almost uniform considering all racks. The variation of mean outlet temperatures for 64% and 32% opening in Figure 23 are within ±0.7 ˚C. Inlet vent opening areas at front (Figure

19) for the middle rack should be half of other opening areas because the middle rack is getting excess airflow as compared to the other two racks. The duct helped to minimize variation of mean outlet temperatures for IT equipment in all racks limiting amount of excess airflow through the middle rack as servers are given fixed airflow, power and temperature rise as boundary condition.

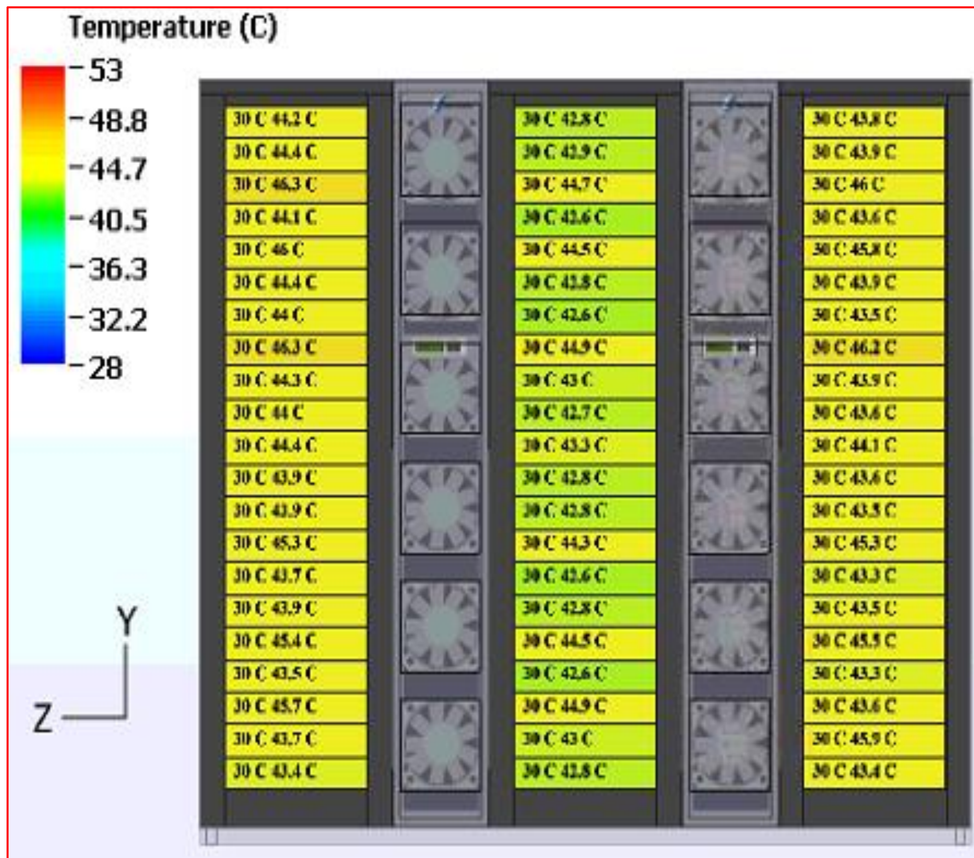

Figure 21 Mean Inlet and Outlet Temperature of IT Equipment With full opening for all vents (1, 2, 3, and 4)

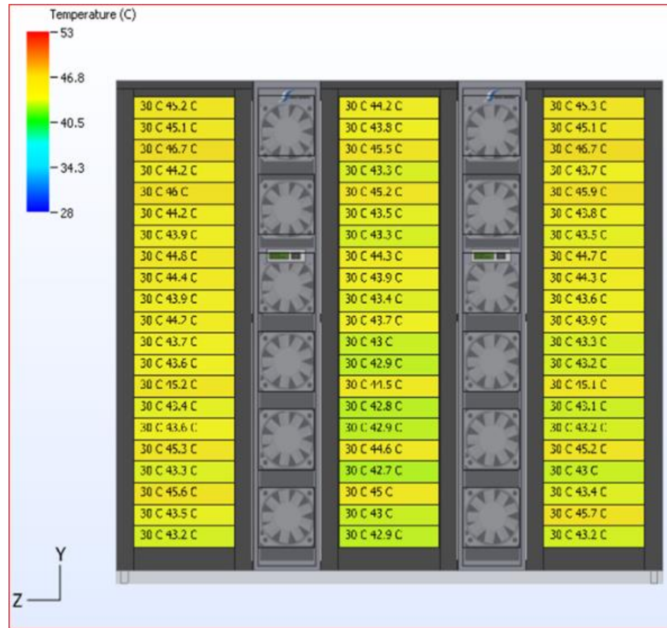

Figure 22 Mean Inlet and Outlet Temperatures for 100% (front) and 50% (rear) Vent Opening Areas of the Two Ducts for Middle Rack.

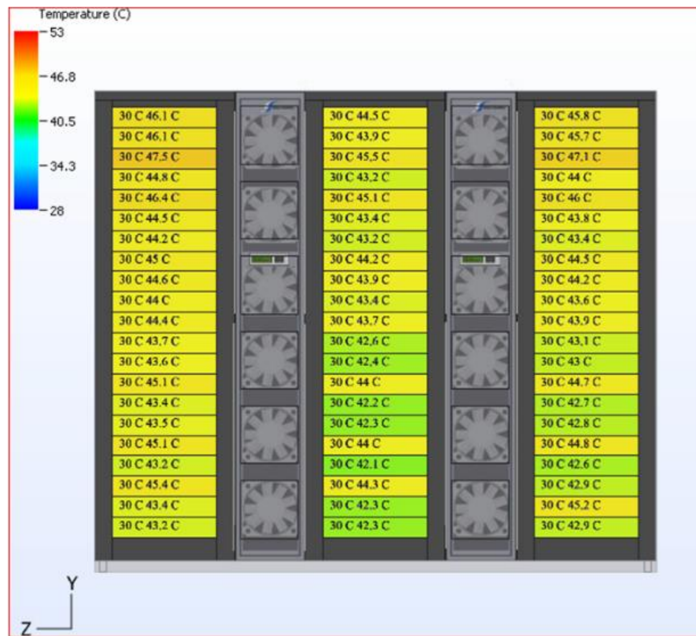

Figure 23 Mean Inlet and Outlet Temperatures for 64%(front) and 32%(rear) Vent Opening Areas of the Two Ducts for Middle Rack

3.1.9 Variable Air Flow Rate from In-Row Coolers

The flow rate from the in-row cooler was varied and the mean outlet temperature was observed from the steady state solutions for different percentage of CFM. The MEC cabinet doors were closed and the racks inside were cooled by in-row coolers. The supply air temperature was fixed at 30°C and the boundary conditions for IT equipment are 375W and 20°C temperature rise. The inlet vents for ducts in between middle rack and in-row coolers are kept as 32 % while rest of the vents are given ass 64% opening area. The plot for the flow rate vs means outlet temperature (Figure 24) for IT equipment also provides the fact that the mean outlet temperature increases with decreased in flow rate.

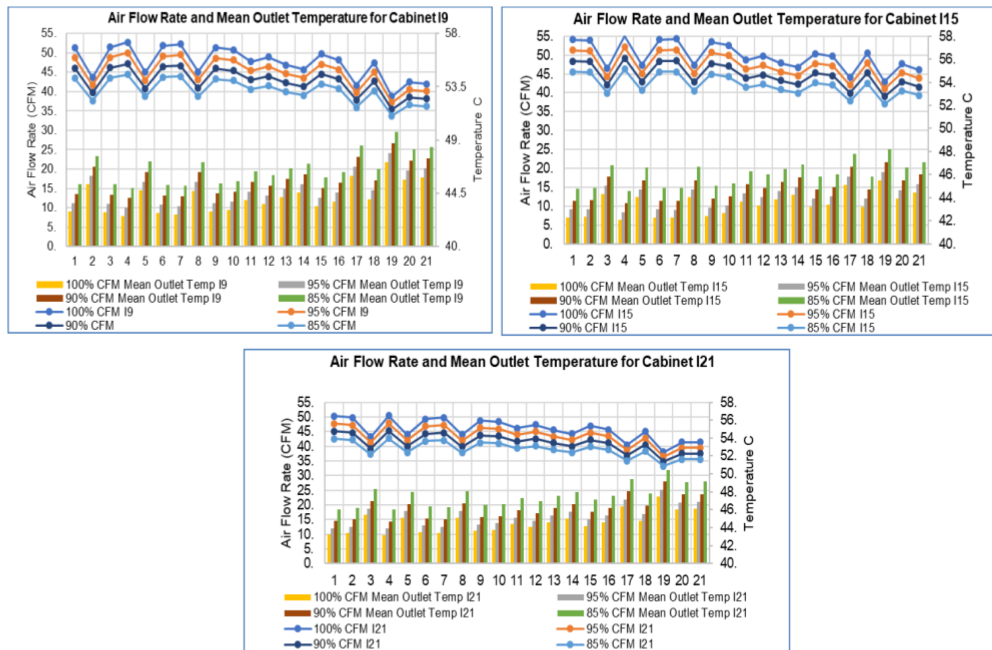

Figure 24 Mean Outlet Temperatures and Flow Rate for Racks (I9, I15, I21) inside MEC for Different Air Flow Rate.

The mean outlet temperatures for servers depend on the flow rates. Small variation in temperatures and flow rates are noticed for recirculation in front of the servers (2, 3, 5, 17, and 19).

3.1.10 Failure Scenarios for In-row Coolers

The cooling system in a data center must operate consistently. "N+1" redundancy ensures that if an ACU unit were to fail, other cooling systems or ACUs would provide adequate airflow at the proper temperature. To simulate the situation for "N+1" redundancy fans in one of the in-row coolers is disabled and worst-case scenarios are also studied by reducing fan power. Air flow inside the IT equipment is decided based on the power and temperature drop provided for each server. There is no backflow from the rear to front of in-row coolers. The fans in the in-row cooler can be controlled by sensing inlet and outlet condition of IT equipment or racks. But there is always a limit up to which it can compensate for the loss of cooling in the event of fan failure of in-row cooler. So, the goal was to find a point of redundancy without affecting IT equipment. The MEC cabinet under this study is also simulated for completely closed or open situations.

3.1.11 Failure Scenario-1

The cooling capacity should always be higher than the heat load of IT equipment. The MEC cabinet contains three racks with 7.88 KW each and two in-row coolers with 24.62 KW cooling capacity. At first, the in-row coolers (12.31 KW, 1500 CFM each) are used to simulate fan failure and the temperature rise was

observed to be too high as active cooling capacity was less than the heat load for MEC cabinet. Then cooling capacity is changed to 24.62 KW and 2900 CFM for each in-row cooler (Figure 25).

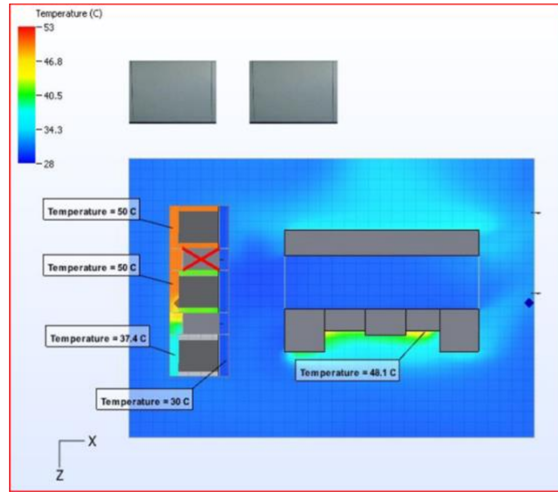

Figure 25 Fan Failure of single in-row cooler (24.62KW): Doors are closed

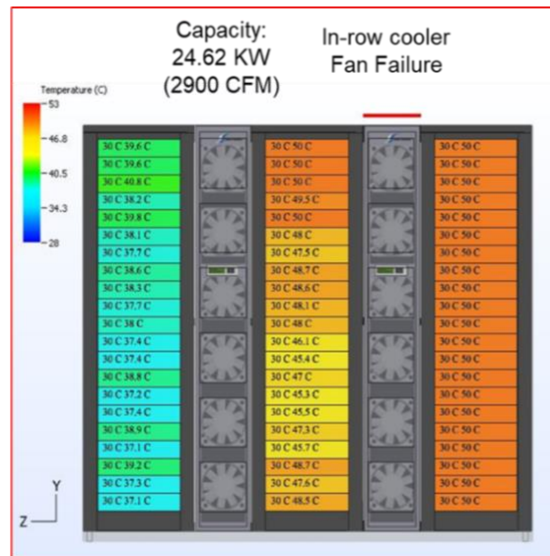

Figure 26 Mean Inlet and outlet temperature of IT equipment for Failure Scenario-1

During the simulation, the doors of the MEC cabinet was closed and the air inside the cabinet was contained. The contour plot of the shelter and the mean outlet temperature from the IT equipment (Figure 26) are given to show the effect of fan failure in a contained situation for MEC cabinet.

3.1.12 Failure Scenario-2

When the doors are open the air inside the room interacts with the air inside the MEC cabinet. As a result, inlet, and outlet air mixes and thus, increases the inlet air temperature for the IT equipment in MEC cabinet. The results are shown for the disabled fans in one in-row cooler (12.31 KW, 1500 CFM).

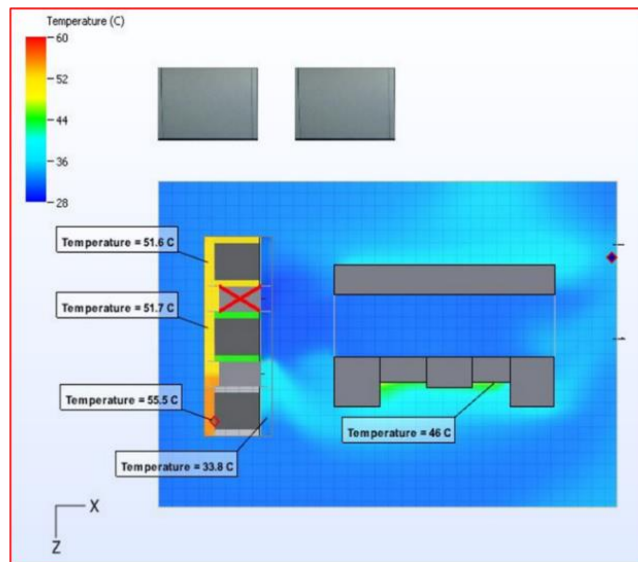

Figure 27 Fan Failure of single in-row cooler (12.34 KW) while doors for MEC are closed

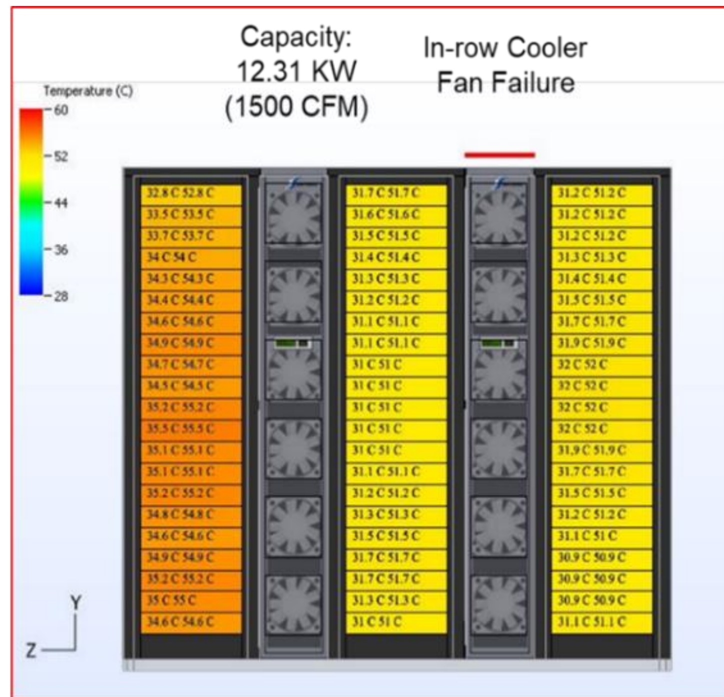

Figure 28 Mean Inlet and outlet temperature of IT equipment for Failure Scenario-2

As the capacity of active in-row cooler is less than the heat load in MEC cabinet (23.63KW, 2900 CFM), front Doors are kept open (Figure 27). Supply air from ACUs and in-row coolers are used to provide the cooling for both the MEC cabinet and existing shelter racks.

The contour plot of the shelter and mean outlet temperature from IT equipment in MEC cabinet are provided to show effect of fan failure for MEC cabinet without containment. The inlet temperature varies and increases for left rack in MEC cabinet (Figure 28) due to getting mixed with the outlet from the racks in MEC cabinet.

Chapter 4

Hybrid Cooling: Server Level

4.1 Server Under Study

The server used for the experimental analysis is an enterprise 1U server from Cisco. There are 8 Hard Disk Drives (HDDs), two central Processing Units (CPUs), 16 Dual In-line Memory (DIMMs), 1 Platform Controller Hub (PCH), 1 chipset, 1 Power supply Unit (PSU) and other components. For hybrid cooled server, the heatsinks are replaced with ASETEK cold plates for cooling the CPUs only. The other components are cooled by air. There are five fans in both the air and hybrid cooled server, but the air-cooled server has a duct between the heatsinks and fans to guide the airflow properly.

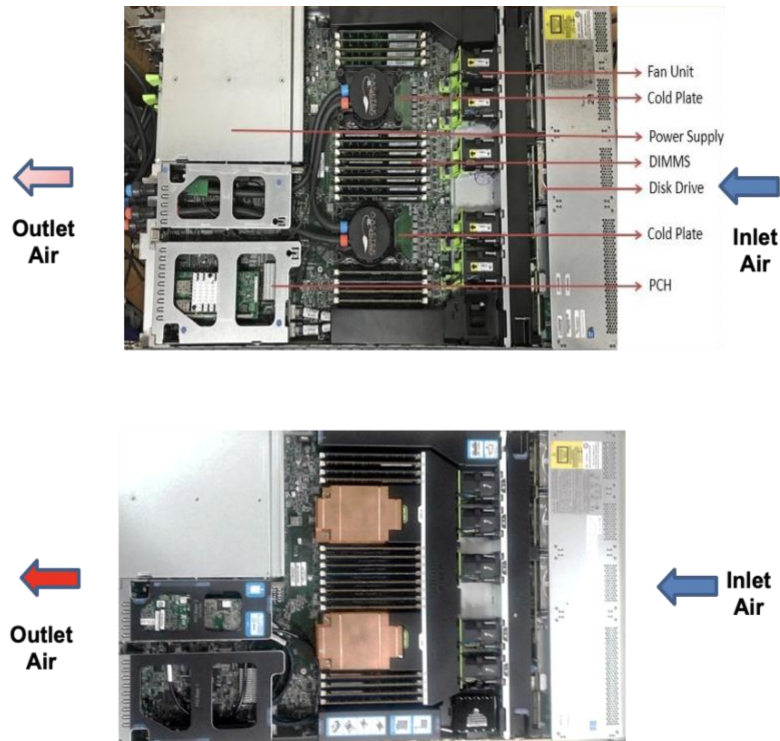

Figure 29 Hybrid and Air Cooled 1U Server. [107]

Table 4 Brief Summary of Components and Cooling in Server [108]

Components	Spec Sheet Data
CPU (2 Processors)	Intel Xeon® E5-2600 v2 or E5-2600 (TDP-135W)
DIMMs (Total 16)	(8x8GB+8x4GB, 1.35V, 1600MHz- 96 GB)
Fan (Total 5)	Delta fan, 40x40x56mm, (TDP-15.6W)

Pump (Total 2)	ASETEK Direct to Chip CPU cooler (Total 2, DP- 4 W)

4.2 Effect of Raised Inlet Coolant Temperature

As the thermo-physical properties of water are superior to air, water using cold plate can carry away the heat from the processors more effectively than heat sinks. The objective of this study is to find out the limits of inlet coolant temperature per ASHRAE liquid cooling guideline for the server under study and lower of coolant flow rate possible in the server cooling loop. The 1U server is retrofitted with cold plates and the external loop consists of quick disconnects connected to a liquid to air heat exchanger (miniature dry cooler). cooled servers. In this experiment, a 1U server is equipped with cold plate to cool the C PUs while the rest of the components are cooled by fans. In this study, predictive fan and pump failure analysis are performed which also helps to explore the options for redundancy and to reduce the cooling cost by improving cooling efficiency. Redundancy requires the knowledge of planned and unplanned system failures. As the main heat generating components are cooled by liquid, warm water cooling can be employed to observe the effects of raised inlet conditions in a hybrid cooled server with failure scenarios. The ASHRAE guidance class W4 for liquid cooling is chosen for our experiment to operate in a range from 25°C-45°C. The experiments are conducted

separately for the pump and fan failure scenarios. Computational load of idle, 10%, 30%, 50%, 70% and 9 8% are applied while powering only one pump and the miniature dry cooler fans are controlled externally to maintain constant inlet temperature of the coolant. As the rest of components such as DIMMs & PCH are cooled by air, maximum utilization for memory is applied while reducing the number fans in each case for fan failure scenario. The components temperatures and power consumption are recorded in each case for performance analysis. An experimental study on the pump and fan failure has been performed on the server level to reduce the cooling power per server. It has been found that 46% cooling power reduction is possible by using liquid cooling in an air-cooled server. The details can be found in this paper published in InterPACK 2017 [63].

4.3 Effect of Raised Inlet Air Temperature on Air Cooler Server

A previous study shows the effect of increasing inlet temperature on the processor temperature and power consumption for air cooled heat sinks and liquid cooled cold plates. There are five fans at the upstream for heat sinks of CPU while a separate liquid cooled server has cold plate with integrated pumps. For the air-cooled server with heat sinks, an environment chamber is used for providing constant inlet air temperature (15-45 °C) to the IT equipment while it was stressed for both CPU and memory following the ASHRAE A1-A4 guidelines. On a separate setup the coolant inlet temperature for liquid cooled server was controlled

for providing constant high inlet temperature (25-50 °C) per ASHRAE W1-W4 guidelines. The effect of high inlet conditions for air and liquid cooled CPUs are summarized and conclusions are made for critical inlet temperature contributing to leakage current effect and increase in static power. The cooling power of air-cooled server is presented as a percentage of total IT power. It was observed that the air-cooled server has limitations for inlet air temperature as 35 °C while the liquid cooled server can have high inlet coolant temperature as high as 45 °C with no increase on static power.

Table 5 Cooling Power Consumption vs IT Power Consumption[109]

Test	15	20	25	30	35	40	45
Idle	5.30%	4.95%	4.88%	4.61%	3.61%	10.05%	12.92%
10%	3.32%	3.69%	5.01%	6.60%	6.89%	6.54%	11.11%
30%	2.68%	3.42%	5.07%	5.01%	4.91%	6.73%	11.19%
50%	2.08%	2.70%	4.01%	3.90%	3.93%	5.93%	9.33%
70%	1.95%	2.56%	3.82%	3.72%	3.64%	5.88%	9.68%
100.00%	1.74%	2.26%	3.39%	3.35%	4.21%	5.88%	11.95%
CPU+MEM	1.55%	2.07%	3.07%	3.13%	4.60%	9.59%	13.35%

4.4 Effect of Raised Inlet Air Temperature on Hybrid Cooler Server

(Reprinted with permission © 2018 ASME)[107]

In a hybrid cooled the server, the high inlet temperature of coolant can be used to minimize the static power increase and increase cooling efficiency. As the rest of components are cooled by air, the inlet air temperature has an effect for DIMMs, PCH, chipset and other auxiliary components depending upon their

respective utilization. The previous comparative study has shown increased power consumption for air cooled server above 35 °C inlet temperature. So, it is crucial to check if the power increase is due to leakage current effect of the CPUs or DIMMs. The hybrid cooled server rejects heat from the CPUs to the coolant liquid, thus it becomes easier to segregate the effect on air cooling from liquid cooling while using high inlet air temperature for the server.

4.5 Numerical Analysis

To evaluate the operating temperatures of DIMMs and other air-cooled components, a numerical analysis on a commercial CFD software (6SigmaET) [110] was performed with the validation of the model with experimental data for pressure drop and air flow rate. The server inlet temperature was varied between 25-45°C with 5°C increase within ASHRAE provided envelopes. The server fan RPM was varied to overserve the effect of reduced flow rate at each inlet air temperature. The results from this study can be helpful in determining the room level operating set points for data centers housing hybrid cooled server racks.

4.5.1 Modeling and Validation

K-Epsilon turbulence model is widely used model for turbulent flow modeling which is also commonly known as two equation model. This model uses two variables: the kinetic energy of turbulence (k) and the dissipation rate of the kinetic energy of turbulence (ε). 6SigmaET is used for numerical analysis. The

dimensions and specifications are measured and collected from the server and online resources as model data is not readily available. 6SigmaET's components like CPUs, DIMMs, HDD, fans, power supply, chipset and heat sinks are used from built-in object panel library. Properties like thermal, material, surface, etc. are defined as per requirements for the developing model. Thermal dissipation power is applied to DIMMs, MOSFETs, chipset, PCI chipset and utilized same as in the experiments performed before. To simplify operations, and match behavior with actual components in a model, changes are made according to the specifications and experimental data. The model is validated with experimental data to define the flow rate and resistance through the server and opening at front, rear and top are adjusted to curve-fit the data. The model is also tested for different gridding to check discrepancy of data and the default grid setting is used while changing the target value for gridding. The final model contained about 8.5 million grids.

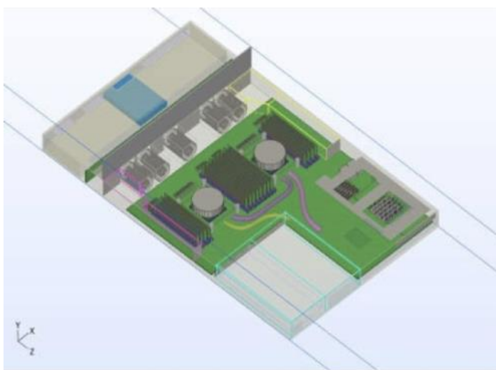

(a)

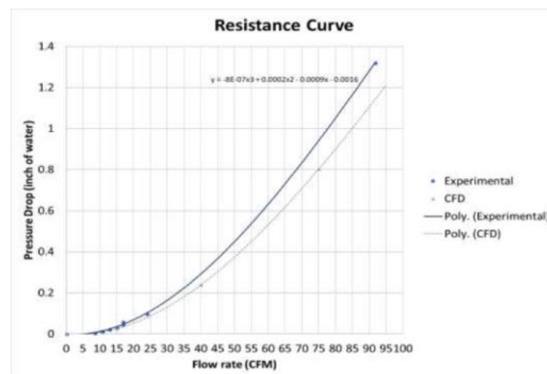

(b)

Figure 30 (a) Isometric View of Server (b) Validation of Resistance Curve of CFD and Experiment.

As it is a simplified model, the details of the other components were not given priority and regarded as obstructions in model. The hybrid cooled server is modelled without the duct between fans and DIMMs as it is absent in hybrid cooled server during experimental studies. The pressure drop values across the server was found to vary up to 7%-8% of the measured values in lab. The pressure plots and velocity plots are shown for low flow rate when fans are observed operating at 3450 rpm for idle state of CPU and memory utilization during the experiments.

4.5.2 CFD Results

The model is updated with fan power curve from experimental results [109]. The inlet air temperature during the experiments was 25˚C ± 1˚C. But choosing the proper the rpm for the fans is a crucial criterion to match with experimental conditions. The fans in air cooled server ramped up for increase in inlet air temperature. The experiments with air cooled server cannot be used to judge the situation in hybrid cooled server as there are changes inside the server for replacing the heat sinks with cold plates and removing duct in hybrid cooled server. But another study previous discussed above [63], showed the effect of flow rate with reduced fans. As the study included five fans with range of rpms for 25 ˚C room temperature, the idle state data is chosen to validate the CFD model data. According to the experimental data, the fans operate at an average rpm of approximately 3450

in a hybrid cooled server. Thus, the recorded temperature by IPMI tool is the baseline of comparison for CFD model. At 25 ˚C and 3450 rpm, the maximum DIMMs and PCH were found to be around 46˚C and 58˚C [63].

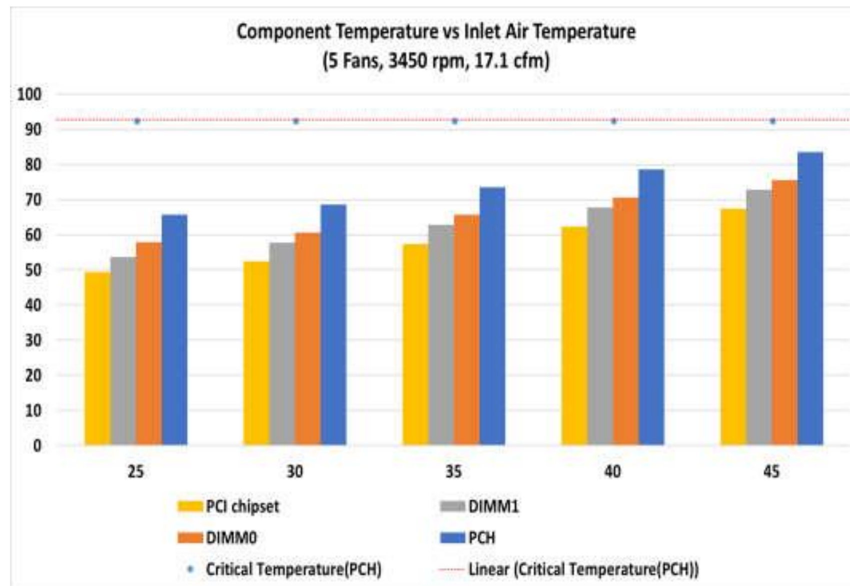

Figure 31 Component temperatures at different inlet air temperatures (5 fans at 3450 rpm).

As during the previous experiments, memory was utilized up to 92.7% (maximum possible), the DIMMs, PCH, PCI chipset, MOSFETs are also stressed accordingly. The CFD results for five fans are plotted and shown here. The most critical component for the air-cooling is the PCH as it lies in a thermal showing zone where warmer air from the DIMMs cools the PCH. The critical value for PCH is shown in a dotted line in Figure 31. Moreover, changing the heat sinks with cold plates changed the impedance to flow. The fans are operated at two different sets of rpms: 3450 and 7000 rpm to overserve the effect of increased air flow rate on

the component temperatures. Similar range of fan speed is observed for experimental analysis when hybrid cooled server was tested with warm water cooling (30-50°C inlet coolant temperature).

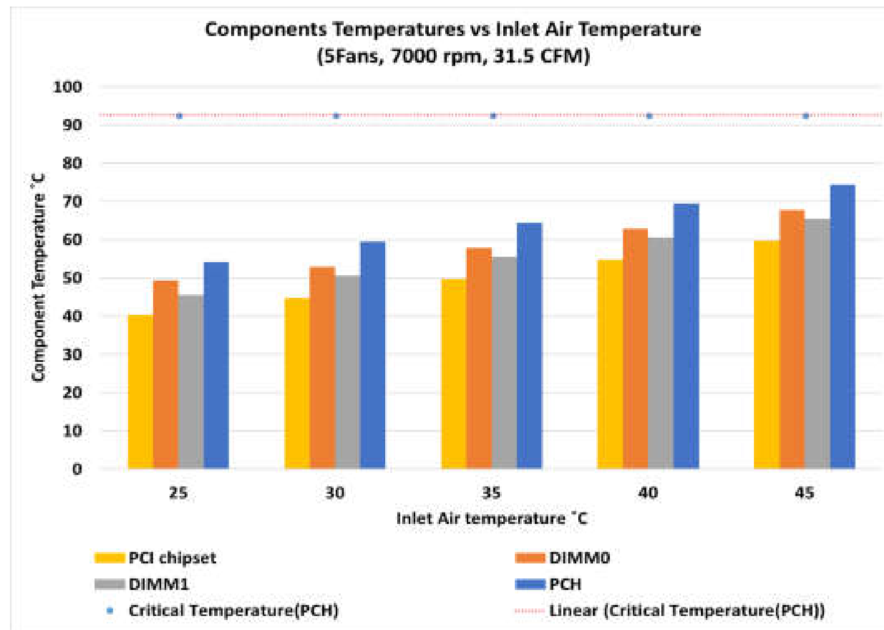

Figure 32 Component temperatures at different inlet air temperatures (5 fans at 7000 rpm).

As in this study we are increasing the inlet temperature, the overheating condition must be avoided, and the component must operate below the critical temperature at worst case scenario when the memory is stressed to the maximum. The contour plots are also provided for 25 ˚C and 45 ˚C for five fans at 3450 rpm. The contour plot below shows the effect of high inlet and reduced flow rate for the hybrid cooled server.

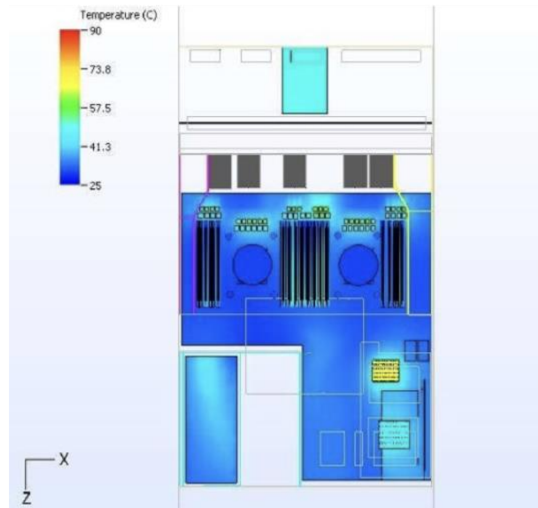

Figure 33 Contour Plot for surface temperature at 3450 RPM for 25˚C

With five fans it is expected that the component temperature should not exceed the critical temperature at stressed condition. Generally, in fans in server are internally controlled and ramps up according to the algorithm when component temperature exceeds the threshold values set in the coding.

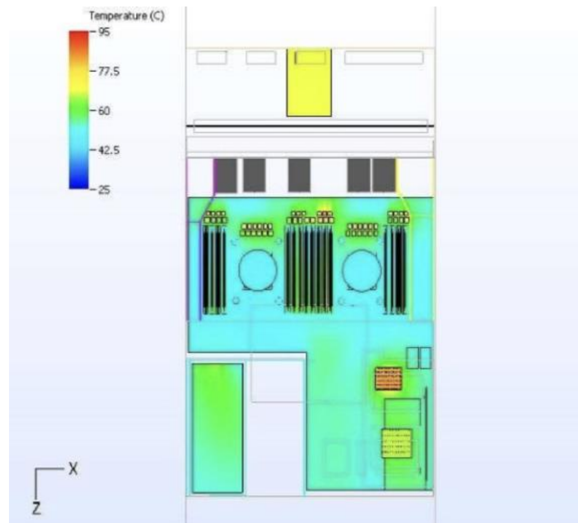

Figure 34 Contour Plot for surface temperature at 3450 RPM for 45˚C

For minimum flow with five fans, the component temperature shows that PCH temperature is 83.51˚C for fans operating at 3450 rpm at 45˚C. For these PCB and DIMMs temperatures also increase. At 7000 rpm for 25 ˚C case, DIMMs and PCH temperature are found to be around 49.2 ˚C and 54.15 ˚C.

4.5.3 Discussion

The IT power consumption increases for raised inlet conditions to provide better heat transfer from the high generating components. On the other hand, increasing inlet air temperature raises the issue of leakage current and increase in power consumption for servers. As the CPUs and other high heat generating components are cooled by liquid, temperatures of auxiliary components depend on inlet air temperature for a hybrid cooled server. This study is performed to understand the effect and determine range of inlet air temperature for a hybrid cooled server which will be eventually helpful to reduce cooling cost of a modular data center. Choice of operating temperature increases with a wider range of inlet air temperatures and data centers in a hot or warm climate can also utilize free cooling using the outside air. For raised inlet temperature the commonly faced challenges are performance, power, and reliability. For optimum performance of IT equipment reasonable air inlet temperature and component temperatures should be maintained. Fan power is a function of the fan rpm and mass flow rate.

One of the ways to reduce total cooling power ($Q_{air} = \dot{m}_{air} C_p \, \Delta T$) is to increase inlet air temperature (T_ambient) while keeping the fan rpm and flow rate constant ($\dot{m}_{air}$=constant). The reliability of components depends on junction and case temperature. In the previous experimental studies, it was found that component (DIMMs and PCH) temperatures are well below critical temperatures when this server is cooled by air. A study by El-Sayed et al. [68] indicate that the effect of temperature on hardware reliability is less than as it is assumed. In a separate study, it was found that DIMMs were operating reliably for elevated rack inlet temperature [111].

4.6 Experimental Analysis of Raised Inlet Temperature for Hybrid Cooled Server

In this experiment the air temperature for the hybrid cooled server is increased from 24 °C to 45°C by 5°C. The respective temperatures for air cooled and liquid cooled components are recorded and compared. The constant inlet temperature was provided by the environmental chamber with the relative humidity varying from 40%-50% following the ASHARE air cooling guidelines (A1-A4). The server is stressed for both CPU and memory to the maximum with a benchmark tool named Prime95. The data from numerical analysis is compared with experimental findings for air cooled components collected by the server Intelligent Platform Management Interface (IPMI) tool. The server power consumption is also

reported for both CPU and memory utilization at different server inlet air temperature while the coolant inlet temperature is kept constant at room temperature (25 °C). Findings from the experiment highlights the similarity and variation of CFD results and provide a margin for air cooling in terms of inlet air temperature for the hybrid cooled server. From the results it is noticed that the hybrid cooled server is not restrained at 35 °C inlet air temperature like the air-cooled server and the limits for air cooling can be expanded if hybrid cooling is used in a data center while decreasing the required air flow rate. Thus, the cooling load on the CRAH or CRAC reduces as we move to larger ASHARE air cooling envelopes without affecting the component performance and reliability and increasing the cooling efficiency.

4.6.1 Experimental Setup

An Environmental Chamber is used to provide constant inlet temperature to the server. The server has two cold plates with integrated pumps (ASETEK) on top of the CPUs for liquid cooling and five fans at the upstream of DIMMs for air cooling. The external loop of liquid cooling consists of a pair of quick disconnect (ASETEK) and a small liquid to air heat exchanger. The coolant temperatures at the inlet and outlet of the server are collected by a penetrable K-type thermocouple without causing extra pressure-drop across the server. The coolant inlet temperature for the liquid cooled loop is kept constant at room temperature (25 °C) by controlling the fan RPM in miniature dry cooler with a LabVIEW code. The fans

have 4 wires where two wires are used to power the fans by external DC Power Supply and third and fourth pins are used to control and read the fan RPM. The fans are controlled by an external function generator for PWM control. The pumps inside the cold plate are provided maximum rated voltage (12V) by a DC Power Supply to run at full speed and circulated the coolant. Following the temperature and relative humidity envelopes set by ASHRAE, the air temperature inside the chamber is controlled and varied from 24 °C to 45 °C by 5 °C for each case. The temperature of server components (CPUs, DIMMs, PCH, Chipset, etc.) and power consumption are collected by IPMI tool. The fan power and pump power consumption were previously reported in these papers. For each case the data is collected after steady state is achieved which takes approximately 30 mins and server is kept at idle for another 30 mins after completion of each case. The repeatability of data is checked by performing same cases twice to provide an average value from the experiments for each case.

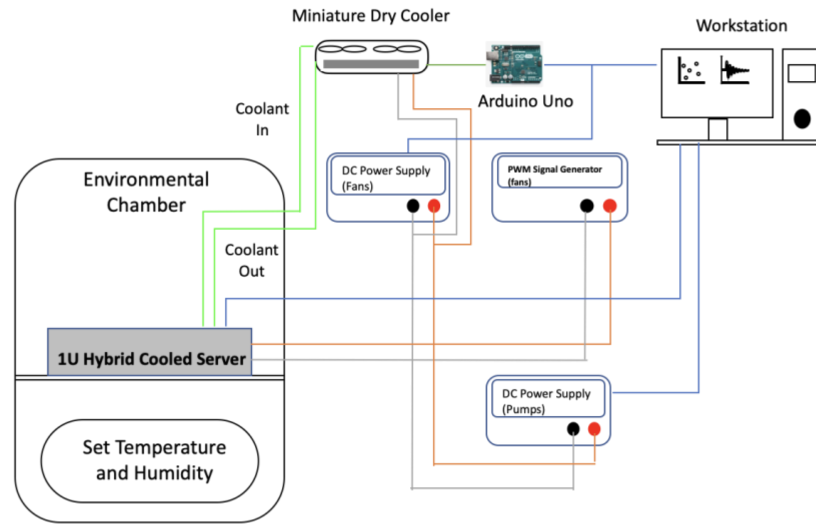

Figure 35 Schematic of Experimental Setup for Testing Hybrid Cooled Server in Environmental Chamber

For experimental study, a precaution was taken to consider the air flow through the top vents on chassis. As 1U servers are placed inside a rack so, there is a minimum gap which provides resistance for the flow rate through the top vents. To observe the effect of top vents being closed, a server is kept on top the experimented server. So, in this analysis two scenarios are compared: one is single server, and another is server on top inside the environment chamber. The scenarios are presented in the schematic below.

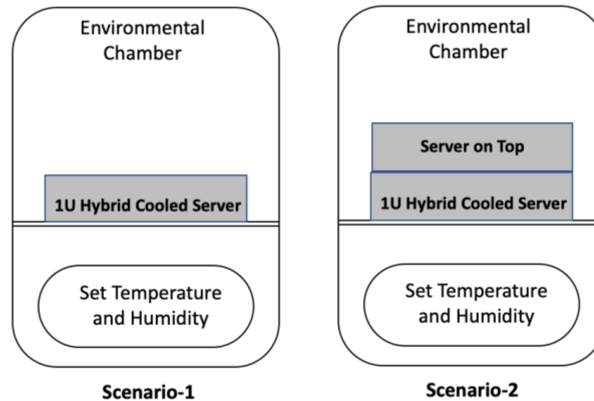

Figure 36 Two Scenarios for Experimentation Inside the Environmental Chamber

The locations of DIMMs and CPUs are shown with the names from the spec-sheet. From the Figure 29 it can be noticed that each CPU has 4 DIMMs on each side and there is total 16 DIMMs in the server. The flow rate from the fans is not guided by the baffle like the air-cooled server as there is no air flow required for cooling the CPUs.

4.6.2 Single Server in Environmental Chamber

The increase in inlet air temperature increases the temperature of air-cooled components. The DIMMs are placed on both sides of CPUs and flow from the fans pushes the air to cool the components. The PCH is thermally shadowed as the air from the DIMMs on the right cools the PCH. On the other hand, as the coolant inlet temperature is kept constant at 25 °C, the CPU temperatures are expected to be similar for all cases studied for single server inside the environmental chamber. The uniformity of CPU temperature is noticed at each case of study and the temperature of both the CPUs is around 45-50 °C.

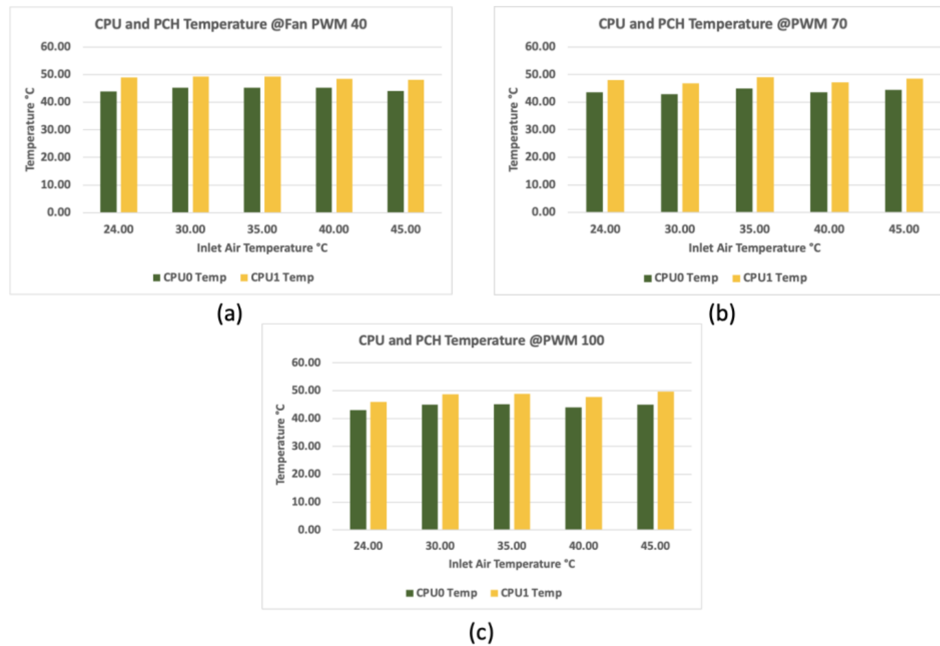

Figure 37 CPU Temperatures for Single Hybrid Cooled Server in Environment Chamber for max. utilization of CPUs and Memory and Variation of Fan PWM: (a) 40% (b) 70% (c) 100%

The DIMMs temperatures are also collected by the IPMI tool, and each fan is controlled at same PWM for each case. Hence, the flow rate from each fan is same and the resultant junction temperature is almost similar as seen from the Figure 38. As the inlet air temperature is increased, the linear pattern of temperature increase is noticed which is logical, but it is far below its critical operating temperature limit of 81 °C. Figure 38 also shows the temperature variation among the DIMMs and it is noticed that due to symmetry of air flow from fans, the temperature rise pattern is symmetric for the location of DIMMs from the center to each side. The maximum temperature for DIMMs is noticed for reduced air flow

rate at 40% PWM setting, and the peak temperature occurs at higher inlet temperature of 45 °C. The corresponding temperature for 40% PWM and 45°C inlet air temperature is approximately 75 °C.

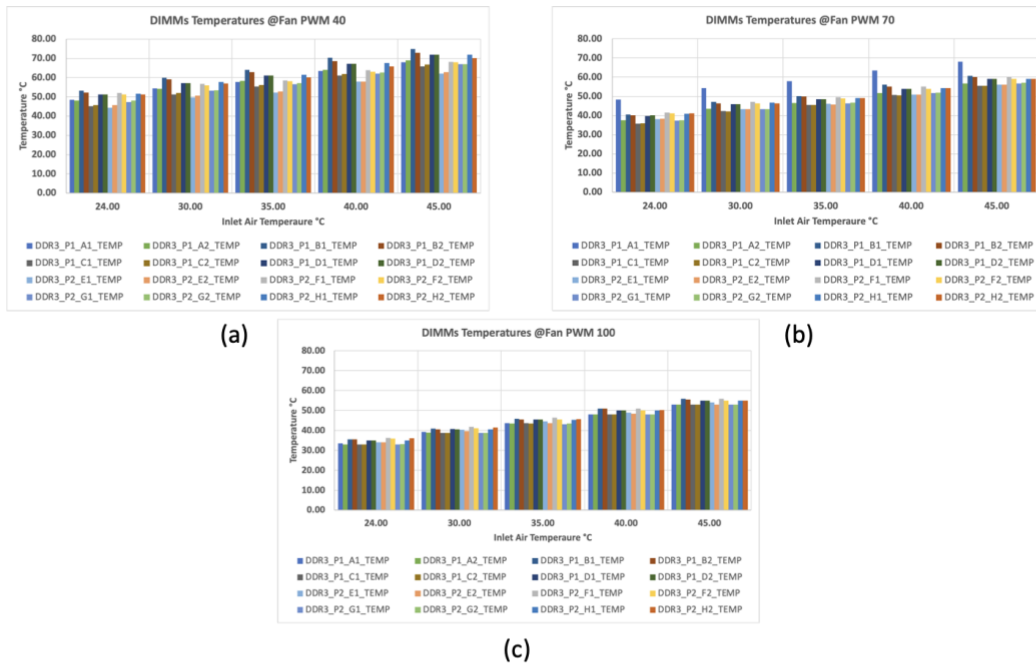

Figure 38 DIMMs Temperatures for Single Hybrid Cooled Server in Environment Chamber for max. utilization of CPUs and Memory and Variation of Fan PWM: (a) 40% (b) 70% (c) 100%

The critical component for air cooling is the Platform Controller Hub (PCH) as it is thermally shadowed and the fans on rights are used to cool the PCH situated at the right side of the server. The maximum temperature is also noticed for PCH as the CPU and memory are utilized to the maximum for each case with variation of inlet air temperature and fan PWM. The maximum temperature of PCH is 88.7°C which is recorded for 45°C inlet air temperature and 40% fan PWM. The critical

temperature of PCH is 92.7°C. So, the server can sustain maximum temperature of 45°C inlet air temperature and fan PWM can be modulated to maintain the PCH temperature far below it's critical limit for safe operation and smooth performance (such as using 70% PWM).

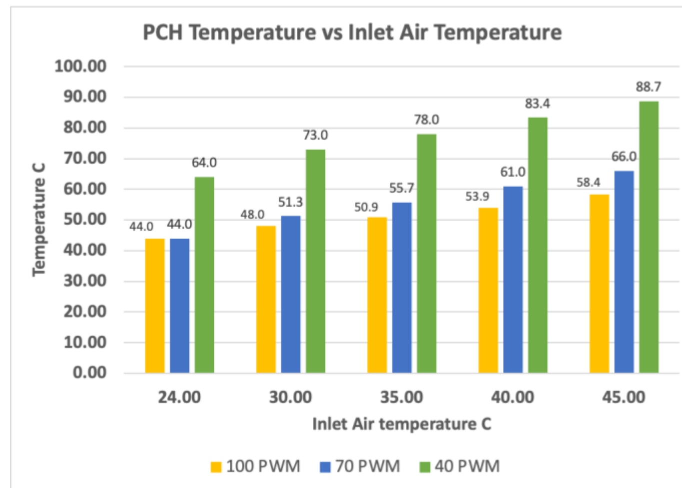

Figure 39 PCH temperature for Max. CPU and Memory Utilization at different inlet air temperature and fan PWMs (40%, 70%, 100%)

4.6.3 Server on Top in Environmental Chamber

The experiment is repeated on the same server but the outlet vents on top are covered, and a minimum gap is kept as two servers are placed on top of each other. As the air flow rate is reduced on top vents, the vents at the rear are the only outlet vents for outgoing air flow rate through the server. The CPUs are utilized to the maximum (99%) with memory at 92% for maximum utilization. The liquid cooling loop is provided with a constant inlet temperature of 24C which results in the similar temperature pattern for all cases when inlet air temperature is varied

inside the environmental chamber and fan flow rate is varied by function generator from outside of the chamber. The junction temperature of CPUs is like the results obtained for single server in environmental chamber and it is ~ 45-50 °C.

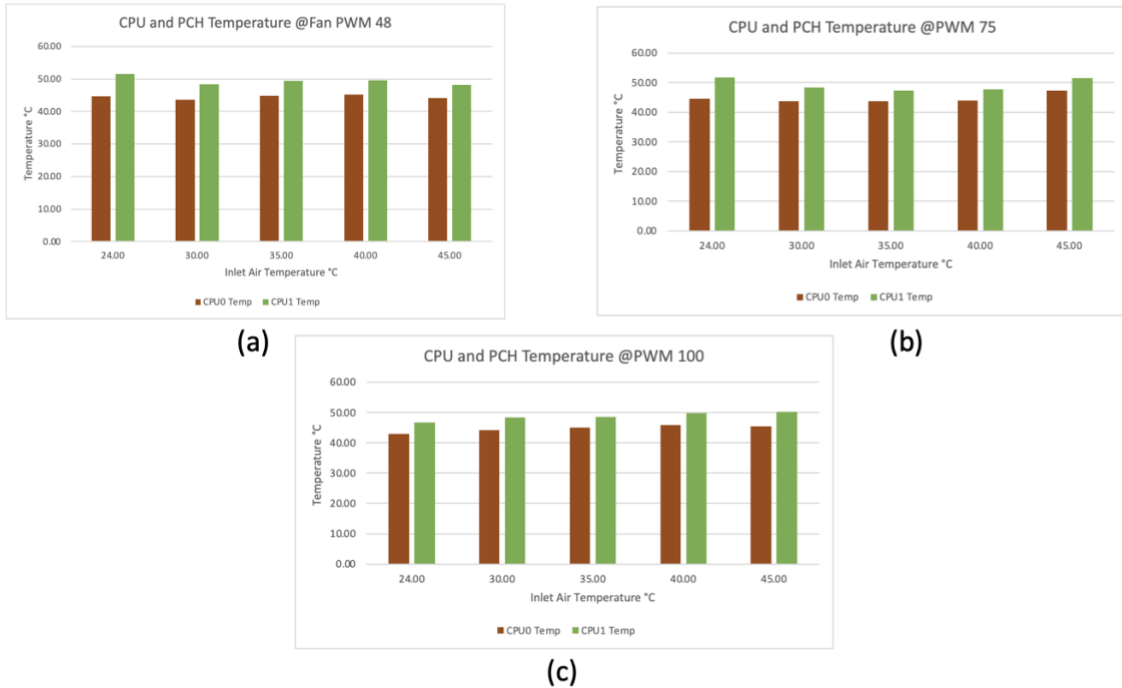

Figure 40 CPU Temperatures for Server on top in Environment Chamber for max. utilization of CPUs and Memory and Variation of Fan PWM: (a) 48% (b) 75% (c) 100%

The DIMMs temperatures also show similar pattern for single server and server on top inside the environmental chamber. The maximum temperature of ~75C is also noticed for server on top scenario. The linear pattern of increase in DIMMs temperature with inlet air temperature is like the single server. But in this case lower PWMs are changed such as 48% and 75% PWMs are used to achieve similar temperature for DIMMs. So, as the vents are closed on top, a minor increase

in PWM was required to maintain the temperature of air-cooled component like previous scenario for a quick comparison. As higher PWM creates higher air flow rate and increase in pressure drop across the server to compensate for the extra resistance provided at the top vents. The results are provided for the variation of DIMMs temperatures in each case in the Figure 41 below.

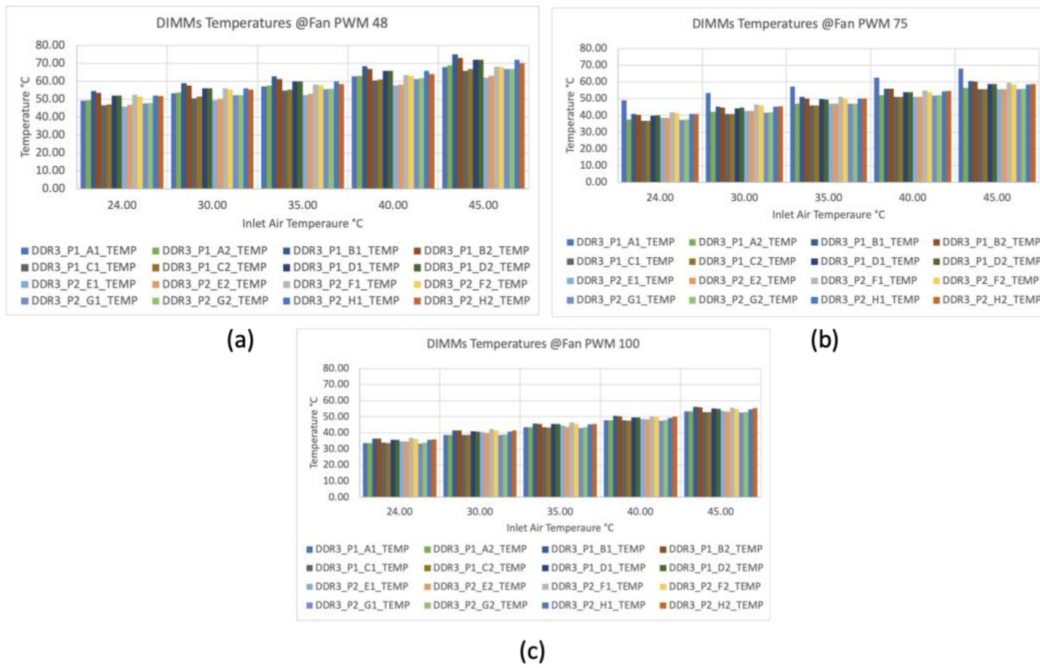

Figure 41 DIMMs Temperatures for Single Hybrid Cooled Server in Environment Chamber for max. utilization of CPUs and Memory and Variation of Fan PWM: (a) 48% (b) 75% (c) 100%

To analyze more, the PCH temperatures are also presented to compare with previous scenario (single server in environmental chamber). The PCH temperature has increased by a little (0.3 °C) although increased PWM (48%) is used for 45 °C inlet air temperature. The temperature for second scenario is higher for other fan

PWM settings considering each inlet air temperature condition. But even in this case, the critical limit is not exceeded and fan PWM can ramped up if necessary, provided that the DIMMs temperature is close to the critical limit for maximum CPU and memory utilization. The 75% PWM setting shows temperature for PCH as low as 68 °C for 45 °C inlet air temperature.

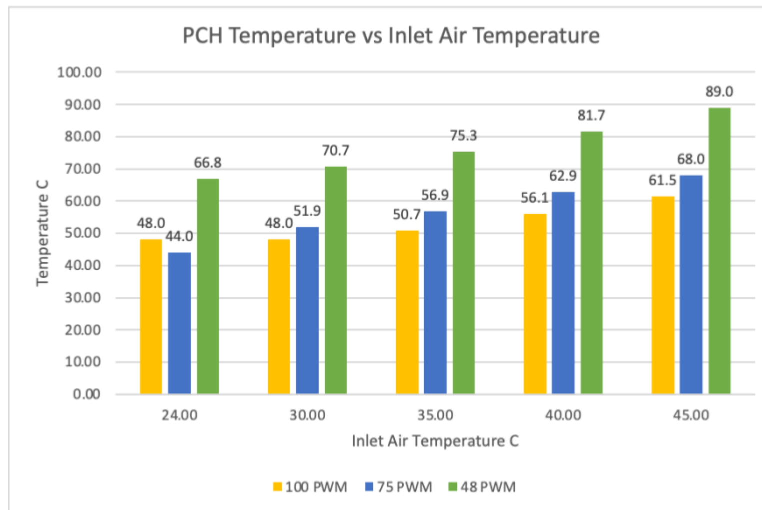

Figure 42 PCH temperature for Max. CPU and Memory Utilization at different inlet air temperature and fan PWMs (48%, 75%, 100%)

4.6.4 Power Consumption

The power consumption is critical when inlet air temperature is increased as it may cause the static power consumption to be increased and thus, increases the server power consumption. The server is segregated from the power input for cooling as the fans and pumps are provided power from external DC power supplies. The lower fan PWM settings causes the fans to operate at lower RPM which draws less power. But the pumps are provided with maximum operating

voltage to operate at maximum RPM. So, in other words, the power consumed by the server is purely IT power and combines the power consumed by the CPUs, DIMMs, PCH, chipset, MOSFET, Power supply, HDDs, and others. The scenarios with single server and server on top for increased air inlet temperature are presented with the data collected from IPMI tool for variation of flow rates by fan PWM settings. Figure 43 shows the power consumption minor variation even at higher air inlet temperature as the server utilization is maxed for CPUs and memory. The temperatures of CPUs and DIMMs are kept within the critical limit which does not result in extra power consumption for leakage current effect. The average power consumption is ~404W per server.

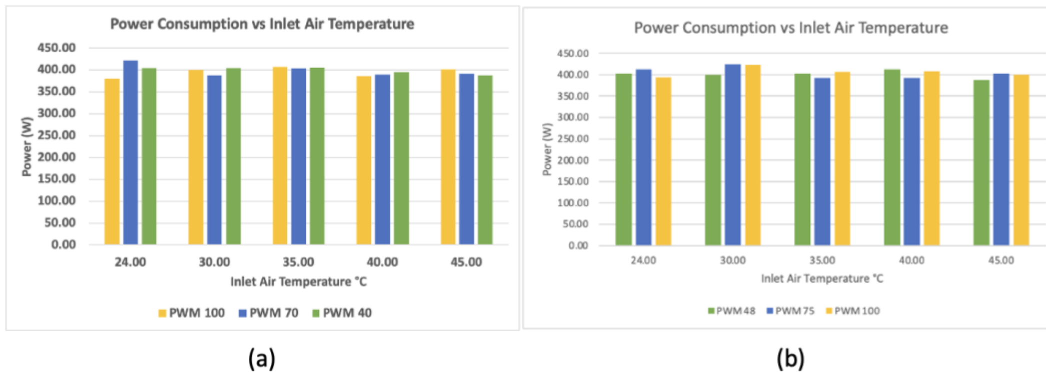

Figure 43 Server (IT) Power Consumption for (a) Single server (b) Server on top inside the Environmental Chamber.

Chapter 5

Flow Network Analysis: Rack and Room Level

One dimensional flow network analysis provides a quick tool to model the liquid cooled loop for IT equipment, rack, and data center. The flow network modeling (FNM) was performed in a commercial 1D flow network solver called "Macroflow"[112].

5.1 Governing Equations

The mass, momentum and energy equations are solved for the fluid flow and thermal analysis. The equations are solved for one dimension only and major and minor losses for pressure drop is calculated based on the friction factor derived from the respective values of Reynold's number and roughness of each pipe. There is a provision of providing the external temperature and atmospheric pressure. At the inlet and outlet of the pipes, constant flowrate and pressure drop can be applied as boundary conditions. In Brief the governing equations are shown below.

Mass Conservation Equation:

$$\sum_{i=1}^{n} \rho Q = 0 \tag{3}$$

Momentum Equation:

$$P_1 - P_2 = S_{cr} + RQ \tag{4}$$

Heat transfer Equation:

$$Nu = CRe^{m}Pr^{n} \tag{5}$$

Pressure-drop for components

$$\Delta P = \frac{1}{2}K\rho\left(\frac{Q}{A}\right)^{2} \tag{6}$$

5.2 FNM and Results

The cold plate from the library is used to present the cold plates being used on top of the CPUs in a server. The fluid flow and thermal properties are provided by using the experimentally or computationally derived pressure drop curve (PQ) and thermal resistance curve (RQ). In this case the PQ and RQ curves for an impingement type cold plate are provided from a published research paper. The proper dimensions (ID: 5 mm) for the tubes are used for the analysis. The equivalent power per CPU is provided for each cold plate to capture the heat dissipated from the CPUs. In this case, the power per CPU is considered higher than the processor TDP used in Cisco Server and 500W is used per cold plate for heat rejection. The server cooling loop consists of two pairs of quick disconnects (inlet and outlet). The quick disconnects (SCG05) provides dripless connection at the inlet and outlet of server liquid loop. The tubes from the server loop are connected to the inlet and outlet rack manifolds. The dimension of rack manifold is chosen as 25mmx25mm. The servers' components are provided with necessary elevations considering each server-to-server distance as 1U (1.75 inch or 44.45mm). The inlet and outlet of the

rack manifold is provided with constant flow rate and zero-gauge pressure boundary condition respectively. A PQ curve is generated for variation in flow rate and water is used as working fluid for the analysis. The derived curves are presented in Figure 44. The RQ curve is caloric thermal resistance curve.

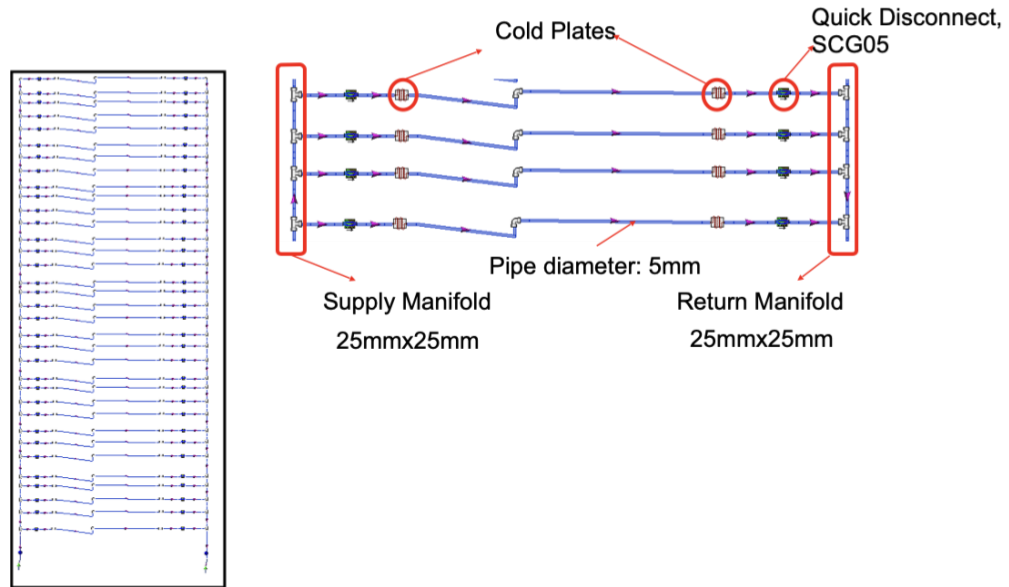

Figure 44 Rack Setup for FNM and Server Loop with cold plates, QDs connected to Rack Manifolds

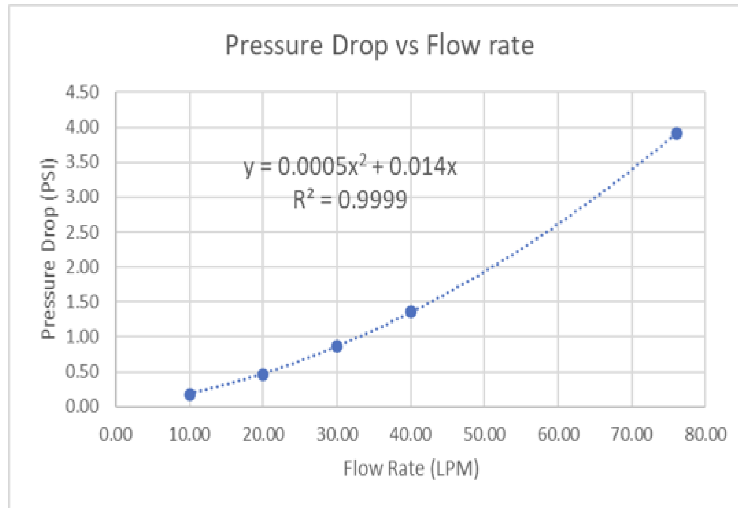

Figure 45 Pressure-drop and thermal resistance curve generated for the rack

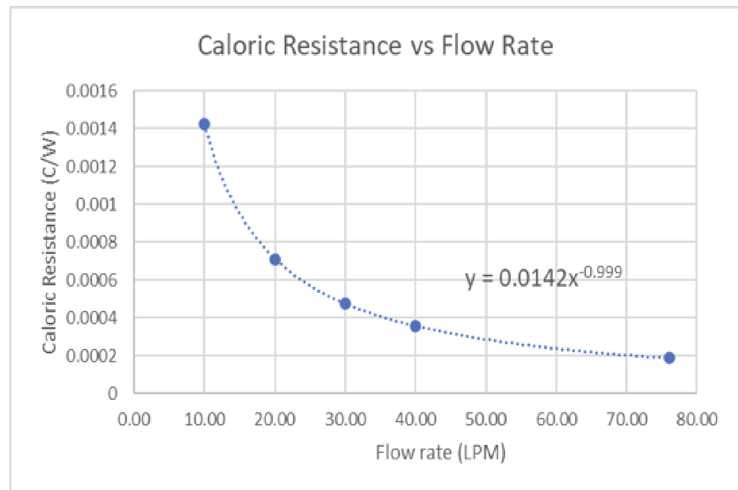

Figure 46 Caloric Thermal resistance curve generated for the rack

The rack manifolds are connected to a row manifold by a quick disconnect (SCG12). The row manifold consists of a header (ID: 2.5 inches) and ports (ID: 0.5 inch). The PQ curve of rack is provided as input for the racks. Propylene glycol (PG) and water mixture (25% PG and 75% DI Water) is used as working fluid. The

thermophysical properties for PG-25 is provide from the open source. Four racks considered for the analysis where each rack has common supply and return row manifold. The inlet of row manifold is provided with a constant flow rate boundary condition and outlet of row manifold is kept at zero-gauge pressure. The inlet and outlet pressure drop for the row manifold is measured at different flowrates for the loop (Figure 47).

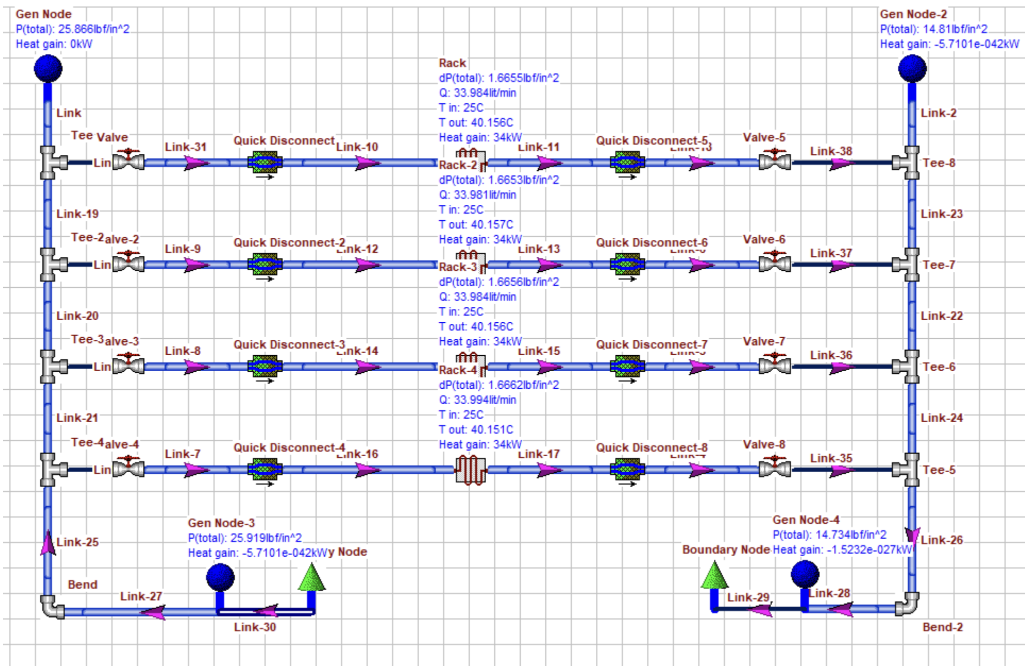

Figure 47 Liquid Cooling loop of a data center with 4 racks (34 servers/rack)

The property variation with temperature has been captured and performance of each component is checked for density and viscosity variation. The software allows for quick calculation of flow resistance curve for cooling loop of data center which can be helpful for selection for proper CDUs and pumps in the loop. The

flow rate for the whole loop depends on the required flow rate per server cooling loop and per cold plate to keep the junction temperature within limits. For the rack, 500W per CPU results in 34KW per rack for heat dissipation. In this case a parametric analysis has been performed for range of flow rate per rack ranging from 10-75 LPM per rack and 60-340LPM for whole data center cooling loop. The pressure inside the loop is also an important factor for which a separated curve of inlet pressure (absolute) values is provided in Figure 48 below.

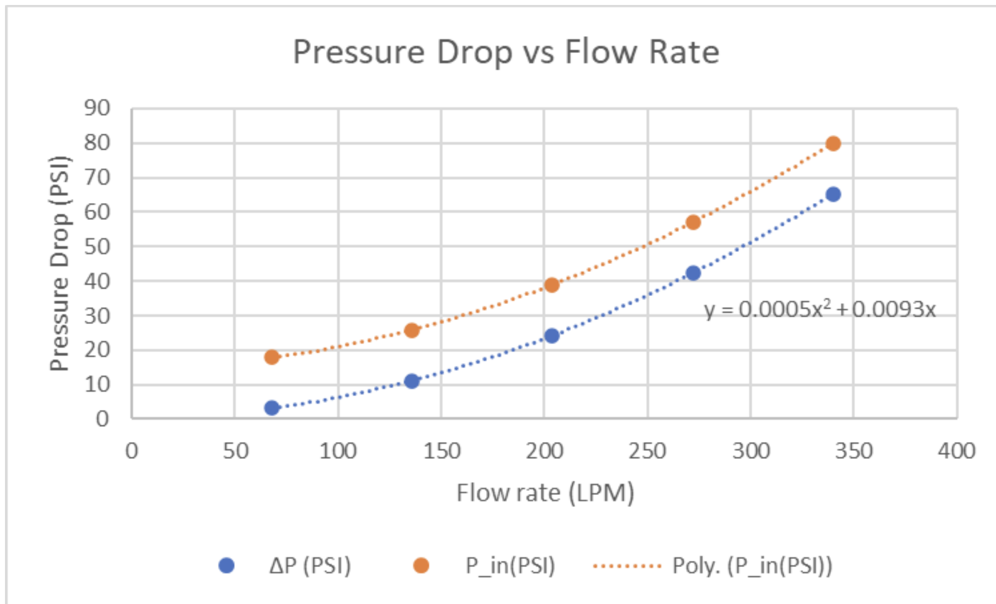

Figure 48 Flow resistance Curve for Data Center Cooling Loop with 4 Racks

From the figure it is noticed that maximum pressure of 80 Psi is possible for inlet to racks as the cooling loop is provided with 350 LPM. The pressure rating of the components should be checked while selecting the pipe and fittings per the ASHARE liquid cooling guidelines and following the operating conditions

described in ASME B31.3 and IEC-62368-1 with allowable (1.5x or 3X) maximum pressure ratings. The cooling capacity of heat exchangers in CDUs are needed to be selected to efficiently remove the heat for chosen coolant flowrate. This analysis helps also to understand amount of cooling power required in terms of pumping power required. The hybrid cooled server has fans and pumps. The fan power can be minimized as described in a paper and kept constant at 12W per sever for this analysis. So, reduction in pumping power for pumps is possible based on the flow rate reduction. The table below shows the possible reduction in cooling power and pPUE values for the flow network model from the derived data for pressure drop and flow rate for calculating the pumping power for the whole data center loop.

Table 6 Cooling power for the liquid cooling loop for 4 racks and pPUE values

Flow rate (LPM)	fan power KW	Pumping power KW	pPUE
68	1.632	0.02426266	1.012178
136	1.632	0.175253768	1.013289
204	1.632	0.56994982	1.016191
272	1.632	1.324358371	1.021738
340	1.632	2.554768283	1.030785

Chapter 6

Total Cost of Ownership (TCO) Analysis for a Hybrid Cooled Data Center

The total cost of ownership is a comprehensive tool which counts the cost of individual components from the chip to chiller involving all capital and operational expenses. The cost calculations include planning, preparation, deployment, power, infrastructure, IT equipment, software, cooling, maintenance, and other expenditures for building and running a data center. There have been many publications for simplifying the cost calculations and preparing methods for cost calculation with the best practices implemented for operating a data center. Over the years, the rack power density is increasing for the use of high-powered compute nodes to meet the ever-growing computational demand. The new cooling technologies are adopted to overcome the cooling challenges to maintain the standard IT equipment reliability. Sometimes, the infrastructure of the data center from inside and outside must be modified to meet the cooling requirements. There are additional costs involved for the right choice of equipment, racks, rails, cable management, aisle containments, heat exchangers, Power Distribution Units (PDUs), software acquisition and security, network equipment, emergency power supply, building management systems etc. So, the cost of the items is interlinked and change in one parameter affects others. So, there are some assumptions and

simplifications being made to use one TCO model to fit for a data center of choice. In this analysis, an established TCO model has been used and change in IT heat load, PUE and cooling modes are used to calculate and compare liquid cooling with air cooling providing the gains in cooling efficiency.

6.1 TCO model

The selected TCO model breaks down the total cost into the following categories. The breakdown of costs includes infrastructure, server, network, power, maintenance, and other costs. The individual cost is described in detail in the paper[100].

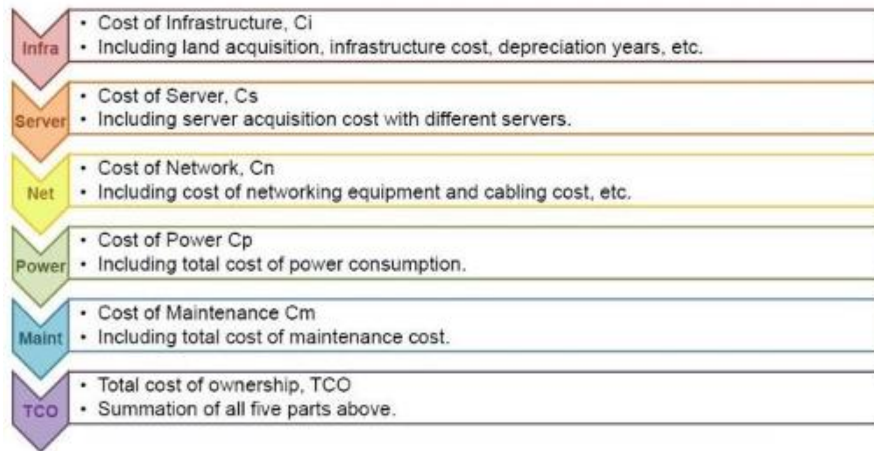

Figure 49 Overview of Cost Model

The infrastructure cost C_i is calculated from the costs involved with server and network power consumption, energy efficiency, occupancy in rack, capital costs involved in land, building and cooling infrastructure.

$$C_i = \frac{C_{sqm} \times A_{rack} \times N_{rack} \times K_{occupancy}}{12 \times T_{building}} + \frac{(SPUE \times P_{server} + P_{net}) \times C_{cp,w}}{12 \times T_{cooling}} \quad (7)$$

The server cost consists of server acquisition cost which can be either a lumped server model or comprising all the components inside a server. The online rate of server is also given inside the model to account for heat dissipation based on usage. The components also include the cost of heatsinks and cold plates for air and liquid cooling in this analysis.

$$C_s = \frac{N_{server} \times C_{server}}{12 \times T_{server}} \quad (8)$$

$$N_{server} = N_{server-IT} \times OR \quad (9)$$

$$C_{server} = \begin{cases} C_{server-v} \\ \sum_i N_{comp,i} \times \left(C_{comp,i} + C_{SLA,i}\right) \end{cases} \quad (10)$$

The network acquisition cost includes the cost of core/cable and rack network equipment for their relative number and power consumption. The cost is kept fixed for the analysis and comparison.

$$C_n = \frac{C_{core-node} \times N_{server}}{12 \times T_{core}} + \frac{C_{netperrack} \times N_{rack}}{12 \times T_{net-rack}} \quad (11)$$

The total electrical power cost consists of the cost per KWh consumed by the IT equipment, PDUs, losses in power distribution, cooling processes. The

power consumption of the server and cooling can be optimized for air and liquid cooling and efficiency metrics such as PUE and SPUE are included in the calculations for the total power consumption.

$$C_p = \frac{C_{e-KWh} \times 30 \times 24}{1000} \times PUE \times (SPUE \times P_{server} + P_{net}) \quad (12)$$

$$P_{server} = \begin{cases} P_{server-peak} = P_{ss-peak} \times U_{ss} \times P_{ss-idle} \times (1 - U_{ss}) \\ P_{server-avg} = P_{ss-avg} \times U_{ss} \times P_{ss-idle} \times (1 - U_{ss}) \end{cases} \quad (13)$$

The maintenance cost can vary but for our analysis the cost is kept same for comparison as the cost is proportional to the failure rate of components.

$$C_m = \left[\frac{C_{server} \times N_{server} \times ARR_{server}}{12} + \left(C_{rep-cost} \times ARR_{server} + \sum_i AFR_{comp,i} \times N_{comp,i} \times C_{comp,i} \right) \times \left(T_{server} - T_{warranty} \right) + C_{labor} \right] \times \frac{1}{12 \times T_{server}} \quad (14)$$

The server is the contributing factor as it is the heat of data center performance and the failure of IT equipment should be given priority. The replacement cost, cold spare cost and labor hourly rate are added in the equation with rates of failure in the cost calculation for maintenance.

The total cost of ownership is calculated by adding all the cost for infrastructure, server, network, power, and maintenance.

$$TCO = C_i + C_s + C_n + C_p + C_m \quad (15)$$

6.2 Assumptions

The costs of land acquisition, power distribution and cooling infrastructure are kept same for the comparison. The rack dimensions are provided for a standard 42U unit rack dimension and an extra area (1.25 times) for cooling and power distribution is considered in the model. The depreciation years for infrastructure, cooling, servers are considered as 15, 10, 5 years respectively. The racks considered to occupy only server of 1U height, and 38 servers are considered in one rack. Total numbers of server and rack are 300,000 and 7895. The electricity cost per KWh is based on average value of 0.1167$/KWh. The peak power for the network equipment is provided as180 W for all cases as an assumption and utilization is provided to the max (100%). Thus, the cost of networking equipment for all the racks are same for all cases being presented for the sake of simplicity. Sever acquisition cost is calculated as a lumped model for air cooling while for liquid cooling it is considered as detailed model considering the cost of components in liquid cooling loop. Duration of warranty for IT equipment is 3 years from the time of acquisition. The number of cold spares and cost of replacement are calculated

based on the depreciation and SLA agreement years with the failure rate of each component and per hour labor cost. For the analysis, the costs per IT equipment and maintenance are kept same for air cooling with the use of CRAC, In-row Cooler (IRC), Overhead Cooling Unit (OCU), Bottom Cooling Unit (BCU) and Indirect Evaporative Cooling (IDEC). But the numbers are changed as the IT equipment component changes for the addition of liquid cooled components. The server power utilization and power consumption (peak and idle) are provided differently for air and liquid cooling. The PUE numbers are also varied in the case studies.

6.3 Case Studies and Results

The average utilization of servers is provided as 80% for air cooling while each server is using the peak load condition. The peak and idle power consumptions are respectively 404W and 160W. The PUE is an important factor as it is used for total power calculation and the values of PUE for CRAC, IRC, OCU, BCU and IDEC are respectively 1.3, 1.21, 1.2, 1.065, 1.035. IDEC and CRAC PUE values are like the used values in the paper.

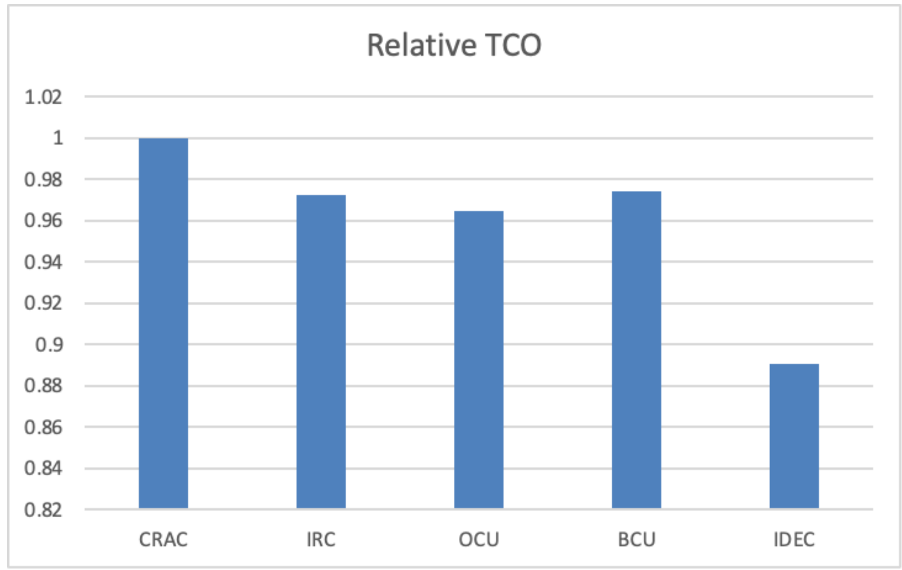

Figure 50 Relative TCO of Different Kind of Cooling Technology with Respect to CRAC

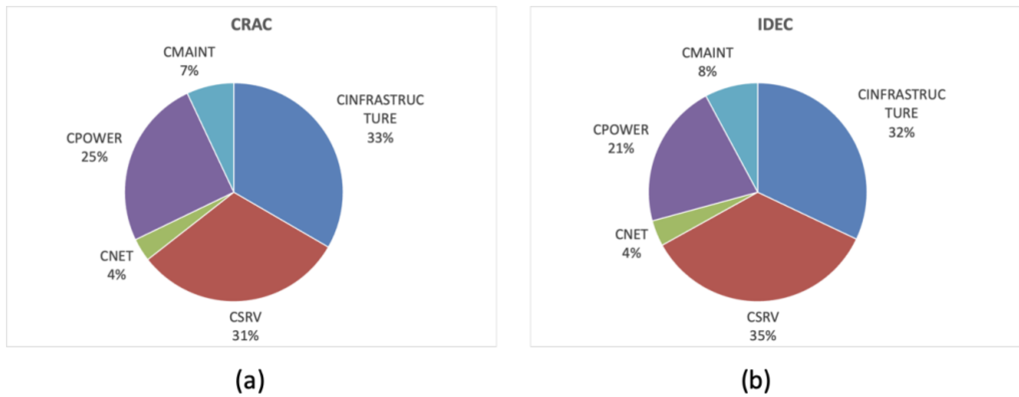

Figure 51 Percentage of costs for infrastructure, maintenance, power, network equipment and server acquisition with (a) CRAC and (b) IDEC

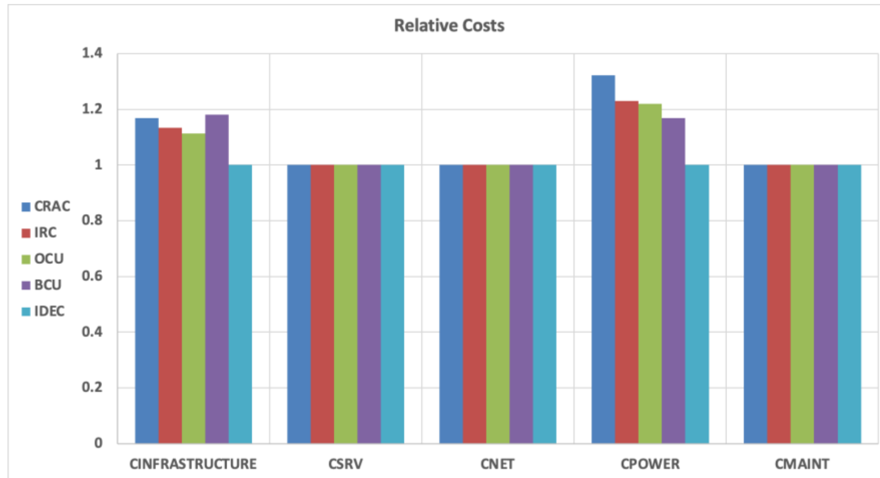

Figure 52 Relative contribution of costs for infrastructure, maintenance, power, network equipment and server acquisition with CRAC, IRC, OCU, BCU and IDEC

The cost reduction for IDEC is due to the lowest PUE and reduction in total infrastructure cost for the elimination of chiller plant outside of data center. Maintenance, server acquisition and network cost are similar but shows different percentage in Figure 51 as the infrastructure and power cost are different for each type of cooling technique shown in Figure 52.

For liquid cooling, the server peak power is increased to 1500W and server power utilization is considered as 98%. The components for liquid cooling components are added to the detailed model for server cost calculation replacing the lumped model used for air-cooling. The maintenance cost is also being impacted by the change in components and failure rates of each component. The infrastructure cost is also highest for liquid cooling deployment than other cooling technologies used in the analysis. The PUE for RDHX is 1.21 and for liquid cooling

it is 1.065 which is assumed to be the lowest of all as minimum fan power and pump power can be considered for hybrid cooling power per server. PUE value for CRAC, OCU and IDEC is kept constant at 1.3. IRC and OCU technology are replaced with Rear Door Heat Exchanger (RDHX) and liquid cooling (LC) in this analysis. The results are presented as relative cost and cost contributions in the TCO model.

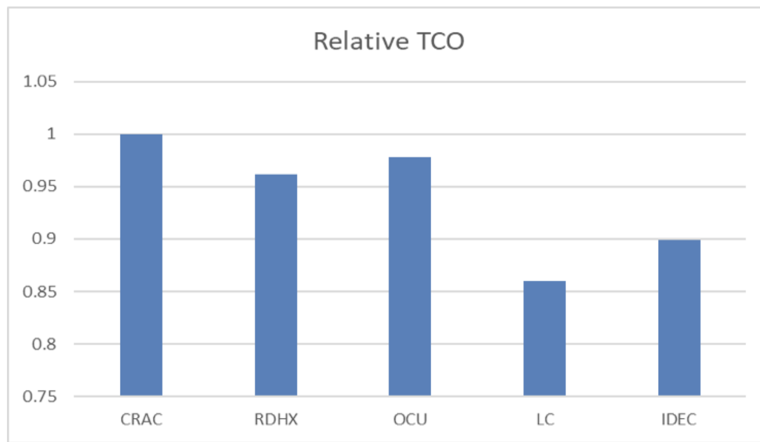

Figure 53 Relative TCO of Different Kind of Cooling Technology with Respect to CRAC

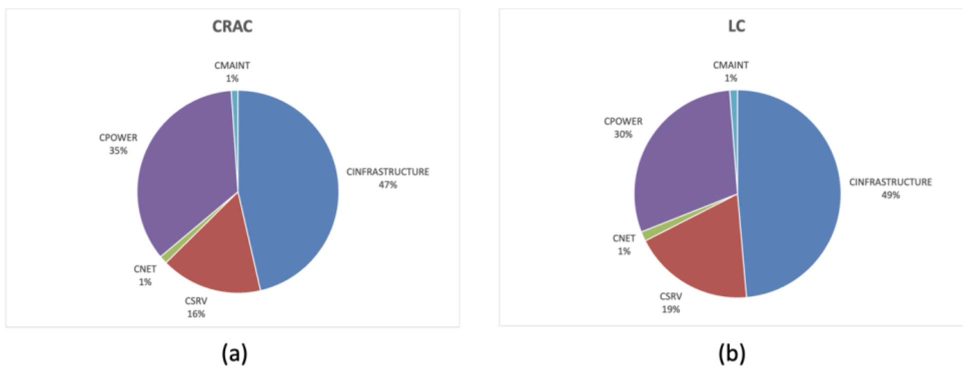

Figure 54 Percentage of costs for infrastructure, maintenance, power, network equipment and server acquisition with (a) CRAC and (b) LC

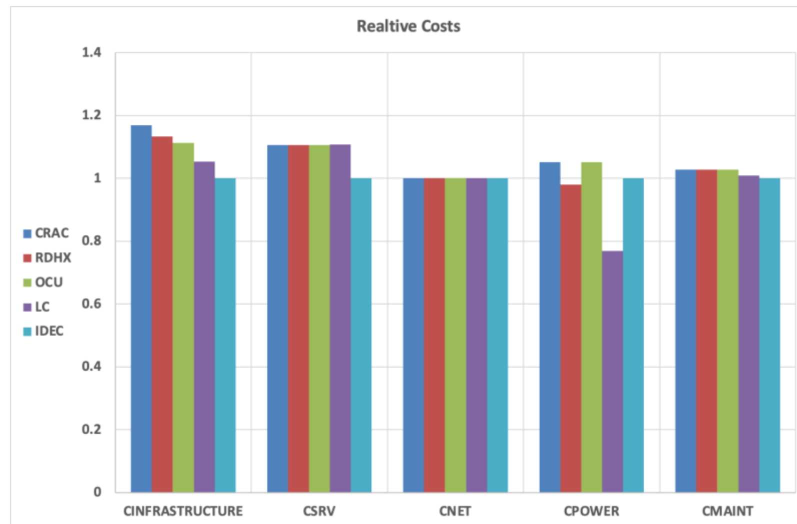

Figure 55 Relative contribution of costs for infrastructure, maintenance, power, network equipment and server acquisition with CRAC, RDHX, OCU, LC and IDEC

The effect of cooling efficiency has a direct impact on the total cost of ownership. More efficient systems provide better cooling with cost minimization which is highlighted in Figure 56 below. When PUE for LC is changed from 1.065 to 1.15, the LC relative cost has increased. So, the efficiency improvement on liquid and air cooling can yield better design of data center.

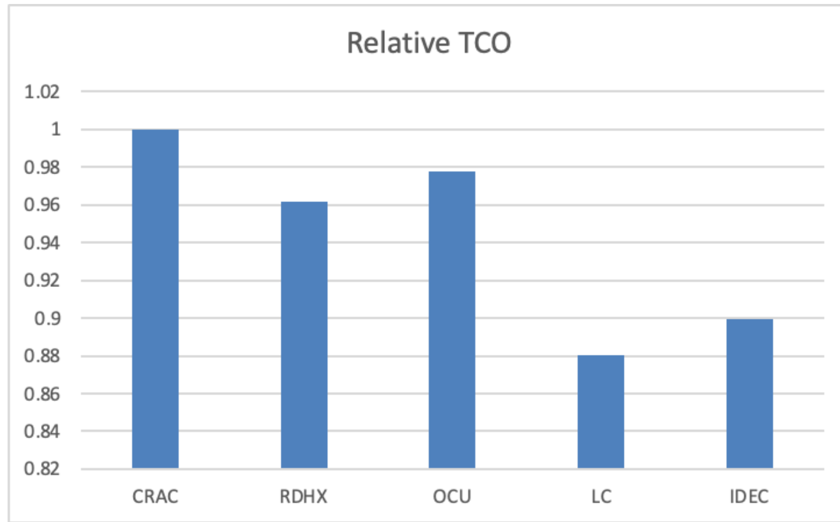

Figure 56 Relative TCO of Different Kind of Cooling Technology with Respect to CRAC when PUE for LC is increased.

Conclusion

6.4 Optimal Design and Modeling of Server Cabinets with In-Row Coolers and Air Conditioning Units in a Modular Data Center

Contained systems work better than open systems but the choice for keeping the doors open or closed can be easily decided based on the results shown for temperatures for different situations. Hot and cold aisle containment is created for MEC cabinet to obtain better results. Rack heat density is increased with two configurations and results are compared for with and without containment for MEC cabinet. With high heat load the temperature values are unrealistic and unacceptable. Closed loop solution for high-powered racks in MEC cabinet is the best available option for ensuring better thermal management of high heat generating servers in MEC cabinet. The failure scenarios provide viable solution for redundancy and show a guideline to choose the optimum level of cooling capacity of in-row coolers. The choices on the numbers of in-row cooler, their capacity can easily be estimated. In-row coolers with 24.62 KW and 2900 CFM works better as it can provide adequate cooling when fans in one of the in-row coolers fail. With containment the rack power density can be increased to 7.88 KW and cooling capacity of external ACUs can also be reduced. This method is useful where only one row of racks is present and hot and cold aisle containment requires a large footprint compared to the room size. More cabinets can be deployed, and

computational capacity can be increased within a small footprint. The flow rate from the in-row cooler can be controlled for optimum delivery of cooling to the IT equipment based on sensor data at server inlet and outlet with sensible cooling. The effective rate of heat removal can be enhanced, and cooling efficiency can also be increased by utilizing free cooling or available supply water. More accurate results can be generated if the servers and racks are designed with flow curves after experimental testing of servers and racks.

6.5 Raised Inlet Temperature of Air and Coolant for Hybrid Cooled Server

The cooling efficiency increases for the reduction in the total cooling power used per IT equipment. So, there is a continuous drive for drive for decreasing the pumping power for fans and pumps and increasing the inlet temperature as it reduces the cooling capacity and power consumption for the CRAH/CRAC and CDUs. As liquid cooling is used on an air-cooled server, warm water cooling can be used and side by side the inlet air temperature can be increased. But the limits can be different based on the thermal margin available from junction to ambient and coolant. It has been observed that higher inlet coolant temperature results in very lower PUE for a data center and even eliminates the use of chiller on the primary side. So, lowering the air-cooling capacity and fan power can help in reducing the total cooling power further. The ASHRAE liquid cooling guidelines

provides the configuration on the primary side (chiller-W3 or chiller less-W4) with the proper selection of inlet coolant temperature for liquid cooling loop. For the air-cooled components, the temperatures and relative humidity for recommended zone in ASHARE air cooling classes can be extended and higher inlet air conditions can be chosen such as A1-A4 based on the component power level and required fan power. The free cooling can be extensively used with the help of evaporative cooling such as direct and indirect evaporative cooling. Thus, there is potential to increase the cooling efficiency without affecting the component reliability and performance.

6.6 One Dimensional Flow Network Analysis

The FNM analysis provided a quick way to check the deployment of cold plates in a rack. For the server as there are two CPUs, two cold plates are used and empirical data for the cold plates are provided to have realistic prediction of heat transfer to the coolant. The flow rate and pressure drop limits show the choice of flow rate and its effect on the similar rack deployment in a data center. The selection of heat exchanger and choice of diameter of pipe also have limitations from the junction temperature limit, cold late performance and diameter of pipes and hoses while considering standards in ASHARE, ASME. The pumping power for liquid loop is used to predict the pPUE.

6.7 Total Cost of Ownership (TCO) Analysis for Hybrid Cooled Data Center

The cost comparison of air and liquid cooling was done with an established TCO model which considers the industrial best practices. As it is based on some assumptions, the variation in actual deployment and performance may be different from the cases presented here. More accurate values can be generated if the model is used with detail analysis of liquid cooling components from primary and secondary sides, power arrangement and management costs and server failure rates and reliability data. The PUE values used in the analysis can also be refined with the values of proper kind of deployment on a large-scale deployment. The land acquisition, rent and interest rates can be added to the model to be more realistic representation. But considering the assumptions in the results being presented, it can be noted that the LC provides better choice for high powered 1U hybrid cooled systems in a data center and the free cooling can be used to manage the air-cooling load with relatively lower cost than other air-cooling technologies. The efficiency improvement can also be focused based on the need for the cost minimization for scope of performance improvement on cold plate, server, rack, and data center level.

References

[1] M. K. Patterson, "Liquid cooling guidelines," in *Proceedings of the 2011 workshop on Energy Efficiency: HPC System and Datacenters - EE-HPC-WG '11*, Seattle, Washington, USA, 2011, p. 155. doi: 10.1145/2159344.2159349.

[2] E. Masanet, A. Shehabi, N. Lei, S. Smith, and J. Koomey, "Recalibrating global data center energy-use estimates," *Science*, vol. 367, no. 6481, pp. 984–986, Feb. 2020, doi: 10.1126/science.aba3758.

[3] "How Much Energy Do Data Centers Really Use?," *Energy Innovation: Policy and Technology*, Mar. 17, 2020. https://energyinnovation.org/2020/03/17/how-much-energy-do-data-centers-really-use/ (accessed Feb. 22, 2021).

[4] C. Malone and C. Belady, Metrics to Characterize Data Center & IT Equipment Energy Use, Proceedings of Digital Power Forum, Richardson, TX. 2006.

[5] A. Shehabi *et al.*, "United States Data Center Energy Usage Report," 2016.

[6] S. Zhang, N. Ahuja, Y. Han, H. Ren, Y. Chen, and G. Guo, "Key considerations to implement high ambient data center," in *2015 31st Thermal*

Measurement, Modeling Management Symposium (SEMI-THERM), Mar. 2015, pp. 147–154. doi: 10.1109/SEMI-THERM.2015.7100153.

[7] A. Habibi Khalaj and S. K. Halgamuge, “A Review on efficient thermal management of air- and liquid-cooled data centers: From chip to the cooling system,” *Appl. Energy*, vol. 205, pp. 1165–1188, Nov. 2017, doi: 10.1016/j.apenergy.2017.08.037.

[8] “ashrae_2011_thermal_guidelines_data_center.pdf.” [Online]. Available: https://tc0909.ashraetcs.org/documents/ASHRAE_TC0909_Power_White_Paper_22_June_2016_REVISED.pdf

[9] “Liquid Cooling Guidelines for Datacom Equipment Centers, 2nd Ed. | ASHRAE Store.” https://www.techstreet.com/ashrae/standards/liquid-cooling-guidelines-for-datacom-equipment-centers-2nd-ed?ashrae_auth_token=&gateway_code=ashrae&product_id=1873288 (accessed Apr. 28, 2021).

[10] R. H. Dennard, F. H. Gaensslen, H.-N. Yu, V. L. Rideout, E. Bassous, and A. R. Leblanc, “Design of Ion-Implanted MOSFET’s with Very Small Physical Dimensions,” *Proc. IEEE*, vol. 87, no. 4, p. 11, 1999.

[11] “The end of Dennard scaling – cartesian product.” https://cartesianproduct.wordpress.com/2013/04/15/the-end-of-dennard-scaling/ (accessed May 13, 2021).

[12] “Is There Finally A Silver Bullet For Software?,” *Semiconductor Engineering*, Feb. 27, 2020. https://semiengineering.com/is-there-finally-a-silver-bullet-for-software/ (accessed May 13, 2021).

[13] H. Esmaeilzadeh, E. Blem, R. Amant, K. Sankaralingam, and D. Burger, *Dark Silicon and the End of Multicore Scaling*, vol. 32. 2011, p. 376. doi: 10.1145/2024723.2000108.

[14] Association for Computing Machinery (ACM), *John Hennessy and David Patterson 2017 ACM A.M. Turing Award Lecture*, (Jun. 04, 2018). Accessed: May 13, 2021. [Online Video]. Available: https://www.youtube.com/watch?v=3LVeEjsn8Ts

[15] S. Paredes, Y. Madhour, G. Schlottig, and C. Ong, *(Invited) Wafer-Level Integration of Embedded Cooling Approaches*, vol. 64. 2014. doi: 10.1149/06405.0253ecst.

[16] White Paper Developed by, “Water-Cooled Servers Common Designs, Components, and Processes,” p. 50.

[17] B. Tschudi and O. VanGeet, “U.S. Department of Energy FEMP william.lintner.ee.doe.gov 202-586-3120,” p. 28.

[18] R. Schmidt *et al.*, “Maintaining Datacom Rack Inlet Air Temperatures With Water Cooled Heat Exchanger,” Mar. 2009, pp. 663–673. doi: 10.1115/IPACK2005-73468.

[19] R. Schmidt, M. Iyengar, D. Porter, G. Weber, D. Graybill, and J. Steffes, “Open side car heat exchanger that removes entire server heat load without any added fan power,” in *2010 12th IEEE Intersociety Conference on Thermal and Thermomechanical Phenomena in Electronic Systems*, Jun. 2010, pp. 1–6. doi: 10.1109/ITHERM.2010.5501423.

[20] L. Silva-Llanca, M. del Valle, A. Ortega, and A. Díaz, “Cooling Effectiveness of a Data Center Room under Overhead Airflow via Entropy Generation Assessment in Transient Scenarios,” *Entropy*, vol. 21, no. 1, p. 98, Jan. 2019, doi: 10.3390/e21010098.

[21] T. Gao *et al.*, “Innovative server rack design with bottom located cooling unit,” in *2016 15th IEEE Intersociety Conference on Thermal and Thermomechanical Phenomena in Electronic Systems (ITherm)*, May 2016, pp. 1172–1181. doi: 10.1109/ITHERM.2016.7517681.

[22] A. C. Kheirabadi and D. Groulx, “Cooling of server electronics: A design review of existing technology,” *Appl. Therm. Eng.*, vol. 105, pp. 622–638, Jul. 2016, doi: 10.1016/j.applthermaleng.2016.03.056.

[23] M. J. Ellsworth, L. A. Campbell, R. E. Simons, M. K. Iyengar, R. R. Schmidt, and R. C. Chu, "The evolution of water cooling for IBM large server systems: Back to the future," in *2008 11th Intersociety Conference on Thermal and Thermomechanical Phenomena in Electronic Systems*, May 2008, pp. 266–274. doi: 10.1109/ITHERM.2008.4544279.

[24] G. Patankar and T. R. Salamon, "Maldistribution of Two-Phase Flow in Parallel Channel Heat Sinks: Effects of Thermal Connection Between Channels," in *2018 17th IEEE Intersociety Conference on Thermal and Thermomechanical Phenomena in Electronic Systems (ITherm)*, May 2018, pp. 653–663. doi: 10.1109/ITHERM.2018.8419551.

[25] T. Salamon, R. L. Amalfi, N. Lamaison, J. B. Marcinichen, and J. R. Thome, "Two-phase liquid cooling system for electronics, part 1: Pump-driven loop," in *2017 16th IEEE Intersociety Conference on Thermal and Thermomechanical Phenomena in Electronic Systems (ITherm)*, Orlando, FL, May 2017, pp. 667–677. doi: 10.1109/ITHERM.2017.7992551.

[26] Yu. F. Maydanik, M. A. Chernysheva, and V. G. Pastukhov, "Review: Loop heat pipes with flat evaporators," *Appl. Therm. Eng.*, vol. 67, no. 1, pp. 294–307, Jun. 2014, doi: 10.1016/j.applthermaleng.2014.03.041.

[27] M. Bulut, S. G. Kandlikar, and N. Sozbir, "A Review of Vapor Chambers," *Heat Transf. Eng.*, vol. 40, no. 19, pp. 1551–1573, Nov. 2019, doi: 10.1080/01457632.2018.1480868.

[28] B. Ramakrishnan, S. H. Bhavnani, J. Gess, R. W. Knight, D. Harris, and R. W. Johnson, "Effect of system and operational parameters on the performance of an immersion-cooled multichip module for high performance computing," in *2014 Semiconductor Thermal Measurement and Management Symposium (SEMI-THERM)*, Mar. 2014, pp. 24–28. doi: 10.1109/SEMI-THERM.2014.6892210.

[29] M. Shojaeian and A. Koşar, "Pool boiling and flow boiling on micro- and nanostructured surfaces," *Exp. Therm. Fluid Sci.*, vol. 63, pp. 45–73, May 2015, doi: 10.1016/j.expthermflusci.2014.12.016.

[30] R. Cardenas and V. Narayanan, "Heat transfer characteristics of submerged jet impingement boiling of saturated FC-72," *Int. J. Heat Mass Transf.*, vol. 55, no. 15, pp. 4217–4231, Jul. 2012, doi: 10.1016/j.ijheatmasstransfer.2012.03.063.

[31] E. A. Silk, E. L. Golliher, and R. Paneer Selvam, "Spray cooling heat transfer: Technology overview and assessment of future challenges for micro-gravity application," *Energy Convers. Manag.*, vol. 49, no. 3, pp. 453–468, Mar. 2008, doi: 10.1016/j.enconman.2007.07.046.

[32] M. Zhang, Z. Zhang, Y. Hu, Y. Geng, H. Huang, and Y. Huang, "Effect of raised floor height on different arrangement of under-floor air distribution performance in data center," *Procedia Eng.*, vol. 205, pp. 556–564, Jan. 2017, doi: 10.1016/j.proeng.2017.10.425.

[33] S. A. Nada, M. A. Said, and M. A. Rady, "CFD investigations of data centers' thermal performance for different configurations of CRACs units and aisles separation," *Alex. Eng. J.*, vol. 55, no. 2, pp. 959–971, Jun. 2016, doi: 10.1016/j.aej.2016.02.025.

[34] S. V. Patankar, "Airflow and Cooling in a Data Center," *J. Heat Transf.*, vol. 132, no. 073001, Apr. 2010, doi: 10.1115/1.4000703.

[35] S. Saini, "AIRFLOW PATH AND FLOW PATTERN ANALYSIS OF SUB-MICRON PARTICULATE CONTAMINANTS IN A DATA CENTER WITH HOT-AISLE CONTAINMENT UTILIZING DIRECT AIR COOLING," p. 58.

[36] S. Saini, P. Shahi, P. Bansode, A. Siddarth, and D. Agonafer, "CFD Investigation of Dispersion of Airborne Particulate Contaminants in a Raised Floor Data Center," in *2020 36th Semiconductor Thermal Measurement, Modeling Management Symposium (SEMI-THERM)*, Mar. 2020, pp. 39–47. doi: 10.23919/SEMI-THERM50369.2020.9142865.

[37] M. Iyengar, R. Schmidt, V. Kamath, and P. Singh, “Energy efficient economizer based data centers with air cooled servers,” in *13th InterSociety Conference on Thermal and Thermomechanical Phenomena in Electronic Systems*, San Diego, CA, USA, May 2012, pp. 367–376. doi: 10.1109/ITHERM.2012.6231453.

[38] Y. Hadad *et al.*, “Three-objective shape optimization and parametric study of a micro-channel heat sink with discrete non-uniform heat flux boundary conditions,” *Appl. Therm. Eng.*, vol. 150, pp. 720–737, Mar. 2019, doi: 10.1016/j.applthermaleng.2018.12.128.

[39] SatishG. Kandlikar and CliffordN. Hayner II, “Liquid Cooled Cold Plates for Industrial High-Power Electronic Devices—Thermal Design and Manufacturing Considerations,” *Heat Transf. Eng.*, vol. 30, no. 12, pp. 918–930, Oct. 2009, doi: 10.1080/01457630902837343.

[40] M. J. Ellsworth and L. A. Campbell, “Theoretical (Ideal) Module Cooling and Module Cooling Effectiveness,” presented at the ASME 2015 International Technical Conference and Exhibition on Packaging and Integration of Electronic and Photonic Microsystems collocated with the ASME 2015 13th International Conference on Nanochannels, Microchannels, and Minichannels, Nov. 2015. doi: 10.1115/IPACK2015-48324.

[41] M. Datta *et al.*, “Liquid Cooling System for Advanced Microelectronics,” *ECS Trans.*, vol. 6, no. 8, p. 13, Sep. 2007, doi: 10.1149/1.2794452.

[42] P. Shahi, S. Agarwal, S. Saini, A. Niazmand, P. Bansode, and D. Agonafer, “CFD Analysis on Liquid Cooled Cold Plate Using Copper Nanoparticles,” presented at the ASME 2020 International Technical Conference and Exhibition on Packaging and Integration of Electronic and Photonic Microsystems, Dec. 2020. doi: 10.1115/IPACK2020-2592.

[43] M. J. Ellsworth, “Flow network analysis of the IBM Power 775 supercomputer Water Cooling System,” in *Fourteenth Intersociety Conference on Thermal and Thermomechanical Phenomena in Electronic Systems (ITherm)*, May 2014, pp. 715–722. doi: 10.1109/ITHERM.2014.6892351.

[44] M. Sahini, C. Kshirsagar, P. McGinn, and D. Agonafer, “Rack-Level Study of Hybrid Cooled Servers Using Warm Water Cooling With Variable Pumping for Centralized Coolant System,” presented at the ASME 2018 International Technical Conference and Exhibition on Packaging and Integration of Electronic and Photonic Microsystems, Nov. 2018. doi: 10.1115/IPACK2018-8255.

[45] C. Kim and J. Chang, “Corrosion in a closed-loop electronic device cooling system with water as coolant and its detection,” in *2017 16th IEEE*

Intersociety Conference on Thermal and Thermomechanical Phenomena in Electronic Systems (ITherm), May 2017, pp. 558–564. doi: 10.1109/ITHERM.2017.7992536.

[46] M. Iyengar *et al.*, “Extreme energy efficiency using water cooled servers inside a chiller-less data center,” in *13th InterSociety Conference on Thermal and Thermomechanical Phenomena in Electronic Systems*, May 2012, pp. 137–149. doi: 10.1109/ITHERM.2012.6231424.

[47] D. Gandhi et al., Computational Analysis for Thermal Optimization of Server for Single Phase Immersion Cooling. 2019. doi: 10.1115/IPACK2019-6587.

[48] J. M. Shah, R. Eiland, P. Rajmane, A. Siddarth, D. Agonafer, and V. Mulay, “Reliability Considerations for Oil Immersion-Cooled Data Centers,” *J. Electron. Packag.*, vol. 141, no. 2, Jun. 2019, doi: 10.1115/1.4042979.

[49] “WP#49 - PUE: A Comprehensive Examination of the Metric | The Green Grid.” https://www.thegreengrid.org/en/resources/library-and-tools/237-PUE%3A-A-Comprehensive-Examination-of-the-Metric (accessed Apr. 29, 2021).

[50] “The Green Grid Unveils Energy Productivity Metric for Data Centers,” *Data Center Knowledge*, Mar. 20, 2014.

https://www.datacenterknowledge.com/archives/2014/03/20/green-grid-unveils-energy-productivity-metric-data-centers (accessed May 13, 2021).

[51] N. Rasmussen and V. Avelar, “Deploying High-Density Pods in a Low-Density Data Center,” p. 21.

[52] M. K. Herrlin, Method for Optimizing Equipment Cooling Effectiveness and HVAC Cooling Costs in Telecom and Data Centers. 2019.

[53] B. A. Rubenstein, R. Zeighami, R. Lankston, and E. Peterson, “Hybrid cooled data center using above ambient liquid cooling,” in *2010 12th IEEE Intersociety Conference on Thermal and Thermomechanical Phenomena in Electronic Systems*, Jun. 2010, pp. 1–10. doi: 10.1109/ITHERM.2010.5501426.

[54] R. Zeighami, W. A. Saunders, H. Coles, and S. Branton, “Thermal performance modeling of hybrid liquid-air cooled servers,” in *Fourteenth Intersociety Conference on Thermal and Thermomechanical Phenomena in Electronic Systems (ITherm)*, May 2014, pp. 583–587. doi: 10.1109/ITHERM.2014.6892333.

[55] T. Gao, M. David, J. Geer, R. Schmidt, and B. Sammakia, “A dynamic model of failure scenarios of the dry cooler in a liquid cooled chiller-less data center,” in *2015 31st Thermal Measurement, Modeling Management Symposium (SEMI-THERM)*, Mar. 2015, pp. 113–119. doi: 10.1109/SEMI-THERM.2015.7100149.

[56] S. Alkharabsheh, U. L. N. Puvvadi, B. Ramakrishnan, K. Ghose, and B. Sammakia, "Failure Analysis of Direct Liquid Cooling System in Data Centers," *J. Electron. Packag.*, vol. 140, no. 2, p. 020902, May 2018, doi: 10.1115/1.4039137.

[57] U. Puvvadi, A. Desu, T. Stachecki, S. Alkharabsheh, K. Ghose, and B. Sammakia, "Flow Disruptions and Mitigation in Virtualized Water-Cooled Data Centers," in *2019 IEEE 17th International Conference on Industrial Informatics (INDIN)*, Jul. 2019, vol. 1, pp. 1435–1442. doi: 10.1109/INDIN41052.2019.8972096.

[58] U. Puvvadi, A. Desu, T. Stachecki, K. Ghose, and B. Sammakia, "An Adaptive Approach for Dealing with Flow Disruption in Virtualized Water-Cooled Data Centers," in *2019 IEEE 12th International Conference on Cloud Computing (CLOUD)*, Jul. 2019, pp. 296–300. doi: 10.1109/CLOUD.2019.00057.

[59] L. Li, W. Zheng, X. Wang, and X. Wang, "Coordinating Liquid and Free Air Cooling with Workload Allocation for Data Center Power Minimization," p. 12.

[60] Xiaojin Wei, G. Goth, P. Kelly, R. Zoodsma, and A. VanDeventer, "Air-water hybrid cooling for computer servers: A case study for optimum cooling energy allocation," in *Fourteenth Intersociety Conference on Thermal and*

Thermomechanical Phenomena in Electronic Systems (ITherm), May 2014, pp. 568–573. doi: 10.1109/ITHERM.2014.6892331.

[61] V. Zavrel, M. Barták, and J. Hensen, "Simulation of a data center cooling system in emergency situation," vol. 24, pp. 155–159, Sep. 2015.

[62] "Thermal Storage System Provides Emergency Data Center Cooling | Connected Social Media." https://connectedsocialmedia.com/6058/thermal-storage-system-provides-emergency-data-center-cooling/ (accessed Feb. 20, 2021).

[63] U. Chowdhury, M. Sahini, A. Siddarth, D. Agonafer, and S. Branton, "Characterization of an Isolated Hybrid Cooled Server With Failure Scenarios Using Warm Water Cooling," in *ASME 2017 International Technical Conference and Exhibition on Packaging and Integration of Electronic and Photonic Microsystems*, San Francisco, California, USA, Aug. 2017, p. V001T02A002. doi: 10.1115/IPACK2017-74028.

[64] R. Kasukurthy, A. Rachakonda, and D. Agonafer, "Design and Optimization of Control Strategy to Reduce Pumping Power in Dynamic Liquid Cooling," *J. Electron. Packag.*, vol. 143, no. 031001, Jan. 2021, doi: 10.1115/1.4049018.

[65] P. R. Parida, T. J. Chainer, M. D. Schultz, and M. P. David, "Cooling Energy Reduction During Dynamically Controlled Data Center Operation,"

presented at the ASME 2013 International Technical Conference and Exhibition on Packaging and Integration of Electronic and Photonic Microsystems, Jan. 2014. doi: 10.1115/IPACK2013-73208.

[66] H.-J. Xu, J.-X. Wang, Y.-Z. Li, Y.-J. Bi, and L.-J. Gao, "A Thermoelectric-Heat-Pump Employed Active Control Strategy for the Dynamic Cooling Ability Distribution of Liquid Cooling System for the Space Station's Main Power-Cell-Arrays," *Entropy*, vol. 21, no. 6, p. 578, Jun. 2019, doi: 10.3390/e21060578.

[67] H. Chen, Y. Han, G. Tang, and X. Zhang, "A Dynamic Control System for Server Processor Direct Liquid Cooling," *IEEE Trans. Compon. Packag. Manuf. Technol.*, vol. 10, no. 5, pp. 786–794, May 2020, doi: 10.1109/TCPMT.2020.2986796.

[68] N. El-Sayed, I. Stefanovici, G. Amvrosiadis, A. A. Hwang, and B. Schroeder, "Temperature Management in Data Centers: Why Some (Might) Like It Hot," p. 12.

[69] N. Ahuja, C. Rego, S. Ahuja, M. Warner, and A. Docca, "Data center efficiency with higher ambient temperatures and optimized cooling control," in *2011 27th Annual IEEE Semiconductor Thermal Measurement and Management Symposium*, Mar. 2011, pp. 105–109. doi: 10.1109/STHERM.2011.5767186.

[70] Y. He *et al.*, “Consideration for Running Data Center at High Temperatures and Using Free Air Cooling,” presented at the ASME 2015 International Technical Conference and Exhibition on Packaging and Integration of Electronic and Photonic Microsystems collocated with the ASME 2015 13th International Conference on Nanochannels, Microchannels, and Minichannels, Nov. 2015. doi: 10.1115/IPACK2015-48169.

[71] T. J. Breen *et al.*, “From Chip to Cooling Tower Data Center Modeling: Chip Leakage Power and Its Impact on Cooling Infrastructure Energy Efficiency,” *J. Electron. Packag.*, vol. 134, no. 041009, Nov. 2012, doi: 10.1115/1.4007744.

[72] S. A. Hall and G. V. Kopcsay, “Energy-Efficient Cooling of Liquid-Cooled Electronics Having Temperature-Dependent Leakage,” *J. Therm. Sci. Eng. Appl.*, vol. 6, no. 011008, Oct. 2013, doi: 10.1115/1.4024843.

[73] M. Iyengar *et al.*, “Server liquid cooling with chiller-less data center design to enable significant energy savings,” in *2012 28th Annual IEEE Semiconductor Thermal Measurement and Management Symposium (SEMI-THERM)*, Mar. 2012, pp. 212–223. doi: 10.1109/STHERM.2012.6188851.

[74] “Department of Energy Using Warm Water to Cool New Data Center | Enterprise Networking Planet.”

https://www.enterprisenetworkingplanet.com/data-center/department-of-energy-using-warm-water-to-cool-new-data-center/ (accessed May 14, 2021).

[75] S. Zimmermann, I. Meijer, M. K. Tiwari, S. Paredes, B. Michel, and D. Poulikakos, "Aquasar: A hot water cooled data center with direct energy reuse," *Energy*, vol. 43, no. 1, pp. 237–245, Jul. 2012, doi: 10.1016/j.energy.2012.04.037.

[76] H. Coles, M. Ellsworth, and D. J. Martinez, "'Hot' for warm water cooling," in SC '11: Proceedings of 2011 International Conference for High Performance Computing, Networking, Storage and Analysis, Nov. 2011, pp. 1–10.

[77] C. D. Patel and A. J. Shah, "Cost Model for Planning, Development and Operation of a Data Center," p. 36.

[78] "Cost Model: Dollars per kW plus Dollars per Square Foot of Computer Floor | Question | Integrity," *Scribd*. https://www.scribd.com/doc/21574994/64-Interview-Questions (accessed Jul. 08, 2020).

[79] M. K. Patterson, D. G. Costello, P. F. Grimm, and M. Loeffler, "Data center TCO; a comparison of high-density and low-density spaces," p. 12.

[80] J. Koomey, "A Simple Model for Determining True Total Cost of Ownership for Data Centers," p. 9.

[81] N. Rasmussen, "Determining Total Cost of Ownership for Data Center and Network Room Infrastructure," p. 8.

[82] C. G. Malone, W. Vinson, and C. E. Bash, "Data center TCO benefits of reduced system airflow," in *2008 11th Intersociety Conference on Thermal and Thermomechanical Phenomena in Electronic Systems*, May 2008, pp. 1199–1202. doi: 10.1109/ITHERM.2008.4544397.

[83] X. Li, Y. Li, T. Liu, J. Qiu, and F. Wang, "The Method and Tool of Cost Analysis for Cloud Computing," in *2009 IEEE International Conference on Cloud Computing*, Sep. 2009, pp. 93–100. doi: 10.1109/CLOUD.2009.84.

[84] J. E. Moreira and J. Karidis, "The Case for Full-Throttle Computing: An Alternative Datacenter Design Strategy," *IEEE Micro*, vol. 30, no. 4, pp. 25–28, Jul. 2010, doi: 10.1109/MM.2010.74.

[85] Yumpu.com, "ibm-blue-gene," *yumpu.com*. https://www.yumpu.com/en/document/view/3676975/ibm-blue-gene (accessed Mar. 11, 2021).

[86] S. Polfliet, F. Ryckbosch, and L. Eeckhout, Optimizing the Datacenter for Data-Centric Workloads.

[87] D. Hardy, M. Kleanthous, I. Sideris, A. G. Saidi, E. Ozer, and Y. Sazeides, "An analytical framework for estimating TCO and exploring data center design space," in *2013 IEEE International Symposium on Performance Analysis of Systems and Software (ISPASS)*, Austin, TX, USA, Apr. 2013, pp. 54–63. doi: 10.1109/ISPASS.2013.6557146.

[88] B. Grot, D. Hardy, P. Lotfi-Kamran, B. Falsafi, C. Nicopoulos, and Y. Sazeides, "Optimizing Data-Center TCO with Scale-Out Processors," *IEEE Micro*, vol. 32, no. 5, pp. 52–63, Sep. 2012, doi: 10.1109/MM.2012.71.

[89] A. Ahuja and V. Gautam, "Towards Cost Effective Data Centers," *J. Technol. Manag. Grow. Econ.*, vol. 3, no. 2, Art. no. 2, Oct. 2012, doi: 10.15415/jtmge.2012.32009.

[90] Shaoming Chen, Yue Hu, and Lu Peng, "Optimization of Electricity and Server Maintenance Costs in Hybrid Cooling Data Centers," in *2013 IEEE Sixth International Conference on Cloud Computing*, Santa Clara, CA, Jun. 2013, pp. 526–533. doi: 10.1109/CLOUD.2013.104.

[91] B. Rubenstein and M. Faist, "Data center cold aisle set point optimization through total operating cost modeling," in *Fourteenth Intersociety Conference on Thermal and Thermomechanical Phenomena in Electronic Systems (ITherm)*, Orlando, FL, USA, May 2014, pp. 1111–1120. doi: 10.1109/ITHERM.2014.6892405.

[92] G. Da Costa, A. Oleksiak, W. Piatek, J. Salom, and L. Sisó, "Minimization of Costs and Energy Consumption in a Data Center by a Workload-Based Capacity Management," in *Energy Efficient Data Centers*, vol. 8945, S. Klingert, M. Chinnici, and M. Rey Porto, Eds. Cham: Springer International Publishing, 2015, pp. 102–119. doi: 10.1007/978-3-319-15786-3_7.

[93] D. W. Demetriou, V. Kamath, and H. Mahaney, “Understanding the True Total Cost of Ownership of Water Cooling for Data Centers,” presented at the ASME 2015 International Technical Conference and Exhibition on Packaging and Integration of Electronic and Photonic Microsystems collocated with the ASME 2015 13th International Conference on Nanochannels, Microchannels, and Minichannels, Nov. 2015. doi: 10.1115/IPACK2015-48152.

[94] V. Sorell, B. Carter, R. Zeighami, S. F. Smith, and R. Steinbrecher, “Liquid-Cooled IT Equipment in Data Centers,” *ASHRAE J.*, vol. 57, no. 12, pp. 12-14,16,18-20,22, Dec. 2015.

[95] D. W. Demetriou, V. Kamath, and H. Mahaney, “A Holistic Evaluation of Data Center Water Cooling Total Cost of Ownership,” *J. Electron. Packag.*, vol. 138, no. 1, p. 010912, Mar. 2016, doi: 10.1115/1.4032494.

[96] Z. Yang, M. Awasthi, M. Ghosh, and N. Mi, “A Fresh Perspective on Total Cost of Ownership Models for Flash Storage in Datacenters,” in *2016 IEEE International Conference on Cloud Computing Technology and Science (CloudCom)*, Dec. 2016, pp. 245–252. doi: 10.1109/CloudCom.2016.0049.

[97] K. Cho, H. Chang, Y. Jung, and Y. Yoon, “Economic analysis of data center cooling strategies,” *Sustain. Cities Soc.*, vol. 31, pp. 234–243, May 2017, doi: 10.1016/j.scs.2017.03.008.

[98] M. Ott, T. Wilde, and H. Huber, “ROI and TCO analysis of the first production level installation of adsorption chillers in a data center,” in *2017 16th IEEE Intersociety Conference on Thermal and Thermomechanical Phenomena in Electronic Systems (ITherm)*, Orlando, FL, May 2017, pp. 981–986. doi: 10.1109/ITHERM.2017.7992594.

[99] T. Rokkas, I. Neokosmidis, D. Xydias, and E. Zetserov, “TCO savings for data centers using NFV and hardware acceleration,” in *2017 Internet of Things Business Models, Users, and Networks*, Nov. 2017, pp. 1–5. doi: 10.1109/CTTE.2017.8260989.

[100] Y. Cui, C. Ingalz, T. Gao, and A. Heydari, “Total cost of ownership model for data center technology evaluation,” in *2017 16th IEEE Intersociety Conference on Thermal and Thermomechanical Phenomena in Electronic Systems (ITherm)*, Orlando, FL, May 2017, pp. 936–942. doi: 10.1109/ITHERM.2017.7992587.

[101] D. Bliedy, S. Mazen, and E. Ezzat, “Datacentre Total Cost of Ownership (TCO) Models : A Survey,” *Int. J. Comput. Sci. Eng. Appl.*, vol. 8, no. 2/3/4, pp. 47–62, Aug. 2018, doi: 10.5121/ijcsea.2018.8404.

[102] D. Bliedy, S. Mazen, and E. Ezzat, “Cost Model for Establishing a Data Center,” *Int. J. Comput. Sci. Eng. Appl.*, vol. 8, no. 2/3/4, pp. 11–30, Aug. 2018, doi: 10.5121/ijcsea.2018.8402.

[103] B. van den Berg, B. M. Sadowski, and L. Pals, “Towards sustainable data centres: Novel internal network technologies leading to sustainable cost and energy consumption in data centres in The Netherlands,” International Telecommunications Society (ITS), 184933, 2018. Accessed: Jul. 08, 2020. [Online]. Available: https://ideas.repec.org/p/zbw/itse18/184933.html

[104] W. Yan, J. Yao, Q. Cao, and Y. Zhang, “LT-TCO: A TCO Calculation Model of Data Centers for Long-Term Data Preservation,” in *2019 IEEE International Conference on Networking, Architecture and Storage (NAS)*, Aug. 2019, pp. 1–8. doi: 10.1109/NAS.2019.8834714.

[105] U. Chowdhury, W. Hendrix, T. Craft, W. James, A. Sutaria, and D. Agonafer, “Optimal Design and Modeling of Server Cabinets With In-Row Coolers and Air Conditioning Units in a Modular Data Center,” in *ASME 2019 International Technical Conference and Exhibition on Packaging and Integration of Electronic and Photonic Microsystems*, Anaheim, California, USA, Oct. 2019, p. V001T02A009. doi: 10.1115/IPACK2019-6522.

[106] “6SigmaRoom CFD Software | Future Facilities.” https://www.futurefacilities.com/products/6sigmaroom/ (accessed Apr. 29, 2021).

[107] U. Chowdhury, A. Siddarth, M. Sahini, and D. Agonafer, “Raising Inlet Air Temperature for a Hybrid-Cooled Server Retrofitted With Liquid Cooled Cold Plates,” in *Volume 8B: Heat Transfer and Thermal Engineering*, Pittsburgh,

Pennsylvania, USA, Nov. 2018, p. V08BT10A044. doi: 10.1115/IMECE2018-88497.

[108] M. M. Islam, U. Chowdhury, N. Inamdar, and D. Agonafer, "Power consumption minimization in hybrid cooled server by fan reduction," in *2017 16th IEEE Intersociety Conference on Thermal and Thermomechanical Phenomena in Electronic Systems (ITherm)*, May 2017, pp. 850–856. doi: 10.1109/ITHERM.2017.7992574.

[109] M. Sahini *et al.*, "Comparative study of high ambient inlet temperature effects on the performance of air vs. liquid cooled IT equipment," in *2017 16th IEEE Intersociety Conference on Thermal and Thermomechanical Phenomena in Electronic Systems (ITherm)*, Orlando, FL, May 2017, pp. 544–550. doi: 10.1109/ITHERM.2017.7992534.

[110] "Home | 6SigmaET by Future Facilities - Thermal Simulation of Electronics." https://www.6sigmaet.info/ (accessed Apr. 28, 2021).

[111] J. Fernandes, "Minimizing Power Consumption At Module, Server And Rack-levels Within A Data Center Through Design And Energy-efficient Operation Of Dynamic Cooling Solutions," *undefined*, 2015, Accessed: May 14, 2021. [Online]. Available: /paper/Minimizing-Power-Consumption-At-Module%2C-Server-And-Fernandes/d7ab2c7ef0dcc81936072282e585231253ab9ed4

[112] "MacroFlow: Overview | Innovative Research, LLC." https://inresllc.com/products/macroflow/overview.html (accessed Apr. 28, 2021).

Biographical Information

Uschas Chowdhury, has received his Bachelor of Engineering degree in Mechanical Engineering from the Bangladesh University of Engineering and Technology (BUET), Dhaka, Bangladesh. He has completed his master's in mechanical engineering from the University of Texas at Arlington, Texas, USA in May 2017. He worked as a Teaching Assistant for an undergraduate course in his second semester and during his Master's, he also worked on projects under Dr Dereje Agonafer in The University of Texas at Arlington. He has again joined the lab for PhD degree and worked on various industry collaborated research projects and studied various topics like air cooling, liquid cooling, and direct/indirect evaporative cooling etc. He has gained theoretical, numerical, and experimental background knowledge while working projects and using CFD codes like 6SigmaET, 6SigmaRoom, ICEPAK and FloTHERM. He was also employed by NVIDIA as Mechanical Engineering Intern for a year and worked on data center air and liquid cooling.